DEVELOPMENT OF RE-HEAT ADSORPTION REFRIGERATION CYCLES

2014.9

GRADUATE SCHOOL OF
BIO-APPLICATIONS AND SYSTEMS ENGINEERING
TOKYO UNIVERSITY OF AGRICULTURE AND TECHNOLOGY
JAPAN

I GUSTI AGUNG BAGUS WIRAJATI

DEVELOPMENT OF RE-HEAT ADSORPTION REFRIGERATION CYCLES

A Dissertation Submitted in Partial Fulfillment of the Requirement for the Award of the Degree of

Doctor of Engineering (Dr.Eng)

By
I GUSTI AGUNG BAGUS WIRAJATI

Supervisor
Prof. Atsushi AKISAWA

Co-Supervisor
Associate Prof. Yuki UEDA

GRADUATE SCHOOL OF BIO-APPLICATIONS AND SYSTEMS ENGINEERING
TOKYO UNIVERSITY OF AGRICULTURE AND TECHNOLOGY, JAPAN

TABLE OF CONTENTS

LIST OF FIGURES

Page

LIST OF TABLES

Page

ABSTRACT

The use of adsorption chiller, as well known as an environmentally friendly chiller, become popular since past decades because of its features such as low heat source temperature utilize, super energy saving, neither using CFCs nor HCFCs, easy maintenance and safe. On the other hand, in tropical country such as Indonesia, many hotels, fishery industries and house-holds are the most common place which is using the air conditioning and refrigerant devices. However, a compression cycle are still using recently, while the advance cycle such as adsorption system as a future plan, and should be implemented almost immediately, in case of reducing the potential ozone depleting onto the planet.

Maintaining a constant chilled water outlet temperature is also of equal importance to improve the conversion efficiency of the chiller so that maximum cooling capacity can be delivered. The possibility of reducing the adsorber/desorber hex's utilization is still promising since the consideration of the smaller adsorption machine to be constructed and can be performed for the relative low heat source temperature below 60^{o}C.

In this thesis, the author concern of studying the conventional adsorption cycle, the re-heat adsorption cycle and the advanced re-heat combined adsorption cycle experimentally and numerically. Developing simulation with cycle time optimization for all of adsorption cycle has been investigated as well.

This thesis comprises 7 chapters. The following is a brief description of the contents of each chapter. Chapter 1 gives a general and specific background of adsorption system and the goal of the research. The mechanism of different types of adsorption systems are discussed in chapter 2. A literature review on the advanced adsorption cooling systems and types of adsorbent/refrigerant pairs which are commonly used in adsorption cooling and heat pump systems are presented therein. Adsorption/desorption phenomena, theory of adsorption and mathematical expression for heat and energy balance of adsorption system are described in Chapter 3. Chapter 4 discussed the experimental investigation of a reheating two-stage adsorption chiller applying fixed chilled water outlet conditions. In Chapter 5 describes a simulation model of the four-bed re-heat adsorption cycles has developed to analyze the optimization of the cycle time, including adsorption/desorption time, mass recovery time and pre-heating/pre-cooling time, with chilled water outlet temperature fixed. Design and performance of an advanced three-bed re-heat conventional and three-bed three-stage re-heat combined adsorption cycle are described in chapter 6. Finally, overall conclusion and remarks on the further development of the adsorption cycle are presented in Chapter 7.

DECLARATION

I hereby declare that the work which is being presented in the thesis entitled "**Development of Re-Heat Adsorption Refrigeration Cycles**" submitted in partial fulfillment of the requirements for the award of the degree of Doctor of Engineering (Dr. Eng), Graduate School of Bio-Applications and Systems Engineering, Tokyo University of Agriculture and Technology, JAPAN, is authentic record of my own research work.

The research work presented in this thesis has not been submitted by me for the award of any degree in this or any other university.

August, 2014

I Gusti Agung Bagus Wirajati

ACKNOWLEDGMENT

The work on this thesis has been an inspiring, often exciting, sometimes challenging, but always interesting experience. It has been made possible by many other people, who have supported me.

First of all I wish to express my sincere gratitude to my supervisor Prof. Atsushi AKISAWA and co-Supervisor Associate Prof. Yuki UEDA, for his valuable comments on my thesis and for being an outstanding advisor and excellent professor. His constant encouragement, support, and invaluable suggestions made this work successful. He has been everything that one could want in an advisor. He has supported me with his encouragement and many fruitful discussions.

I would like also acknowledge to the Directorate General of Higher Education of Indonesia for the financial support of the 3 years doctoral course scholarship.

I am deeply and forever indebted to Ratu Aji Ida Bagus Putu WIDIARTA, for his trust on me, and Prof. Takahiko MIYAZAKI, for his support, cooperation and help during my research work. And would like also to thankfully for all friendly students and staff of Akisawa and Ueda Laboratories for their charming cooperation during my study.

The author wishes to express his love and sincere gratitude to my parents, my parents in law and my beloved wife BINTANG and my daughter NAWA, for their deep understanding and moral support and their praying throughout this long-term study in Japan. I also dedicate this thesis to my ancestor and my spiritual organization of GHANTA YOGA.

NOMENCLATURES

Nomenclature

A	area	(m2)
C	specific heat	(J kg-1 K-1)
D_o	pre-exponential constant in Eq. (10)	(m2s-1)
E_a	activation energy	(J mol-1)
L	latent heat of vaporization	(J kg-1)
$\dot{m}$	mass flow rate	(kg s-1)
P_s	saturated vapor pressure	(Pa)
q	amount of adsorbed water	(kg refrigerant/kg adsorbent)
q*	equilibrium amount of adsorbed water	(kg refrigerant/kg adsorbent)
Q_s	isosteric heat of adsorption	(J kg-1)
R	gas constant	(J mol-1 K-1)
R_p	average radius of a particle	(m)
T	temperature	(K)
t	time	(s)
U	overall heat transfer coefficient	(Wm-2K-1)
W	weight	(kg)
γ	bed connection indicator	-
δ	adsorption indicator	-
ε	heat exchanger efficiency	-

Subscripts

ads	adsorption
ads-eva	adsorbed vapor from evaporator to adsorber
hex	heat exchanger
con	condenser
chill	chilled
cw	cooling water
cycle	cycle
des	desorption

des-con	desorbed vapor from desorber to condenser
eva	evaporator
HEX	heat exchanger
hw	hot water
i	inlet
o	outlet
s	sorption element
v	vapor
w	water

CHAPTER 1

1.1 BACKGROUND

The adsorption refrigeration chiller has sustained an increased interest over the past three decades. The adsorption refrigeration chiller system is regarded not only as an alternative cooling system for reducing chlorofluorocarbons (CFCs) and hydro fluorocarbons (HCFCs) use but also as an energy-efficient technology. Reduction of primary energy consumption is strongly required to mitigate global warming caused by fossil fuel consumption. By using of waste heat thermal energy or renewable energy in order to increase energy conversion process especially in refrigeration process, is one of the alternative way to achieve this objective. At the moment, absorption (liquid vapor) refrigeration cycles are most promising technologies, however, the adsorption (solid vapor) cycles have distinct advantage over the other heat driven refrigeration cycle, in their ability to be driven by heat of relatively low, near-environmental temperature. Under the cycle, waste heat below 100^{o}C can be recovered.

On the other hand, in tropical country such as Indonesia, many hotels, fishery industries and house-holds are the most common place which is using the air conditioning and refrigerant devices. However, a compression cycle are still using recently, while the advance cycle such as adsorption system as a future plan, and should be implemented almost immediately, in case of reducing the potential ozone depleting onto the planet.

1.2 INTRODUCTION

The use of adsorption chiller, as well known as an environmentally friendly chiller, become popular since past decades because of its features such as low heat source temperature utilize, super energy saving, neither using CFCs nor HCFCs, easy maintenance

and safe [1]. The Adsorption refrigeration chiller system regarded not only as an alternative for reducing CFCs and HCFCs uses but also as an energy-efficient technology. Furthermore, adsorption cycle has a distinct advantage over other systems for their ability to be driven by heat of relatively low, near-environmental temperatures, can be recovered, which is highly desirable and investigated by Kashiwagi et al. [18].

Many theoretical and experimental investigations have been conducted not only on a single stage (conventional stage) chiller but also on the advanced stages of the operational chiller [2-7]. The reheating two-stage adsorption chiller is one of the advanced stages of the adsorption chiller. Saha et al. [8] investigated the performance of a thermally activated silica gel–water adsorption refrigeration cycle by applying a multi-bed scheme. Boelman et al. [9] experimentally evaluated the commercial two-bed adsorption chiller under a typical cyclic steady state operation. Chua et al. [10] investigated the improvement of the utilization of waste heat and reduction of the chilled water outlet temperature fluctuation. Kim et al. [11] and Wang et al. [12] also investigated the performance of the adsorption chiller experimentally, but the temperature of the chilled water outlet was not fixed. The reheating two-stage adsorption chiller has also been investigated experimentally. Alam et al. [13] investigated the performance of the chiller and compared the reheating two-state adsorption chiller with the conventional single and two-stage chillers. The chilled water outlet in this experiment operated with fluctuating temperatures. Khan et al. [14] also investigated the reheating two-stage adsorption chiller, but the temperature of the chilled water outlet was not fixed.

Maintaining a constant chilled water outlet temperature is also of equal importance to improve the conversion efficiency of the chiller so that maximum cooling capacity can be delivered [15]. However, maintaining a constant chilled water outlet temperature during the experiments is difficult because the outlet water temperature cannot be set up automatically. From this point of view, the main objective of this investigation was to identify the effects of

heat source temperature and the effect of cycle time on performance while the chilled water outlet temperature was kept constant at 9°C. The total cycle times of 1000 s and 2500 s are representative of the reheating adsorption chiller with short and long cycles. Understanding of the short and long cycles is based on how long (time in seconds) a cycle time is applied in the experiment.

The possibility of reducing the adsorber/desorber hex's utilization is still promising since the consideration of the smaller adsorption machine to be constructed [24, 38-40] and can be performed for the relative low heat source temperature below 60^{o}C. By reducing the hex utilization and introducing the new mode operational strategy which is applied in the present chiller, the smaller compact machine can be designed.

In this thesis, the author concern of studying the conventional adsorption cycle and re-heat adsorption cycle experimentally and numerically, while the advanced cycle namely three-bed re-heat conventional and three-bed three-stage re-heat combined cycle also investigated since the consideration of exploiting the low heat source temperature and reducing the Hex's utilization which are the highlight in presents work.

1.3 PROBLEM STATEMENT

Four-bed conventional cycle is not suitable to work for the heat source temperature lower than 60^{o}C if the chilled water out temperature fixed in 9^{o}C. Since our concentration research focused on utilizing the low heat source temperature, then the other cycle namely four-bed re-heat cycle was developed and have been investigated numerically and experimentally. The main advantage of these cycles is their ability to utilize low temperature waste heat (below 60°C) as driving heat sources while chilled water out arranged in fixed condition at 9^{o}C. However, four-bed re-heat cycle can only work at the lowest temperature 55 ^{o}C if the chilled water outlet fixed in 9 ^{o}C. On the other hand, reducing the adsorber/desorber hex's utilization is still promising to consider to make the smaller adsorption machine and can

to be performed for the relative low heat source temperature below 60^{o}C. From this point of view, the advanced three-hex re-heat combined cycle introduced. Unfortunately, the lowest temperature heat source of this cycle was similar than the four-bed re-heat cycle, with the advantages is only using three bed.

Since our consideration are exploiting the low heat source temperature and reducing the bed's utilization, then the new advanced three-bed three stage re-heat combined cycle was investigated numerically, to answer the highlight problem in this study. Our target is to gain the heat source temperature below 50 ^{o}C.

1.4 OBJECTIVES

There are three main objectives of the present research work i.e:

1. Conducting the experiment to investigate the performances of four-bed adsorption chiller with conventional and re-heat cycle.
2. Developing a simulation of multi-bed adsorption chiller with re-heat cycle.
3. Introducing a newly simulation model of the advanced three-bed re-heat combined adsorption cycle to investigate the performances.

1.5 THESIS OUTLINE

This thesis comprises 7 chapters describing the various theories of adsorption and simulations to achieve the research objectives. The following is a brief description of the contents of each chapter.

Chapter 1 gives a general and specific background of adsorption system and the goal of the research. The mechanism of different types of adsorption systems are discussed in chapter 2. A literature review on the advanced adsorption cooling systems and types of adsorbent/refrigerant pairs which are commonly used in adsorption cooling and heat pump systems are presented therein. Adsorption/desorption phenomena, theory of adsorption and mathematical expression for heat and energy balance of adsorption system are described in

Chapter 3. Chapter 4 discussed the experimental investigation of a reheating two-stage adsorption chiller applying fixed chilled water outlet conditions. In Chapter 5 describes a simulation model of re-heat adsorption cycles has developed to analyze the optimization of the cycle time, including adsorption/desorption time, mass recovery time and pre-heating/pre-cooling time, with chilled water outlet temperature fixed. Design and performance of an innovative advanced three-bed re-heat conventional and the advanced three-bed three-stage re-heat combined adsorption cycle are described in chapter 6. Finally, overall conclusion and remarks on the further development of the adsorption refrigerator are presented in Chapter 7.

CHAPTER 2

DEVELOPMENT OF ADSORPTION SYSTEM

The adsorption system, as well known as an environmentally friendly chiller, become popular since past decades because of its features such as low heat source temperature utilize, super energy saving, neither using CFCs nor HCFCs, easy maintenance and safe[1-2]. The Adsorption refrigeration chiller system regarded not only as an alternative for reducing CFCs and HCFCs uses but also as an energy-efficient technology [3]. Furthermore, adsorption cycle has a distinct advantage over other systems for their ability to be driven by heat of relatively low, near-environmental temperatures, can be recovered, which is highly desirable and investigated by Kashiwagi et al. [18].

2.1. THEORY OF ADSORPTION

Adsorption is a surface phenomenon occurring at the interface of refrigerant phase (gas phase) and adsorbent phase (solid phase) in such a way that Van der Waals forces and hydrogen bonding act between the molecules of substances, irrespective of their state of aggregation. The substance on whose surface the adsorption occurs is known as adsorbent and whose molecules get adsorbed on the surface of the adsorbent (i.e., solid or liquid) is known as adsorbate. Depending upon the nature of forces existing between adsorbate molecules and adsorbent, the adsorption occurs through physical (Vander Waal's forces which is weak) and chemical sorption (chemical bonds known as Langmuir adsorption). Physical adsorption can be easily reversed by heating or by decreasing the pressure. In chemical sorption, the force of attraction is very strong, therefore adsorption cannot be easily reversed.

Desorption is a phenomenon whereby a substance is released from or through a surface. It is exactly opposite of either adsorption or absorption. The adsorption and desorption process is simply shown in Figure 2.1. During adsorption water vapor molecules attach to the surface of silica-gel particle, whereas during desorption it is removing from the surface.

The use of solids for removing substances from either gaseous or liquid solutions has been widely used since biblical times. This process is know as adsorption, involves nothing more than the preferential partitioning of substances from the gaseous or liquid phase onto the surface of a solid substrate. Therefore, the adsorption process is essentially an attraction

of a gaseous or liquid adsorbate molecules into a porous adsorbent surface. From the early days of using bone chare for decolorizition of sugar solutions and other foods, to the later implementation of activated carbon for removing never gases from the battlefield to today's thousands of applications, the adsorption phenomenon has become a useful tool for purification, separation and refrigeration. Adsorption phenomena are operative in most natural, physical, biological, and chemical systems, and adsorption operations employing solids such as activated carbon and synthetic resins are used widely in industrial applications and for purification of waters and waste water. The process of adsorption involves separation of a substance from one phase accompanied by its accumulation or concentration at the surface of another. Adsorption is thus different from absorption, a process in which material transferred from one phase to another (e.g. liquid) interpenetrates the second phase to from a "solution". The term sorption is a general expression encompassing both processes.

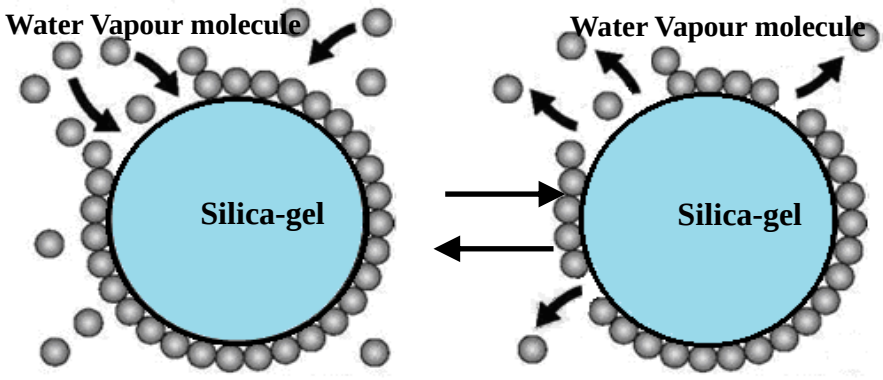

Figure 2.1: Adsorption and desorption process.

2.2. ADSORPTION AND DESORPTION PROCESS

Adsorption and desorption are the most common words or terms that often heard when we discuss about the process in the ab/ad-sorption chiller.

Refrigerant (water) in evaporator is evaporated at the temperature (T_{eva}) and seized heat (Q_{eva}) from the chilled water. The evaporated vapor is adsorbed by the adsorbent (silica gel bed), at which point the cooling water removes the adsorption heat (Q_{ads}).

The desorption process takes place at pressure (P_{cond}). The desorbers(silica gel bed) are heated up to the temperature (T_{des}) by driving heat source (Q_{des}). The resulting refrigerant vapor in condensor is cooled down to the temperature (T_{cond}) by the cooling water, which removes the heat (Q_{cond}).

2.3. ABSORPTION AND/OR ADSORPTION SYSTEM

Adsorption is different from absorption. In absorption, the molecules of a substance are uniformly distributed in the bulk of the other, whereas in adsorption molecules of one substance are present in higher concentration at the surface of the other substance.

On the other hand, since the adsorption and/or absorption are playing an important part of the chiller system, then both terms become clearly if they compare not only by definition but also by adsorbant/refrigerant pairs and by commercialized.

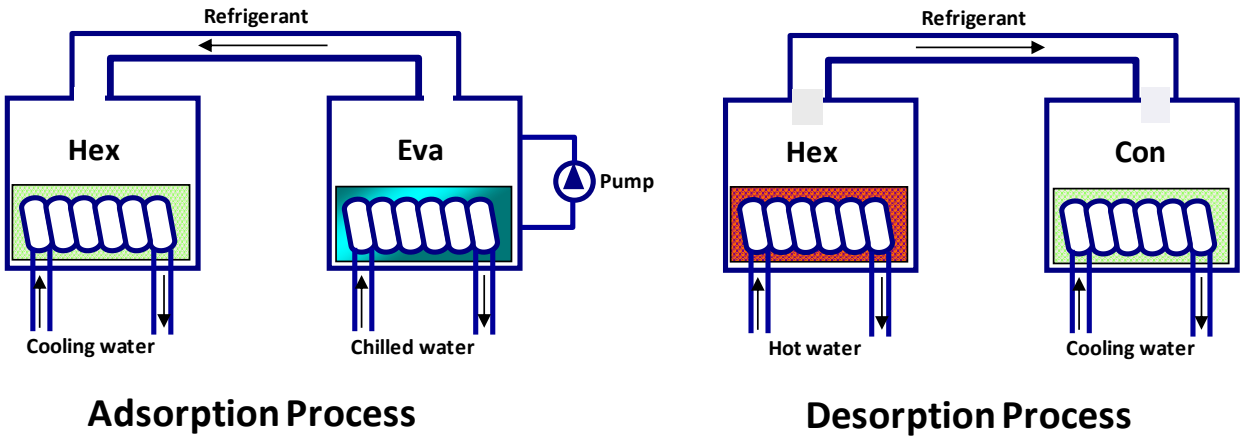

Figure 2.2: Adsorption and desorption process in the system

In the adsorption chiller, cold generated through the process of adsorption on porous material, whilst the absorption chiller that cold generated through the process of sorption by liquid solution. The adsorbant-refrigerant pairs in the adsorption chiller are solid-vapor such as silica gel/tap water or zeolite/tap water. Meanwhile, lithium bromide (LiBr)/destiled water or Amonia (Nh3)/destiled water are the adsorbant-refrigerant pair in the absorption chiller.

In the market, absorption chiller is a mature technology and several product comercialised. However, adsorption chiller constitutes as a developing technology and only a few products on the market.

Generally, the main difference between absorption and adsorption is the nature of the sorbent pair as well as the cycle duration time Fan et al.[41]. It is reported that absorption cycle performance is higher than that of adsorption cycle. However, the main drawback of absorption cycles is that it needs a high temperature heat source to maintain its operation. All absorption cycles are closed cycles. On the other hand adsorption cycles can be classified into open and closed cycles. The open cycle is applied in the field of desiccant cooling and

dehumidification applications. Calcium chloride, lithium bromide and silica gel are commonly used as desiccants. Closed adsorption systems can be classified into high pressure (above atmospheric pressure) and low pressure (sub-atmospheric pressure) depending on the type of adsorbent-refrigerant employed in the system as well as the system application. Flowchart of simple classification of heat pump system is shown in Figure 2.3. A short description of vapor compression, absorption and adsorption systems is given below:

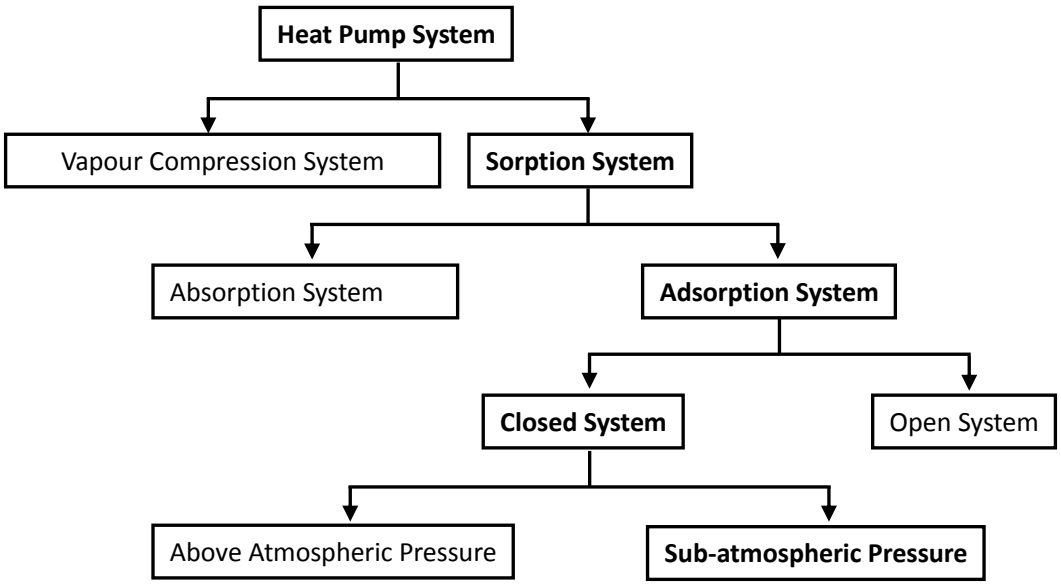

Figure 2.3: Classification of heat pump system

2.4. ADSORBENT/ADSORBATE PAIRS

Adsorbent is a thing or substance that has capability to adsorb vapor or gaseous substance, while adsorbate is a substance that is adsorbed by adsorbent. Thus, the adsorbing phase is the adsorbent, and the material concentrated or adsorbed at the surface of that phase is the adsorbate. In refrigeration and heat pump application adsorbate is mainly known as refrigerant. The first criterion for a material to be an adsorbate is whether the material has a high internal volume which is accessible to the components being removed from the fluid. Such a highly porous solid may be carbonaceous or inorganic in nature, synthetic or natural occurring. The internal surface area for the adsorbent ranges is between 100 ~ 3000 m^2/g. The performance of adsorbent used in physorption is governed mainly by surface properties, such as surface area, micro-pores and macro-pores, size of granules in powders, crystal or in pellets. Adsorbent having specila affinity with polar substances like water are termed “hydrophilic”. These include silica gel, zeolites and porous or active alumina. Non-polar

adsorbent, termed “hydrophobic” have more affinity for oils and gases than fro water. These substances include activated carbons, polymer adsorbent and silicalites. Adsorptions is always accompanied by evolution of heat, the quality of which depend upon the magnitude of the Van der Waal forces involved, phase change, electrostatic energies and chemical bonds.

When the adsorbate (refrigerant) is adsorbed on the adsorbent surface, it is called adsorbent bed. The adsorbent bed may directly be equipped with collector and directly heated or it is heated indirectly by using some heat transferring medium between collector absorber and adsorbent bed.

Thermo physical properties of some adsorbent/adsorbate pairs are presented in Table 2.1.

Table 2.1 Thermo physical properties of some adsorbent/adsorbate pairs

Adsorbent/Adsorbate Pairs	**Maximum adsorption capacity (kg refrigerant/kg adsorbent)**	**Average adsorption heat (kJ/kg refrigerant)**
Active Alumina/H_2O	0.19	3000
Chabazite/ H_2O	0.17	3000
Charcoal/ H_2O	0.32~0.38	2300~2600
Silica gel/ H_2O	0.4	2800
Zeolite/ H_2O	0.2~0.27	3300~4200
AC35/CH_3OH	0.32	1400
Zeolite/ CH_3OH	0.17~0.20	2300~2600
Silica gel/Methyl Alcohol	0.17~0.22	1000~1500
AC35/NH_3	0.3~0.36	2000~2700
Zeolite/NH_3	0.22~0.32	4000~6000

At present, silica gel/water, zeolite/water, zeolite/ammonia, active carbon/ammonia and active carbon/methanol are most commonly used as adsorbent/adsorbate pairs. The adsorbent/adsorbate pairs for adsorption refrigeration system selected from the following distinct point of views [42]:

- Adsorption/desorption temperature limit
- Adsorption/desorption heat of adsorbent
- Adsorption/desorption capacity of adsorbent
- Boiling/freezing temperature of adsorbate
- Environmental impact of adsorbent/adsorbate pair.

Silica gel-water pair is one of working pairs, which is commonly used in adsorption cooling system. Silica gel has large capacity to adsorb water, especially at high vapor pressure. Therefore, it is widely used as a desiccant for dehumidification purposes. Silica gels with pore sizes range from 2 to 3 nm (Type A) to about 0.7 nm (Type B), are mostly used in commercial applications. Specifically, Type A is used for general drying and Type B is for relative humidity's greater than 50% [43]

Some characteristic of adsorbent/refrigerant pair has been presented in Table 2.2.

Table 2.2 Characteristic of Adsorbent-Refrigerant Pairs

Adsorbent/ Refrigerant	**Driving Temperature**	**Refrigerated Space Temp.**	**ODP/ GWP**	**Toxicity/ Flammable**	**Applications**
SiO_2-H_2O	50~100 ^oC	0 ^oC	0	No	Air-Conditioning
$CaCl_2$-NH_3	100~130 ^oC	-10 ^oC	0	Yes	Refrigeration
AC35-CH_3OH	90~150 ^oC	-10 ^oC	0	Yes	Refrigeration Air-Conditioning
AC35-NH_3	120~300 ^oC	-10 ^oC	0	Yes	Refrigeration Heating
NaX-H_2O	140~300 ^oC	0 ^oC	0	Yes	Air-Conditioning Heating
NaX-NH_3	300~550 ^oC	-	0	Yes	Heating

ODP: **O**zon **D**epleting **P**otential; GWP: **G**lobal **W**arming **P**otential

Source: Saha (1997)

2.5 CONVENTIONAL VAPOR COMPRESSION SYSTEM

A simple vapor compressor system consists of four basic components, namely, 1) evaporator, 2) compressor, 3) condenser and 4) expansion valve. The schematic diagram of the arrangement is as shown in Figure 2.4. Except these, a heat transfer fluid known as refrigerant is required to transfer heat. The refrigerant passes through these four components

of the system and performs compression, condensation, expansion and evaporation, respectively. Liquid refrigerant is allowed to evaporate in the evaporator at low temperature and pressure. Heat is required for vaporization and hence, a refrigerating effect is produced during the vaporization. After evaporating vapor into evaporator, it enters to the compressor and compressed by mechanical compressor to increase the pressure as well as temperature. When the pressure of vapor reaches at the pressure of condenser, the vapor is allowed to condense in condenser. The pressure at this state is sufficiently high and vapor is condensed into high pressure liquid in the condenser where heat is removed from it by either water or air. After the condensation, the liquid refrigerant passes through the expansion valve. Here, the vapor is throttled down to a low pressure liquid and goes to the evaporator. The cycle repeats again and again. The exchange of energy is as follows:

- During evaporation, heat which is equivalent to latent heat of vaporization is absorbed by the refrigerant.
- Compressor requires work, which is supplied to the system from the surroundings.
- During condensation, heat, equivalent of latent heat of condensation etc, is lost from the refrigerator.
- There is no exchange of heat during throttling process through the expansion valve as this process occurs at constant enthalpy.

The performance of a vapor-compression system is defined as the coefficient of performance (*COP*), which can be calculated as follows;

$$COP = \frac{refrigeration\ effect}{work\ input}$$

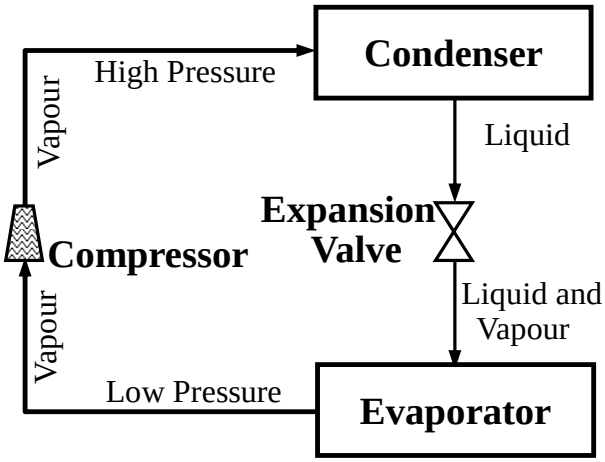

Figure 2.4: Typical vapor compressor refrigeration system.

Typically, for domestic refrigeration, the coefficient of performance (*COP*) of vapor compression system lays around 3. Up to the recent regulation, the usual refrigerant was CFC's. However, because of the ozone layer depletion and global warming problems, more and more substitutes are under development.

2.6 ABSORPTION SYSTEM

The absorption system differs from the vapor compression system in a way that it uses heat energy instead of mechanical energy to make a change in the conditions necessary to complete the refrigeration cycle. It can be said that absorption system is heat powered system in which a secondary fluid, known as sorbent, is used to absorb the primary fluid i.e., gaseous refrigerant, which has been vaporized in the evaporator. A basic absorption system consists of one or more absorber, a pump, a generator, a condenser and an evaporator. Schematic of a basic absorption system is shown in Figure. 2.5.

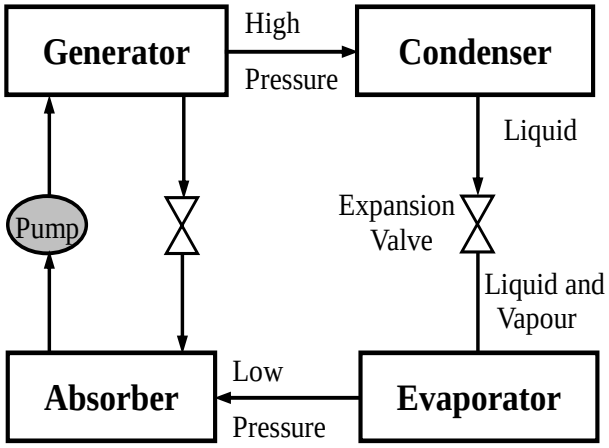

Figure 2.5: Typical absorption refrigeration system.

Condenser and evaporator of absorption system act as similar as the condenser and evaporator of compression system. In compression system only one suitable refrigerant is used whereas in absorption system sorbent and refrigerant pair is needed. In absorber, at low pressure sorbent absorb the refrigerant vapor of evaporator. Pump is used to send low pressure sorbent-refrigerant solution to the generator, which works at higher temperature and pressure. Pump is similar as the compressor of vapor compression system. Generator separate the solution into liquid sorbent and refrigerant vapor through heating and rectification process

and then refrigerant vapor goes to the condenser and liquid sorbent return to the absorber. At the same time refrigerant vapor condense in the condenser and then go to the evaporator through expansion valve. The cycle is repeats.

2.7 ADSORPTION SYSTEM

Adsorption system is environmental friendly whereas vapor compression system has weakness in this point. It can work at lower heat source temperature compare to absorption system. Adsorption system is very simple compare to compression and absorption system because it has no extra component such as compressor, generator and pump. The simplest heat powered adsorption system composes of three heat exchangers namely, sorption bed or adsorber/desorber bed, condenser and evaporator, as shown in Figure. 2.6. Adsorber/desorber bed can compare with compressor of compression system but electric power is needed to operate compressor whereas heat power is used in bed to change it mode from adsorber to desorber. Adsorption system needed adsorbent-adsorbate pair similar as sorbent-refrigerant pair of absorption system. Adsorption system will be described elaborately in subsequent sections.

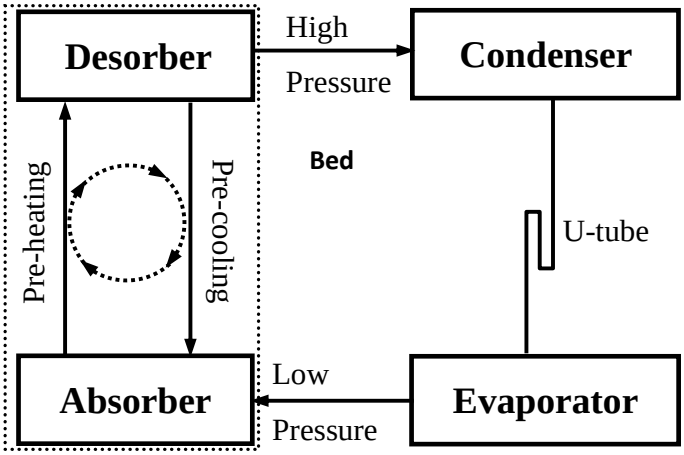

Figure 2.6: Typical adsorption refrigeration system.

An adsorption cycle for refrigeration or heat pumping does not use any mechanical energy, but only heat energy. Moreover, this type of cycle basically is a four temperature discontinuous cycle. An adsorption unit consists of one or several adsorbers plus a condenser plus an evaporator, connected to heat sources. The adsorber (or system consisting of the absorbers) exchanges heat with a heating system at high temperature (HS) and a cooling

system at intermediate temperature (CS), while the system consisting of the condenser plus evaporator exchangers heat with another heat sink at intermediate temperature (not necessarily the same temperature as the CS), and a heat source at low temperature. Vapor is transported between the adsorber(s) and the condenser and evaporator.

The cycle consists of four periods:

1: Heating and Pressuration

During this period, the adsorber receives heat while being closed. The adsorbent temperature increases, which induces a pressure increase, from the evaporation pressure up to the condensation pressure. This period is equivalent to the "compression" in compression cycles.

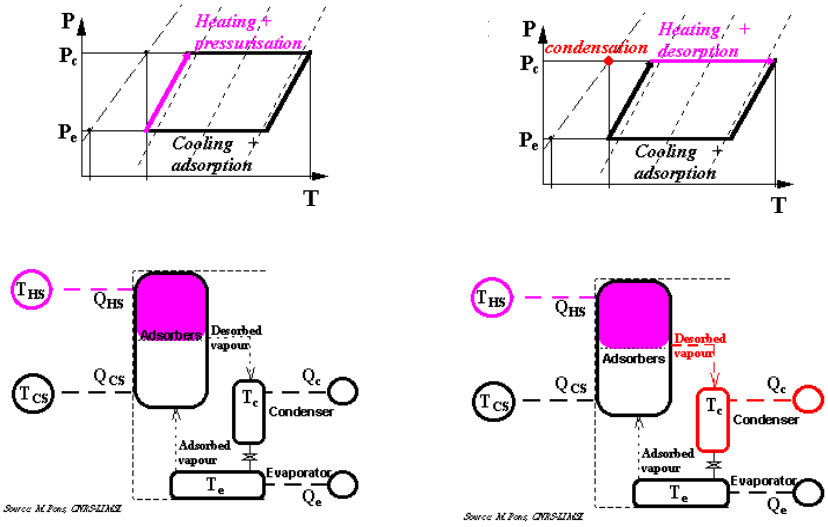

Source: http://perso.limsi.fr/mpons/pricyc.htm

2: Heating and Desorption + Condensation

During this period, the adsorber continues receiving heat while being connected to the condenser, which now superimposes its pressure. The adsorbent temperature continues increasing, which induces desorption of vapour. This desorbed vapour is liquified in the condenser. The condensation heat is released to the second heat sink at intermediate temperature.

This period is equivalent to the "condensation" in compression cycles.

3: Cooling and Depressurization

During this period, the adsorber releases heat while being closed. The adsorbent temperature decreases, which induces the pressure decrease from the condensation pressure

down to the evaporation pressure.

This period is equivalent to the "expansion" in compression cycles.

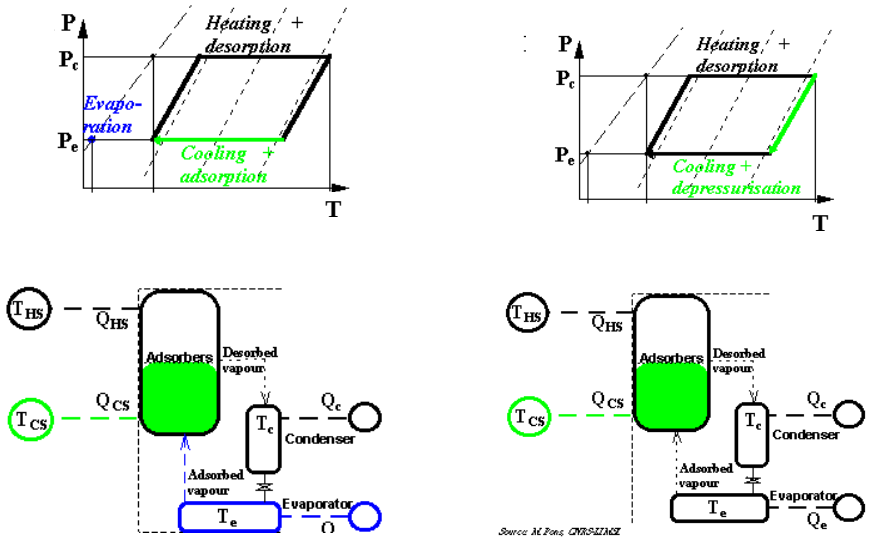

Source: http://perso.limsi.fr/mpons/pricyc.htm

4: Cooling and Adsorption + Evaporation

During this period, the adsorber continues releasing heat while being connected to the evaporator, which now superimposes its pressure. The adsorbent temperature continues decreasing, which induces adsorption of vapour. This adsorbed vapour is vaporised in the evaporator. The evaporation heat is supplied by the heat source at low temperature.

This period is equivalent to the "evaporation" in compression cycles

2.8. FOUR-HEX's ADSORPTION SYSTEM

Four-hex's adsorption system means that the chiller operates by utilizing four-adsorber/desorber heat exchanger in their system. In this thesis, the author has been investigated three types of adsorption cycle experimentally and numerically.

2.8.1. Conventional Four-Hex Adsorption Cycle

Figure 2.7 present the schematic of the conventional four-hex adsorption cycle. In this chiller, both upper hex (Hex1 and Hex3) and lower hex (Hex2 and Hex4) never interact with evaporator and condenser, respectively.

To complete a full cycle, the chiller operates through simple four processes such as desorption, pre-cooling, adsorption and pre heating. In the heating process, system provides driving heat to Hex1 and Hex2 for the desorption process. The heating process provides

sufficient energy for releasing refrigerant from adsorbent pores, and the refrigerant then vaporizes to the condenser. By opening valve V1 and V2, the refrigerant vapor will flow to the condenser. The resulting refrigerant from desorption process is cooled down in the condenser by circulating cooling water from the cooling system, which removes condensation heat, Q_{cond}. The desorption-condensation process takes place at pressure P_{cond}, as shown in Figure 2.8, point 1 - 2. After the condensation process, liquid refrigerant flows to the evaporator

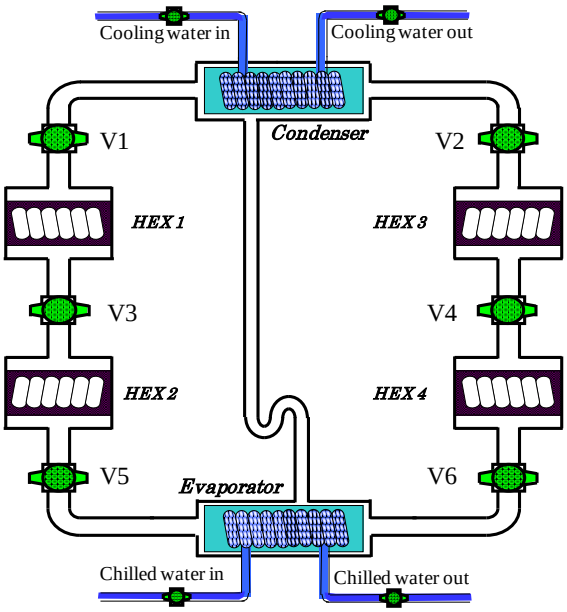

Figure 2.7: The Conventional Four-Hex Adsorption Cycle.

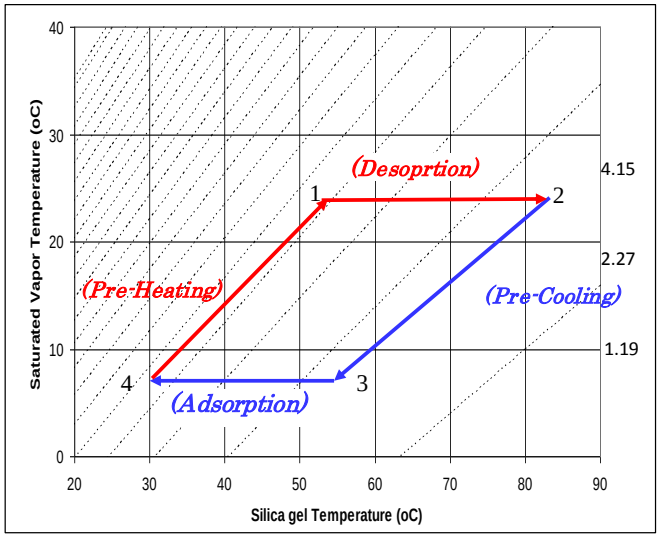

Figure 2.8: The P-T-X Diagram of Conventional Four-Hex Adsorption Cycle.

The evaporator is connected to Hex2 and Hex4 by opening valves V5 and V6, respectively. In the adsorption‑evaporation process, the refrigerant in the evaporator is evaporated at low evaporation temperature (T_{eva}) and captured heat (Q_{eva}) from chilled water. The evaporated vapor is adsorbed by Hex2 and Hex4. The cooling system also supplies cooling water to Hex2 and Hex4 to remove adsorption heat released during the adsorption process. The adsorption‑evaporation process occurs at evaporation pressure (P_{eva}). The process can be seen in Figure 2.8 at points 3‑4.

During pre-cooling and pre-heating process, all Hexes' are cooled down and heated up by cooling water and hot water, respectively. All hexes are isolated from adsorber/desorber by closing valves V1-V6 and there is no refrigerant circulation.

2.8.2. Advanced Four-Hex Re-Heat Adsorption Cycle

Figure 2.9 shows advanced four-hex re-heat adsorption cycle, while Figure 4 shows the P-T-X diagram for standard conditions. The chiller consists of four heat exchangers (i.e., HEX1, HEX2, HEX3 and HEX4), one evaporator and one condenser. The adsorbent heat exchangers of the chiller are operated through six thermodynamic processes in a full cycle, namely adsorption (1-2), mass recovery with cooling (2-3), pre-heating (3-4), desorption (4-5), mass recovery with heating (5-6) and pre-cooling (6-1). In the adsorption process, refrigerant (water) is evaporated in the evaporator and the temperature (T_{eva}) and heat (Q_{eva}) are seized isobarically from the chilled water. An evaporation process occurs and produces a cooling effect. Heat for the evaporation of the water is supplied by flowing chilled water at a low heat source temperature. In the first half cycle, HEX1 is heated by hot water and HEX3 is cooled by cooling water. When the pressures of HEX1 and HEX2 are nearly equal, both are then connected by opening the connecting valve V4, allowing vapor to flow from HEX1 into HEX2. This process is known as the mass recovery process. Heating and cooling processes are continued during the mass recovery process. Since the concentration of refrigerant in HEX1 and HEX2 are near to the equilibrium level, then the next process call pre-cooling/pre-heating begin.

During pre-cooling/pre-heating process, HEX1 is heated by hot water, and HEX2 is cooled by cooling water to provide more cooling capacity. During this process, refrigerant circulation is stopped by closing all refrigerant valves.

When the pressures of HEX1 and HEX2 are nearly equal to the pressures of the condenser and the evaporator, the valve between HEX1 and the condenser (as well as the

valve between HEX2 and the evaporator) is opened, allowing refrigerant to flow. The adsorption and desorption process then begins. In this process, refrigerant from HEX1 is transferred to the condenser, and then it will condense by releasing heat to the heat sink.

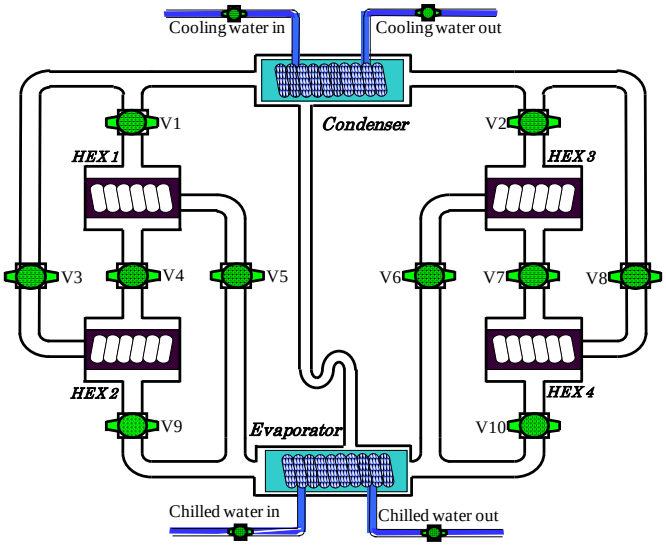

Figure 2.9: The Advanced Four-Hex Re-Heat Adsorption Cycle

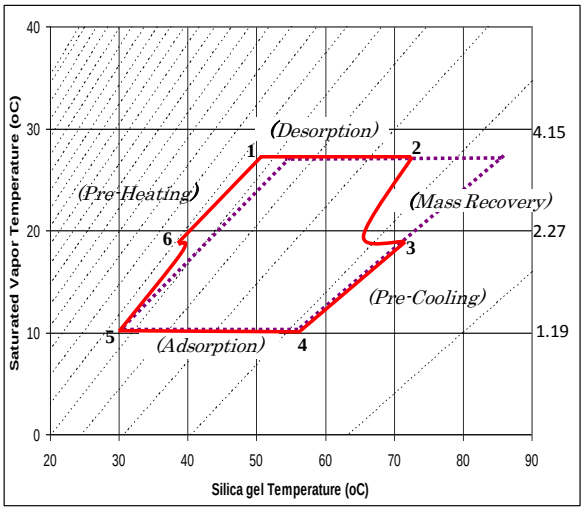

Figure 2.10: The P-T-X Diagram of Four-Hex Re-Heat Adsorption Cycle

Finally, the liquid refrigerant flows from the condenser to the evaporator through a u-shaped tube to control the pressure differential between the condenser and the evaporator. To complete one cycle, the next part of the process is the same as the first half-cycle, but HEX3 is the desorber and HEX1 is the adsorber. HEX2 and HEX4 also follow a process

similar to HEX 1 and HEX 3 in the full cycle

2.8.3. Advanced Three-Hex Re-Heat Combined Adsorption Cycle

2.8.3.1 Advanced Three-Bed Conventional Re-Heat Combined Cycle

The advanced three-bed conventional re-heat combined adsorption chiller schematic and the Pressure-Temperature-Concentration (PTX) diagram are present in Figure 2.11 and Figure 2.12, respectively. There are three HEXs namely HEX1, HEX2 and HEX3. To complete a full cycle, HEX1 and HEX2 consist of six processes while HEX3 only four processes respectively. The HEXs operates continuously all together in ten modes.

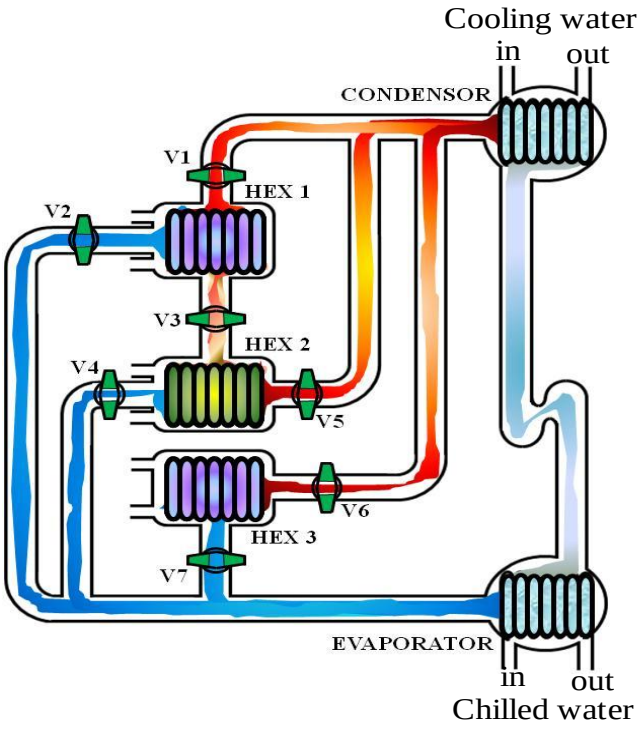

Figure 2.11: The Advanced Three-Hex Re-Heat Combined Adsorption Cycle

In the beginning of the process, the valves (V1, V4 and V6) are opened. HEX1 and HEX3 will connect to the condenser and the desorption process started, while HEX2 will connect to the evaporator and the adsorption process started as well. The desorption and the adsorption process take place at the condenser pressure (P_c) and the evaporator pressure (P_e) respectively, that is shown in PTX diagram. During the desorption process, HEX1 and HEX3 are heated up by hot water (Q_{des}) to the condenser temperature (T_{des}), provide by the driving heat source. The resulting refrigerant vapor is cooled down to the condenser temperature (T_c)

by the cooling water, which removes the heat (Q_c). During the adsorption process, refrigerant in evaporator is evaporated at evaporation temperature (T_e) and seized heat (Q_e) from the chilled water. The adsorber (HEX2) will absorb the evaporated vapor and the adsorption heat (Q_{ads}) is removed by the cooling water. Since the concentration of refrigerant in the desorber (HEX1) and adsorber (HEX2) are near to the equilibrium levels, the process continue to the next process.

In the next process, all HEXs out of connects to the condenser or evaporator. HEX1 was at the end position of desorption process and HEX2 was at the end position of adsorption process. HEX1 is connected with HEX2 through opened the valve (V3) with continuing cooling water in HEX2 and hot water in HEX1. The process called mass recovery with cooling for HEX2 and mass recovery with heating for HEX1. In this process, HEX3 is cooled down by cooling water called pre-cooling process. When the pressure of both HEX1 and HEX 2 nearly equals, then the process will continue to the next process.

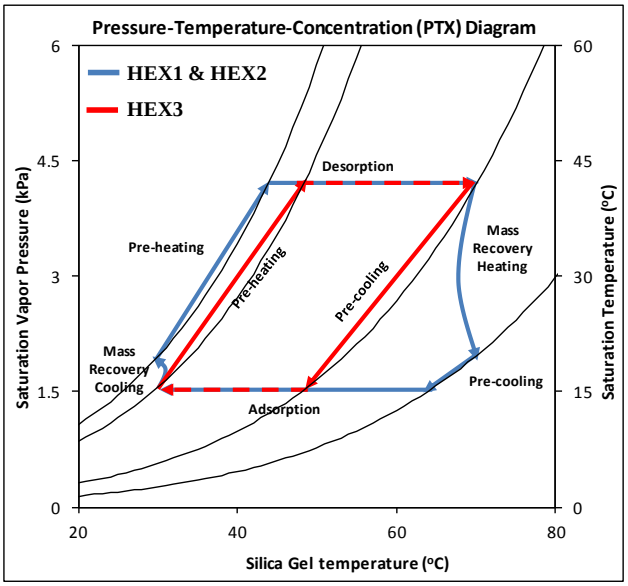

Figure 2.12: The P-T-X Diagram of Three -hex Re-heat Combined Adsorption Cycle.

In the next process, all HEXs are in warm up process. HEX1 and HEX3 are cooled down by cooling water, called pre-cooling process, and HEX2 is heated up by hot water, called pre-heating process. When the pressure of HEX1 and HEX3 nearly equal to the pressure of evaporator; and the pressure of HEX2 nearly equal to the pressure of condenser, then the valve (V2, V5and V7) are opened to flow the refrigerant. HEX1 and HEX3 are connected with evaporator and HEX 2 is connected with condenser respectively.

2.8.3.2 Advanced Three-Bed Three-Stage Re-Heat Combined Cycle

A schematic of the three-bed three-stage adsorption cycle and its behavior are presented in Figure 2.13 in the Dühring diagram, and the mode strategy of the proposed cycle is shown in Figure 2.14. The cycle consists of three adsorber/desorber beds, one condenser, and one evaporator. It is assumed that silica-gel A type is used in the cycle simulation of this study. The Dühring diagram reflects the adsorption isotherm, but the hysteresis of adsorption/desorption is neglected in the simulations, which may give rise to a factor of uncertainty. To complete a full cycle, the system operates continuously throughout eight modes.

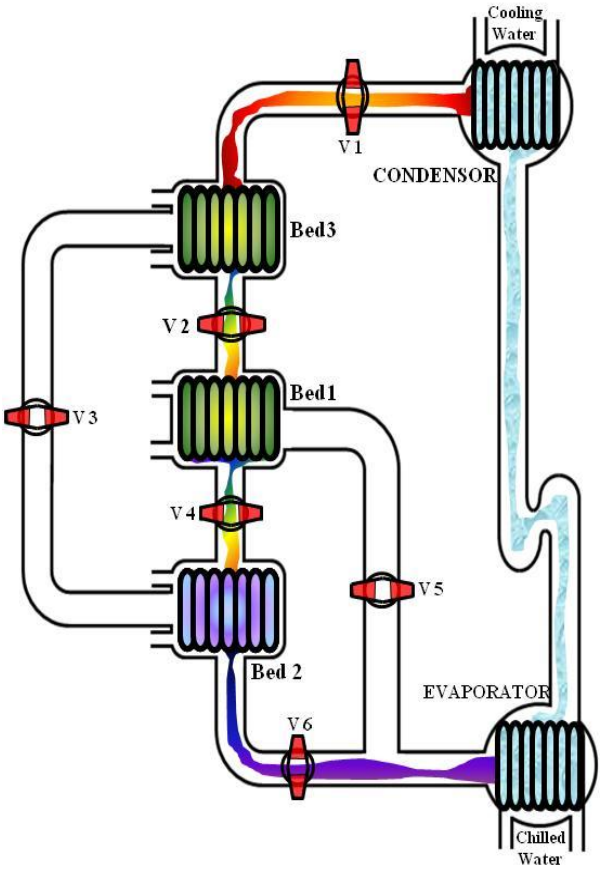

Figure 2.13: The Advanced Three-Hex Three Stage Re-Heat Combined Adsorption Cycle

At the beginning of the process (mode A), valves V2 and V6 are opened. Bed1 connects to bed3, and vapor is transferred into bed3, which is recognized as the adsorption process for bed3 and the desorption process for bed1. In this mode, bed2 connects to the evaporator, and the adsorption process begins. The desorption and adsorption processes take place at the condenser pressure (Pc) and the evaporator pressure (Pe), as shown in the Dühring diagram. During the desorption process, bed1 is heated by hot water (Qdes) to the

heat source temperature (Tdes). The refrigerant vapor is cooled to the condenser temperature (Tc) by the cooling water, which removes the condensation heat (Qc). During the adsorption process, refrigerant in the evaporator is evaporated using the evaporation temperature (Te) and seized heat (Qe) from the chilled water. The adsorbers of bed2 and bed3 absorb the evaporated vapor. Then, the adsorption heat (Qads) is removed by the cooling water. When the concentration of refrigerant in all of the adsorber/desorber beds is near the equilibrium level, the process continues into mode B.

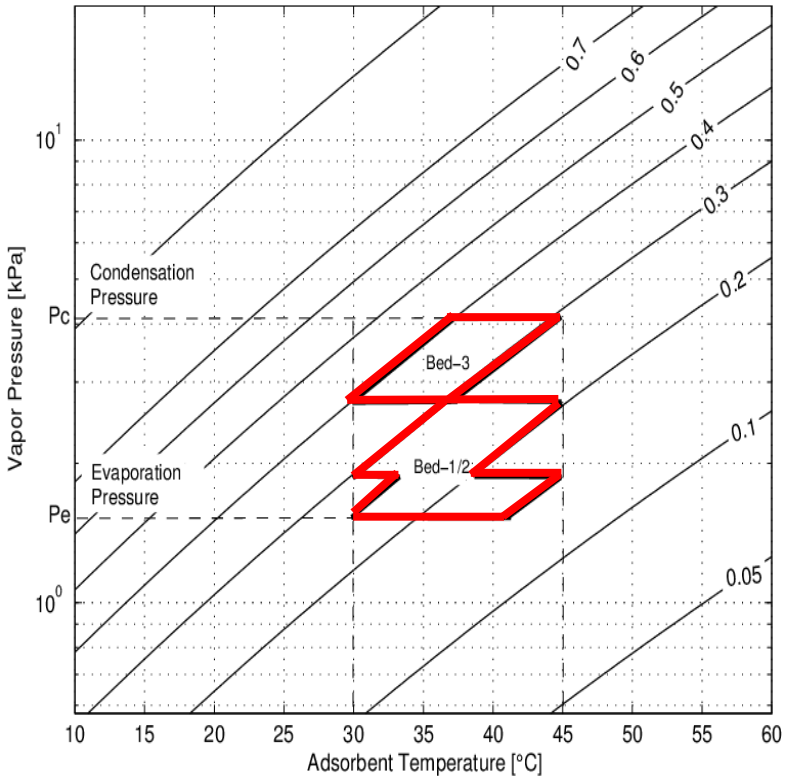

Figure 2.14: The P-T-X Diagram of Three-Bed Three-Stage Re-heat Combined Adsorption Cycle.

In mode B, all beds are un-connected to the condenser or evaporator. Bed1 is positioned at the end position of desorption process and the other beds (bed2 and bed3) at the end position of the adsorption process. Bed1 is connected with bed2 through valve V4 with continuous cooling water in bed2 and hot water in bed1. The bed2 cooling process is referred to as mass recovery cooling, and the heating process of bed1 is known as mass recovery heating. During these processes, vapor is transferred from bed1 to bed2. If the pressure of both bed1 and bed2 are nearly equal, then the process continues to mode D. In mode B, bed3

is heated by hot water in the pre-heating process. If the pressure of bed3 is nearly equal to the condenser pressure, then the process continues to mode C in which valve V1 is opened, and the desorption process for bed3 begins.

In mode D, all beds are included in the pre-heating or pre-cooling process. Bed1 and bed3 are cooled by cooling water in pre-cooling process, and bed2 is heated by hot water in pre-heating process. If the pressures of bed1 and bed3 are nearly equal to the pressure of evaporator, and the pressure of bed2 is nearly equal to the pressure of the condenser, then valves V3 and V5 are opened to refrigerant flow. Bed2 and bed3 are now connected, and bed1 is connected with the evaporator.

Mode D occurs at the end of the half cycle of the process. To complete a full cycle, the next process is the same as the previous half-cycle referred to in the mode operational strategy of Table 6.4.

In this cycle, the pressure rise from the evaporator level to the condenser level is split into three progressive smaller pressure rises, as seen in Figure 2.14. Bed1 and bed2 pressurize the vapor from the evaporation level to the intermediate level. Next, bed3 pressurizes the vapor from the intermediate level to the condensation level.

In mode B, all beds are un-connected to the condenser or evaporator. Bed1 is positioned at the end position of desorption process and the other beds (bed2 and bed3) at the end position of the adsorption process. Bed1 is connected with bed2 through valve V4 with continuous cooling water in

CHAPTER 3

MATERIAL AND METHODS

3.1. EXPERIMENTAL SETUP MACHINE

The experimental setup of the re-heat adsorption cycle, which has been installed in the laboratory of the Tokyo University of Agriculture and Technology, is shown in Figure 3.1. and the schematic of the chiller shown in Figure 3.2, respectively.

The experimental setup is designed to test various operating modes of the adsorption cycle. The chiller has six adsorption/desorption heat exchangers (HEXs), two condensers and two evaporators. Though the chiller has six HEXs, only four HEXs (i.e., HEX1, HEX2, HEX5 and HEX6) were used in this experiment, and the other two HEXs (i.e., HEX3 and HEX4) were not used. The chiller also has three types of reservoir tanks that have been installed outside the room, namely a hot water tank, a cooling water tank and a chilled water tank. Silica gel type A, which consists of spherical particles 2-20 nm in size, and water are used as the adsorbent/refrigerant pair in this chiller.

3.1.1 Instrument and Test Procedure

Three kinds of measurements are used in the experiment. They are temperature, pressure, and mass flow rate. Bed concentration cannot be measured directly, so it is approached by using temperature and bed pressure calculations. In beds, thermocouple sensors are used to measure temperature of beds, vapor refrigerant, and inlet-outlet water temperature of beds. In condensers and evaporators, thermocouple sensors are used to measure temperature, inlet-outlet of water cooling condensers, and chilled water inlet-outlet.

Pressure sensors are used to measure the pressures of bed, condenser, and evaporator. Electro magnetic flow meters are used to measure the flow rate of cooling water and heating water, the flow rate of cooling water into condenser, and the flow rate of chilled water into evaporator.

All sensors are connected to data logger. The data are collected in every second. A computer is used to save measurement data. The position of measurement point as marked in Figure 3.3.

During one cycle, a bed will go through half-cycle of heating process and half-cycle of cooling process. Heating process cycle consists of pre-heating, desorption process, and

mass recovery process with heating. Cooling process consists of pre-cooling, adsorption process, and mass recovery process with cooling. Chiller modes have been changes automatically by opening and closing the GV and AV valves which are set in control panel as can be shown in Table 3.5 shows operational valves for each mode.

3.1.2 Parameter Settings

Table 3.1 presented the experimental parameter which is applied during the experiment and standard operating condition can be shown in Table 3.2.

Table 3.1 Experimental conditions

Parameter		Value	Unit
Hot water	Temp	60,65,70,75	^{o}C
	Flow	1.7	kg/s
Cooling water in	Temp	30	^{o}C
	Flow	3	kg/s
Chilled water in	Temp	14	^{o}C
	Flow	0.7	kg/s
Chilled water out	Temp	9	^{o}C
	Flow	0.25-0.45	kg/s
Cycle time	RS	(200+30+420)x2=1300 mr ph/pc ad/des	s
	RL	(600+30+970)x2=3200 mr ph/pc ad/des	s
	S	(30+420)x2=900 ph/pc ad/des	s

Note:
mr= mass recovery
ph/pc= preheating/precooling
ad/des= adsorption/desorption
RS= reheat short cycle
RL= reheat long cycle
S=single stage

Table 3.2 Standard operating condition

Hot Water in		Cooling water in			Chilled water in	
Temp (oC)	Flow (Kg/s	Temp (oC)	Flow (Kg/s)		Temp (oC)	Flow (Kg/s
			Ads	Cond		
70	1.2	30	1	0.778	14	0.2

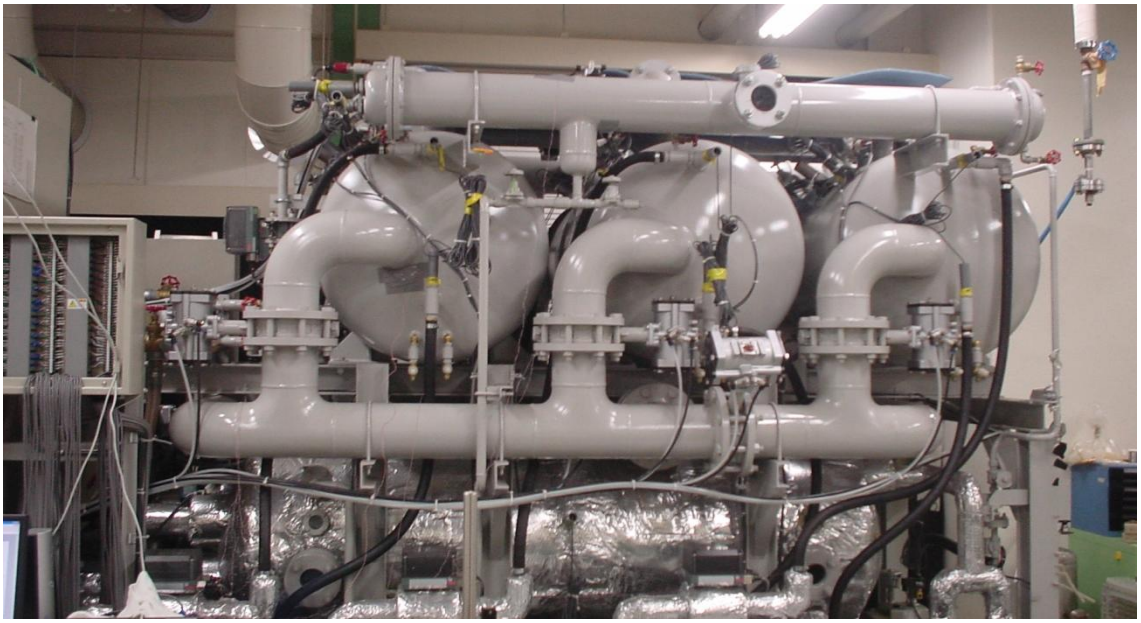

(a) Front view

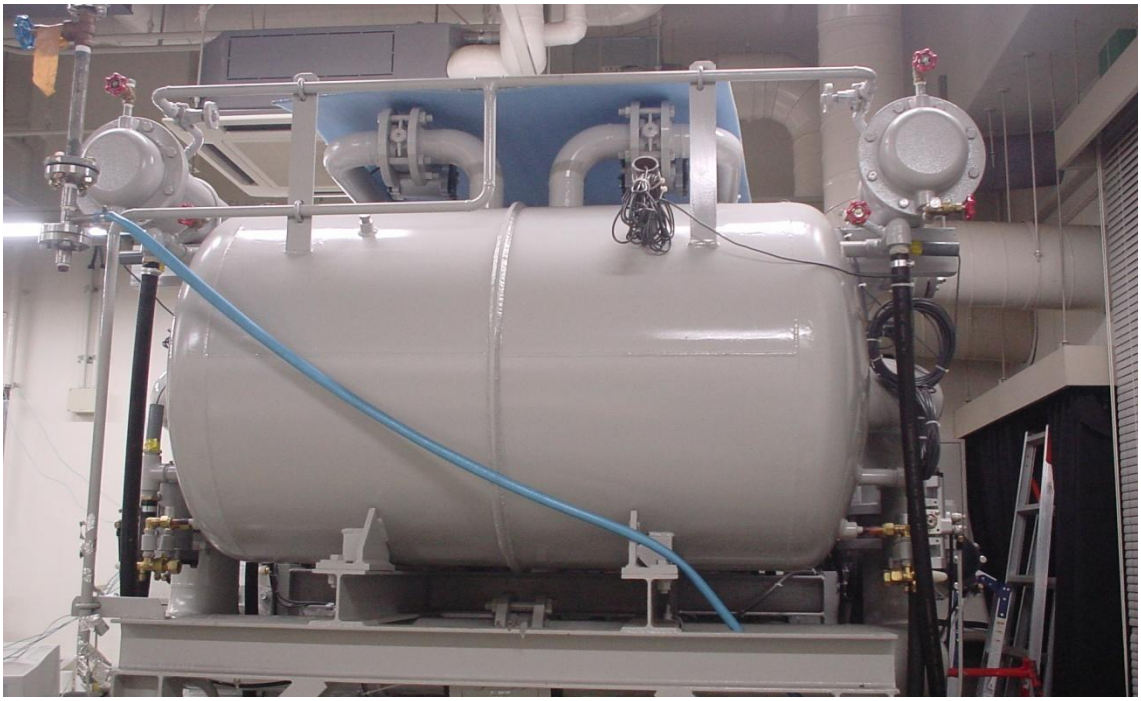

(b) Side view

Figure 3.1 Six-Bed Adsorption Chiller Experimental Machine

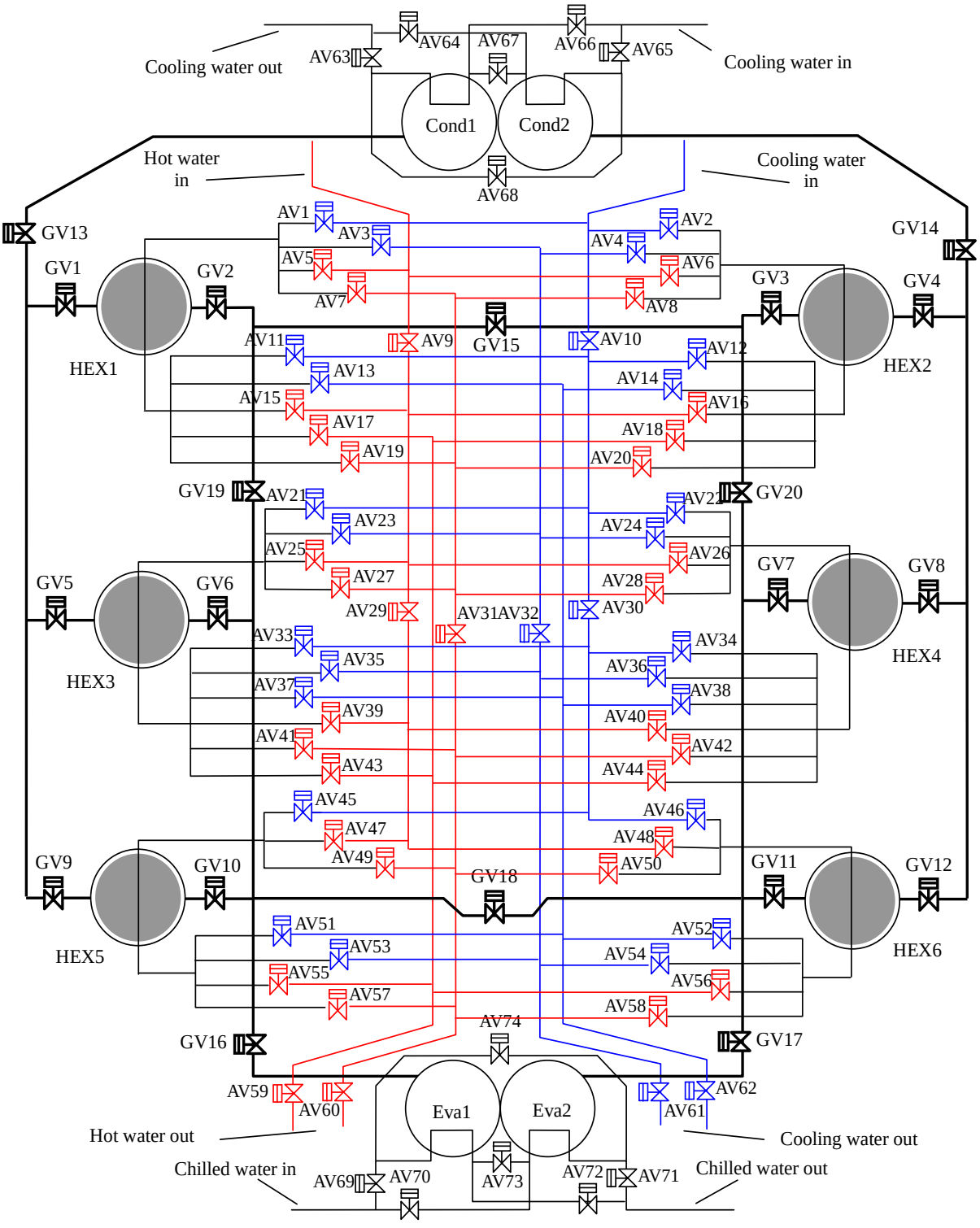

Figure 3.2 Schematic of Six-Bed Adsorption Chiller

GV is the valves which are connecting bed with condenser, evaporator, or other bed. This valve controls the refrigerant flow.

AV is the valves which are control heating or cooling water flows into bed.

Table 3.3 Experimental Chiller Specifications

Items		**Note**
Adsorbent	Silica Gel	Type A
Refrigerant	Water	
Beds (Adsorber-Desorber)	6	Plate Fin Type
Evaporator	2	Shell-Tube Type
Condenser	2	Shell-Tube Type

Table 3.4 Adsorber, Condenser, and Evaporator Specifications

	Adsorber	**Desorber**	**Evaporator**	**Condenser**
Heat Transfer Cooefficient	2001 $Wm^{-2}K^{-1}$	2233 $Wm^{-2}K^{-1}$	2360.7 $Wm^{-2}K^{-1}$	4061.8 $Wm^{-2}K^{-1}$
Heat Capacity	1260 $JK-^{1}$/kg.adsorbent	1260 $JK-^{1}$/kg.adsorbent	260000 JK^{-1}	109000 JK^{-1}
Silica Gel Diameter	355-1000 X 10-6 m (0.35-1.0 mm)			
Silica Gel Mass	16 kg/bed (total : 16 X 6= 96 kg)			

Table 3.5 Operational Valves

GV	Mode									
	A	**B**	**C**	**D**	**E**	**F**	**G**	**H**	**I**	**J**
1	O	O	O	O	X	X	X	X	O	X
2	X	X	X	X	X	O	O	O	X	X
3	X	X	O	O	O	X	X	X	X	X
4	O	X	X	X	X	O	X	O	O	O
5	X	X	X	X	X	X	X	X	X	X
6	X	X	X	X	X	X	X	X	X	X
7	X	X	X	X	X	X	X	X	X	X
8	X	X	X	X	X	X	X	X	X	X
9	X	X	X	O	X	O	O	O	O	
10	O	O	O	O	X	X	X	X	X	X
11	X	X	X	X	X	X	X	O	O	O
12	O	X	O	X	O	O	X	X	X	X
13	O	O	O	X	X	O	O	O	X	X
14	X	X	O	X	O	X	X	O	O	O
15	X	X	X	X	X	X	X	X	X	X
16	O	O	O	X	X	O	O	O	X	X
17	X	X	O	O	O	X	X	O	O	O
18	X	X	X	X	X	X	X	X	X	X
19	X	X	X	X	X	O	O	O	X	X
20	X	X	O	O	O	X	X	X	X	X

O : Valve opened
X : Valve closed

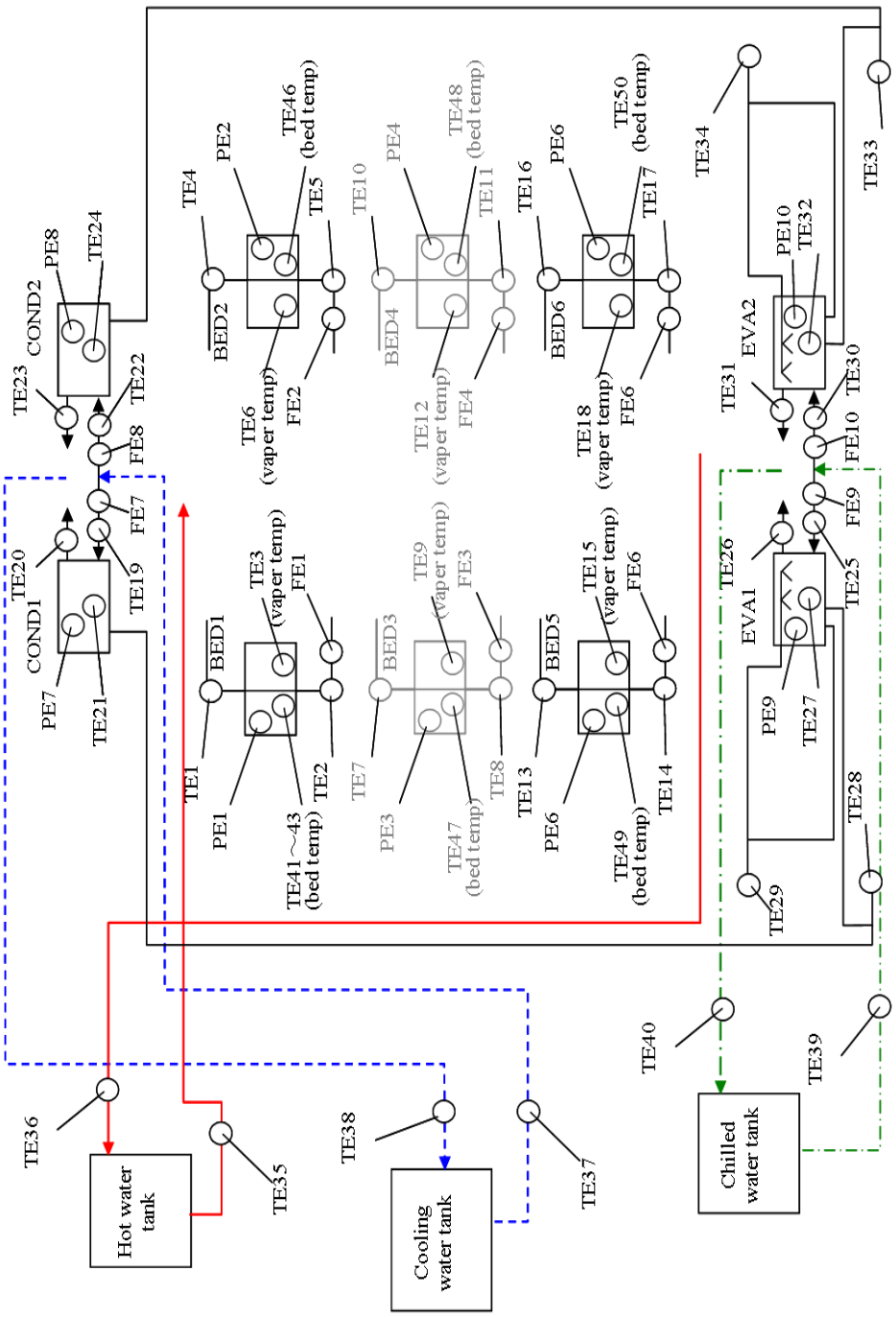

Figure 3.3 Measurement Point on Six-Bed Chiller

3.2. MATHEMATICAL MODELING

3.2.1. Heat Transfer and Energy Balance of Adsorber/Desorber Hex

The heat transfer equation of adsorbent bed can be described as follows:

$$T_o = T + \left(T_i - T\right) \exp\left(\frac{U_{bed} A_{bed}}{\dot{m}_w . C_w}\right) \tag{3.1}$$

Here, T denotes bed temperature. The adsorbent bed temperature, pressure and concentration are assumed to be uniform throughout the adsorbent bed. We have taken the specific heat of refrigerant (water) in liquid phase as our system works in the low concentration range. Heat transfer fluid (water) temperature term T_i and T_o denote cooling water upon adsorption and hot water upon desorption.

The energy balance equation of adsorbent bed is shown below:

$$(W_s.C_s + W_s.C_w.q + W_{bed}.C_{bed})\frac{dT}{dt} = W_s.Q_s\frac{dq}{dt} - W_s.C_v.\delta[\gamma(T - T_{eva})(T - T_{wv})]\frac{dq}{dt}$$

$$+ \dot{m}_w.C_w.\varepsilon_{bed}\left(T_i - T\right) \tag{3.2}$$

where δ is either 0 or 1 depending whether the adsorbent bed is working as desorber or adsorber and γ is either 1 or 0 depending on whether the bed is connected with evaporator or another bed. Eq. (1) expresses the importance of heat transfer parameters, namely heat transfer area A_{bed} and overall heat transfer coefficient U_{bed}. The left-hand side of the adsorber/desorber energy balance equations (Eq. (3.2)) provides the amount of sensible heat required to cool or heat the silica-gel (s), water (w) as well as metallic (bed) parts of the heat exchanger during adsorption or desorption. This term accounts for the input/output of sensible heat required by the batched-cycle operation. First term on the right-hand side of Eq. (3.2) constitutes the release of adsorption heat or the input of desorption heat, while the second terms for the sensible heat of the adsorbed vapor. The last term on the right-hand side of Eq. (3.2) refers the total amount of heat released into the cooling water upon adsorption or provided by the hot water for desorption. Eq. (3.2) does not account for external heat losses into the environment as all the beds are considered to be well insulated. ε_{bed} in Eq. (3.2) expresses the heat exchanger effectiveness that came from log mean temperature difference of heat exchanger (bed) in the flow system.

3.2.2 Heat Transfer and Energy Balance of Condensor

Equation (3.3) represents as the heat transfer of the condenser while equation (3.4) as energy balances for condenser, and can be expressed as:

$$T_{con,o} = T_{con} + \left(T_{cw,i} - T_{con}\right) \exp\left(\frac{U_{con}A_{con}}{\dot{m}_w.C_w}\right) \tag{3.3}$$

$$\left(W_{con,w}.C_w + W_{con,bed}.C_{con,bed}\right)\frac{dT_c}{dt} = \dot{m}_{cw}.C_w.\varepsilon_{con}\left(T_{cw,i} - T_{cw,o}\right)$$

$$- W_s.\left(\frac{dq_{des}}{dt}\right)\left(L + C_v(T_{des} - T_{con})\right) \tag{3.4}$$

The first term on the right-hand side of Eq. 3.(4) gives the amount of heat released into the cooling water, the second-term accounts for the latent heat of vaporization (L) for the amount of refrigerants desorbed (dq_{des}/dt) and the amount of heat that the liquid condensates carries away when it leaves the condenser to the evaporator. ε_{con} in Eq. (3.4) expresses the heat exchanger effectiveness that came from log mean temperature difference of heat exchanger (condenser) in the flow system. The left-hand side of Eq. (3.4) represents the sensible heat required by the metallic parts of heat exchanger tubes due to the temperature variations in the condenser.

3.2.3 Heat Transfer and Energy Balance of Evaporator

Equation (3.5) represents the heat transfer of evaporator and equation (3.6) as energy balances for evaporator, respectively:

$$T_{chill,o} = T_{eva} + \left(T_{chill,i} - T_{eva}\right) \exp\left(\frac{U_{eva}A_{eva}}{\dot{m}_{ch}.C_{ch}}\right) \tag{3.5}$$

$$\left(W_{eva,w}.C_w + W_{eva,bed}.C_{eva,bed}\right)\frac{dT_e}{dt} = \dot{m}_{chill}.C_{chill}.\varepsilon_{eva}\left(T_{chill,i} - T_{chill,o}\right)$$

$$- W_s.\left(\frac{dq_{ads}}{dt} + \frac{dq_{des}}{dt}\right)\left(L + C_v(T_{con} - T_{eva})\right) \tag{3.6}$$

The first term on the right-hand side of Eq. (3.6) represents the total amount of heat from chilled water, the second-term accounts for the latent heat of vaporization (L) for the amount of refrigerants adsorbed (dq_{ads}/dt) and the sensible heat required to cool down the

incoming condensate from the condensation temperature T_{con} to evaporation temperature T_{eva}. ε_{eva} in Eq. (3.6) expresses the heat exchanger effectiveness that came from log mean temperature difference of heat exchanger (evaporator) in the flow system. The left-hand side of Eq. (3.6) represents the sensible heat requirement by the liquid refrigerant and the metal of heat exchanger tubes in the evaporator.

3.2.4 Total Mass Balance

The total mass balance of refrigerant (water) can be expressed as:

$$dW_{eva,w} = -W\left(\frac{dq_{ads\text{-}eva}}{dt} + \frac{dq_{des\text{-}con}}{dt}\right) \tag{3.7}$$

where subscript des-con and ads-eva refer to the vapor flow from desorber to condenser and from evaporator to adsorber.

3.2.5 Adsorption Rate

The combination of silica-gel adsorption rate was modeled by Sakoda and Suzuki [27] as a function of temperature:

$$\frac{dq}{dt} = k_s a_p.\left(q^* - q\right) \tag{3.8}$$

The overall mass transfer coefficient, $k_s a_p$, was estimated by Eq.(9) and (10).

$$k_s a_p = \frac{15D}{R_p 2} \tag{3.9}$$

$$D = D_0 \exp\left(-E_a/RT\right) \tag{3.10}$$

where D refers the surface diffusivity. D_0 is a constant, and is given as 25.4 x 10^{-4} m^2/s. E_a expressed the activation energy of surface diffusion, and is given as 4.20 x 10^4 J/mol. R is the universal gas constant and equals 8.314 J/mol K.

The amount adsorbed in equilibrium, q^*, is predicted by equation as follows:

$$q^{*} = \frac{0.8\,x\left[P_S(T_W)/P_S(T_S)\right]}{1+0.5\,x\left[P_S(T_W)/P_S(T_S)\right]} \tag{3.11}$$

where $P_s(T_w)$ and $P_s(T_s)$ are the saturation vapor pressure at temperature T_w (water vapor) and T_s (silica gel), respectively. The saturation vapor pressure and temperature are correlated by Antoine's equation, as bellows:

$$P_S = 133.32\,x\exp\left(18.3-\frac{3820}{T-46.1}\right) \tag{3.12}$$

3.2.6 System Performance

Coefficient of performance (COP) and cooling capacity (CC) are mainly characteristics on the performance of the re-heat adsorption cycle, can be measured as:

$$COP = \dot{m}_{ch}.C_w \int_0^{t_{cycle}} \left(T_{ch,i}-T_{ch,o}\right)dt \Big/ \dot{m}_h.C_w \int_0^{t_{cycle}} \left(T_{h,i}-T_{h,o}\right)dt \tag{3.13}$$

$$CC = \dot{m}_{ch}.C_w \int_0^{t_{cycle}} \left(T_{ch,i}-T_{ch,o}\right) dt \Big/ t_{cycle} \tag{3.14}$$

$$SCP = \dot{m}_{ch} C_w \int_0^{t_{cycle}} \left(T_{ch,i}-T_{ch,o}\right) \;/\; t_{cycle} W_{s,total} \tag{3.15}$$

3.3. OPTIMIZATION METHOD

A cyclic simulation using MATLAB software with ode-45 solver was developed to solve the performance of the re-heat cycle based upon the equation (1)-(14) and the Particle Swarm Optimization (PSO) is applied to optimized the cycle time components (i.e. adsorption/desorption time, pre-heating/pre-cooling time and mass recovery time). In the PSO, cycle time components were chosen as the variable and COP and cooling capacity as the objective function, respectively. The number of particles 20 and the number of iteration 1000 were considered during running the PSO, and that all of the particles reached their best position before the end of the iterations. The operation mode of the cycle refers to the Table 1 during running the simulation. All input parameters and standard operating condition are given in Table 2 and Table 3 respectively.

3.3.1 Optimization of Adsorption System

Role of optimization is to find values of the variables that minimize or maximize the objective function while satisfying the constraints. In this dissertation the objective function is chosen as COP and Cooling Capacity, variables were cycle time components and chilled water flow rate and fixed chilled water outlet temperature.

It can be precise as

Objective: To maximize the objective function

Objective function: COP and Cooling Capacity

Variables: Cycle time components such as adsorption/desorption, pre-cooling/pre-heating and mass recovery time

Boundary Conditions: Chilled water outlet temperature

Input parameters: Hot and cooling water inlet temperature, chilled water inlet temperature, adsorbent mass etc. Parameters values are shown details in Table 4.3, Table 5.2 and Table 6.3).

There are some methods of optimization among them particle swarm optimization (PSO) method is applied for optimizing of cycle time to maximize COP and Cooling Capacity of adsorption system. PSO in detail given below;

3.3.2 Particle swarm optimization (PSO) methodology

Particle swarm optimization (PSO) is a stochastic population based optimization technique that was first introduced by James Kennedy (a Social Psychologist) and Russel Eberhart (an Electrical Engineer) in 1995 [60], inspired by social behavior and movement of birds and fishes. It is an evolutionary computational technique based on the movement and intelligence of swarms looking for the most fertile feeding location and it is globally acceptable methods for optimization.

Swarm is an apparently disorganized collection (population) of moving individuals that tend to cluster together while each individual seems to be moving in a random direction. Swarm picture of birds and fish are shown in Figure 3.3.

PSO applicable to optimize the nonlinear function based on swarm of particles (e.g., birds and fishes). The particle swarm consists of 'n' particles. These particles are moved around in the search space according to formulae. The dimension or number of variables are indicated by z.

The particles of the swarm is represented by $x_{z1}, x_{z2}, x_{z3} \ldots\ldots x_{zn}$ and the best particle of

the swarm, i.e. the particle with the maximum function value, is denoted by index g. The best previous position (i.e. the position giving the maximum function value) of the i-th particle is recorded and represented as $p_{z1}, p_{z2}, p_{z3}.....p_{zn}$ and the position change (velocity) of the particles are represented as $v_{z1}, v_{z2}, v_{z3}.....v_{zn}$.

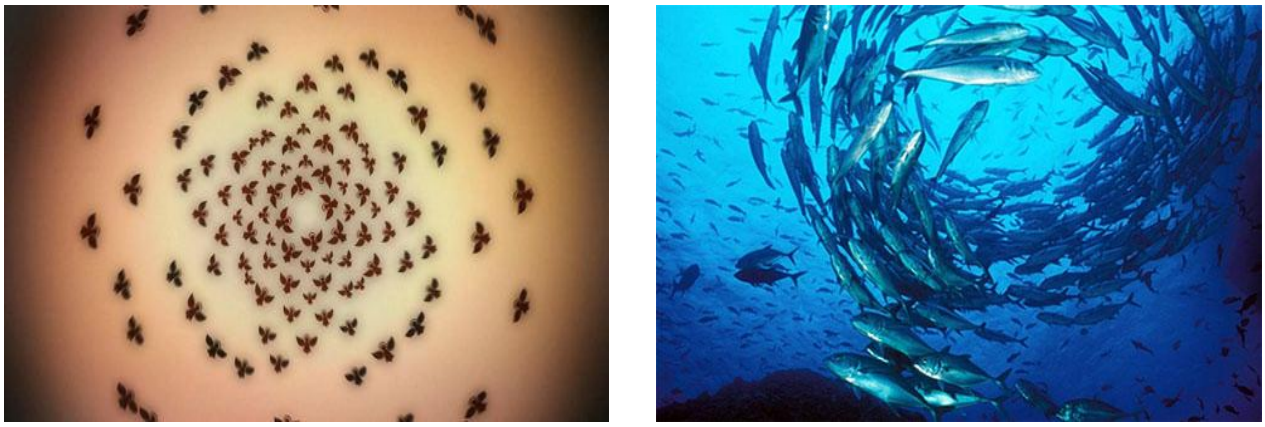

(a) (b)

Figure 3.4: Swarm of (a) birds and (b) fishes.

The formula to update a particle's velocity and position can be written as

$$v_{zi}^{k+1} = \omega \cdot v_{zi}^{k} + C_1 \cdot r_1 \cdot (p_{zi}^{k} - x_{zi}^{k}) + C_2 \cdot r_2 \cdot (p_{zg}^{k} - x_{zi}^{k}) \quad (3.15)$$

$$x_{zi}^{k+1} = x_{zi}^{k} + v_{zi}^{k+1} \quad (3.16)$$

where x_i and v_i are the position and velocity of the ith particle. p_i is the personal best position that the ith particle had reached and p_{zg}, is the group best position that all the particles had reached. k represents the number of iteration. ω is the inertia weight; r_1 and r_2 are two random numbers either 0 or 1 and C_1 and C_2 are two positive constant, called the cognitive and social parameter, respectively.

The equation 3.15 is used to calculate at each iteration, the i-th particle's new velocity. Three terms are taken into consideration. The first term, ωv_{zi}^{k} is the particle's previous velocity weighted by the inertia weight ω w. The second term, $(p_{zi}^{k} - x_{zi}^{k})$, is the distance between the particle's best previous position and its current position. Finally, the third term, $(p_{zg}^{k} - x_{zi}^{k})$, is the distance between the swarm's best experience and the i-th particle's current position.

Equation 3.16 provides the new position of the i-th particle, adding its new velocity, to its current position. The particles change its condition according to the following three principles: (1) to keep its inertia (2) to change the condition according to its most optimist position (3) to change the condition according to the swarm's most optimist position. The positions of the particles are guided by their own best known position (i.e., personal best or pbest) as well as the entire swarm's best known position (i.e., group best or gbest). When better positions are being discovered these will then come to guide the movements of the swarm.

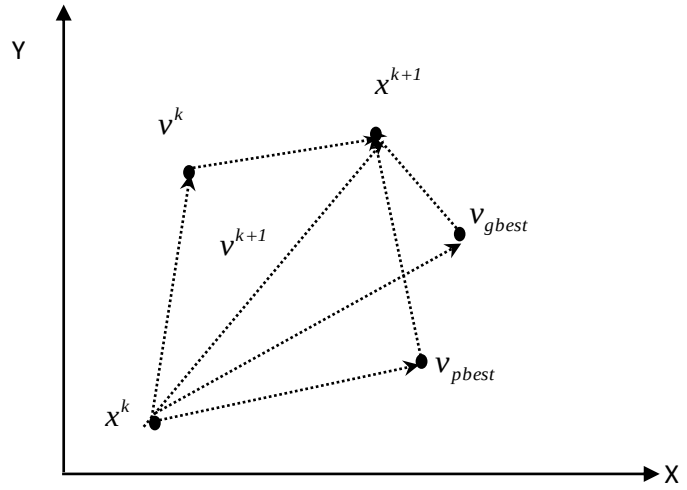

Figure 3.5: Concept of modification of a searching position by PSO.

The modification of search particle position and velocity graphically shown in Figure 3.5. In general, the performance of each particle is measured according to a fitness function, which is problem dependent. In optimization problems, the fitness function is usually the objective function under consideration. More descriptions of PSO technique are given in Figure 3.6(a). Optimization of cycle time components to maximize the COP and Cooling capacity based on PSO is shown in the Figure 3.6(b).

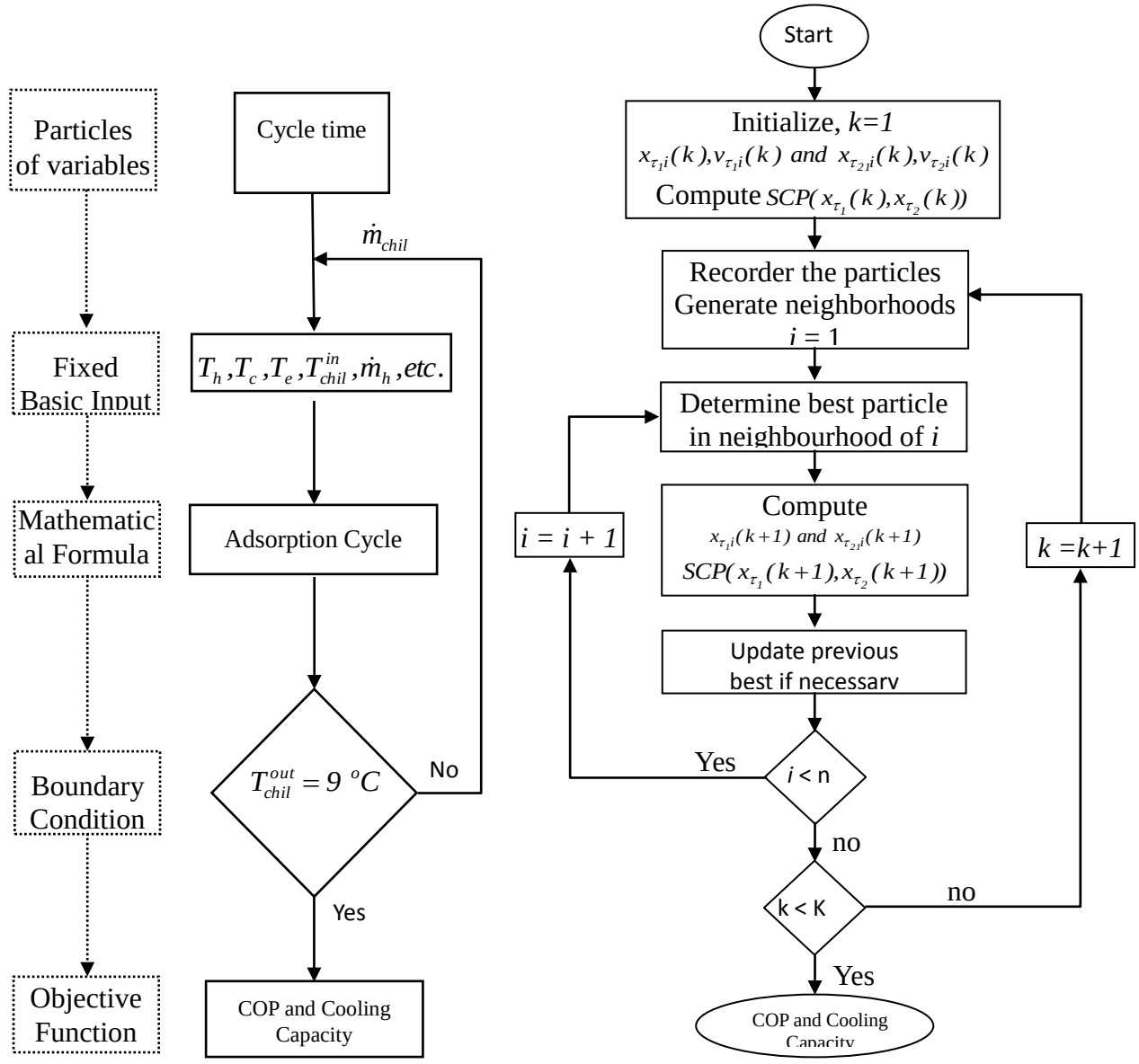

(a) (b)

Figure 3.6: Flow chart of (a) COP and cooling capacity simulation and (b) optimization of cycle time based on PSO.

CHAPTER 4

EXPERIMENTAL INVESTIGATION OF A RE-HEATING ADSORPTION CYCLE APPLYING FIXED CHILLED WATER OUTLET CONDITIONS

In this chapter, an experimental investigation of a re-heating adsorption cycle was conducted, and the working principle of the cycle was also introduced. The coefficient of performance and the cooling capacity were calculated to analyze the performance of the chiller. The objective was to identify the effect of the heat source temperature, the effect of cycle time on performance, the effect of mass recovery time on performance and predicts the optimum global value if the chilled water outlet temperature is fixed at 9°C during the experiment.

4.1. WORKING PRINCIPLE OF RE-HEATING ADSORPTION CYCLE

Figure 4.1(a) shows a re-heat adsorption cycle schematic diagram, while Figure 4.1(b) shows the P-T-X diagram for standard conditions. The chiller consists of four heat exchangers (i.e., HEX1, HEX2, HEX3 and HEX4), two evaporators and two condensers. The adsorbent heat exchangers of the chiller are operated through six thermodynamic processes in a full cycle, namely adsorption (1-2), mass recovery with cooling (2-3), pre-heating (3-4), desorption (4-5), mass recovery with heating (5-6) and pre-cooling (6-1). In the adsorption process, refrigerant (water) is evaporated in the evaporator and the temperature (T_{eva}) and heat (Q_{eva}) are seized isobarically from the chilled water. An evaporation process occurs and produces a cooling effect. Heat for the evaporation of the water is supplied by flowing chilled water at a low heat source temperature. In the first half cycle, HEX1 is heated by hot water and HEX3 is cooled by cooling water. When the pressures of HEX1 and HEX3 are nearly equal, both are then connected by opening the connecting valve, allowing vapor to flow from HEX1 into HEX3. This process is known as the mass recovery process.

Heating and cooling processes are continued during the mass recovery process. HEX1 is heated by hot water, and HEX3 is cooled by cooling water to provide more cooling capacity. During this process, refrigerant circulation is stopped by closing all refrigerant valves. This process is known as the pre-heating/pre-cooling process.

When the pressures of HEX1 and HEX3 are nearly equal to the pressures of the condenser and the evaporator, the valve between HEX1 and the condenser (as well as the valve between HEX3 and the evaporator) is opened, allowing refrigerant to flow. The adsorption and desorption process then begins. In this process, refrigerant from HEX1 is transferred to the condenser, and then it will condense by releasing heat to the heat sink.

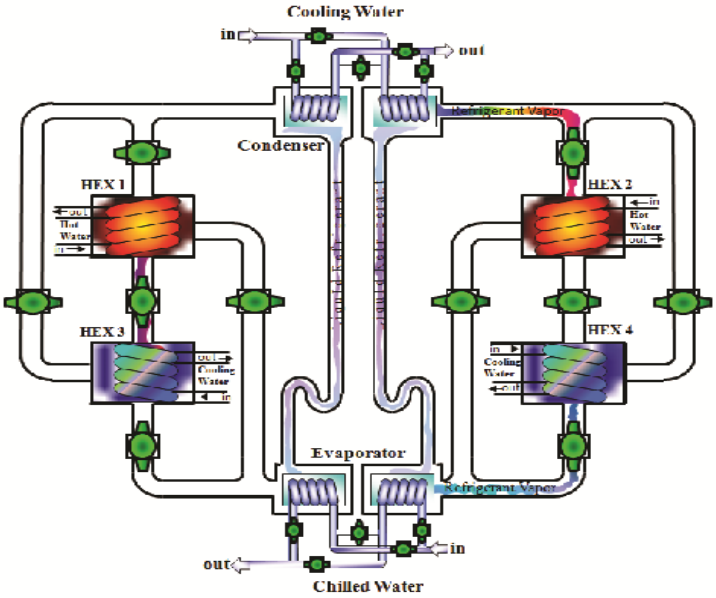

(a)

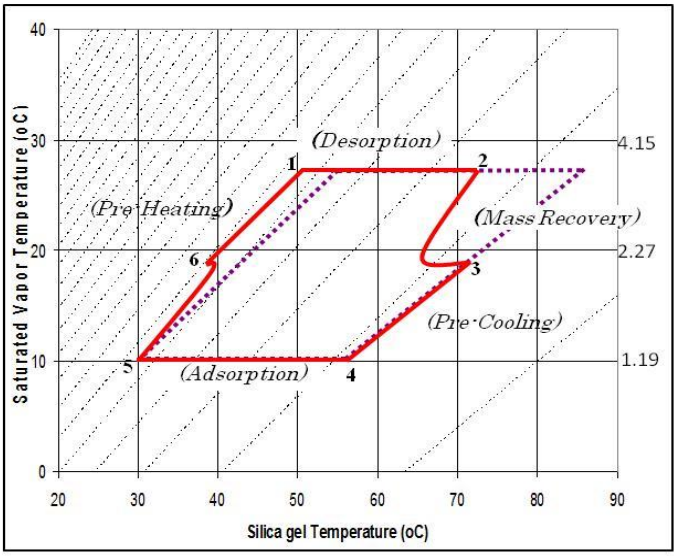

(b)

Figure 4.1: (a) Re-heat two-stage adsorption chiller scheme (b) P-T-X Diagram

Finally, the liquid refrigerant flows from the condenser to the evaporator through a u-shaped tube to control the pressure differential between the condenser and the evaporator. To

complete one cycle, the next part of the process is the same as the first half-cycle, but HEX3 is the desorber and HEX1 is the adsorber. HEX2 and HEX4 also follow a process similar to HEX 1 and HEX 3 in the full cycle

4.2. EXPERIMENTAL PROCEDURE FOR THE RE-HEAT ADSORPTION CYCLE

4.2.1 Experimental apparatus

The experimental setup of the re-heat adsorption cycle, which has been installed in the laboratory of the Tokyo University of Agriculture and Technology, is shown in Figure 3.1.

The experimental setup is designed to test various operating modes of the adsorption cycle. The chiller has six adsorption/desorption heat exchangers (HEXs), two condensers and two evaporators. Though the chiller has six HEXs, only four HEXs (i.e., HEX1, HEX2, HEX5 and HEX6) were used in this experiment, and the other two HEXs (i.e., HEX3 and HEX4) were not used. The chiller also has three types of reservoir tanks that have been installed outside the room, namely a hot water tank, a cooling water tank and a chilled water tank. Silica gel type A, which consists of spherical particles 2-20 nm in size, and water are used as the adsorbent/refrigerant pair in this chiller.

Table 4.1 shows the chiller operating strategy to complete one full cycle of the reheating two-stage chiller. The cycle consists of ten operational modes (A-J). There are two pairs of HEXs: one pair is HEX1 and HEX 5, and the other pair is HEX 2 and HEX6. The mass recovery process occurs between each pair. In the first half-cycle, when one pair of HEXs (1 and 5) is in the desorption-adsorption process (mode A to C), at the same time, another pair of HEXs (2 and 6) is completing the mass recovery process (mode A) and the pre-heating/pre-cooling process (mode B). After one HEX pair (2 and 6) has gone into the adsorption-desorption process (mode C to F), at the same time, the other HEX pair (1 and 5) is completing the mass recovery process (mode D) and the pre-cooling/pre-heating process (mode E). In the second half-cycle (i.e., mode F to mode J), HEX pair (1 and 5) acts the same as HEX pair (2 and 6) and vice versa. In mode C and mode H, there are two HEX pairs undertaking the adsorption-desorption process simultaneously.

4.2.2 Instrument and Test Procedures

Three types of measurements were performed in the experiment: temperature, pressure and mass flow rate. In HEXs, thermocouple sensors are used to measure the temperature of the HEXs, refrigerant vapor and inlet-outlet water temperature.

Similarly, in condensers and evaporators, thermocouple sensors were also used to

measure the temperature of the condenser and the evaporator, the inlet-outlet of the condensers and the inlet-outlet temperature of the chilled water. Pressure sensors were used to measure the pressures of the HEX, condenser and evaporator. Electromagnetic flow meters are used to measure the flow rate of the cooling water and the heating water of the HEXs, the flow rate of the cooling water into the condenser and the flow rate of chilled water into the evaporator. All sensors were connected to a data logger, and the measurements were performed every second. A computer was used to save the measured data. The position of the measurement point is marked in Figure 3.2

Table 4.1. Chiller operating strategy of the reheating two-stage chiller.

HEX	Mode									
	A	B	C	D	E	F	G	H	I	J
1	Des			Mrh	Pc	Ads			Mrc	Ph
2	Mrh	Pc	Ads			Mrc	Ph	Des		
3	Ads			Mrc	Ph	Des			Mrh	Pc
4	Mrc	Ph	Des			Mrh	Pc	Ads		

Ads=adsorption Mrh=mass recovery with heating Pc = pre-cooling
Des=desorption Mrc=mass recovery with cooling Ph= pre-heating

4.2.3 Parameter Settings

Table 4.2 presents the standard experimental parameters applied during the experiment. The important point of the experiment was that the chilled water outlet temperature was maintained constant at 9°C. Applying this extent of control over this parameter required extra attention during the experiment because the chilled water outlet temperature cannot be set up automatically on the machine. The chilled water outlet temperature was controlled by adjusting the flows for the chilled water outlet temperature. The cycle time parameters (in Table 4.3) were distributed in every mode based on Table 1 to observe the effect of cycle time on the performance.

4.3. PERFORMANCE INDICATOR INDEX

The performance of the re-heat adsorption cycle is indicated mainly by the coefficient of performance (COP) and the cooling capacity (CC), which can be shows in equation 3.13

and 3.14 respectively

Table 4.2 Standard experimental conditions

Parameter		Value	Unit
Hot water	Temperature	60,65,70,75	^{o}C
	Flow rate	1.8	kg/s
Cooling water in	Temperature	30	^{o}C
	Flow rate	1.4	kg/s
Chilled water in	Temperature	14	^{o}C
	Flow rate	0.17	kg/s
Chilled water out	Temperature	9	^{o}C
	Flow rate	0.1-0.4	kg/s

Table 4.3. Cycle Time Parameter

Re-heat Cycle

A	B	C	D	E	F	G	H	I	J	Cycle time (s)
100	30	240	100	30	100	30	240	100	30	1000
200	30	290	200	30	200	30	290	200	30	1500
300	30	340	300	30	300	30	340	300	30	2000
400	30	390	400	30	400	30	390	400	30	2500
500	30	440	500	30	500	30	440	500	30	3000
600	30	490	600	30	600	30	490	600	30	3500
700	30	540	700	30	700	30	540	700	30	4000

Single Stage

420	30	420	30		900

4.4. RESULTS AND DISCUSSION

4.4.1 Temperature and Pressure Histories

Figure 4.2 illustrates the temperature and pressure histories of the four HEXs of the chiller with the heat source temperature at 60°C and a total cycle time of 2000 s.

In the beginning (300 s), HEX2 and HEX6 are in the mass recovery process, HEX2 is in the heating mode, and HEX6 is in the cooling mode (mode A). At the beginning, the

temperature and pressure of HEX2 decrease and that of HEX6 increase suddenly after the temperature of HEX2 is increased and HEX6 is decreased due to heating by hot water and cooling by cool water.

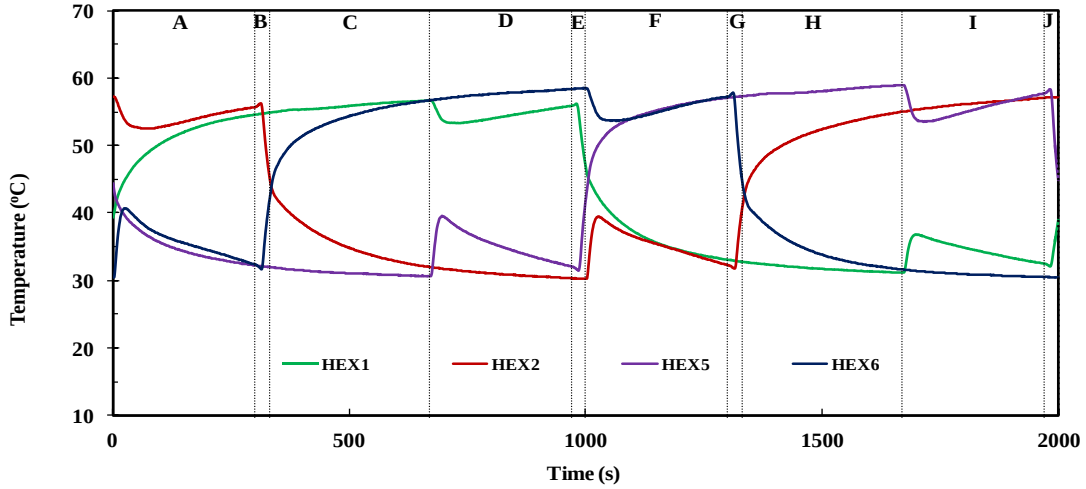

(a)

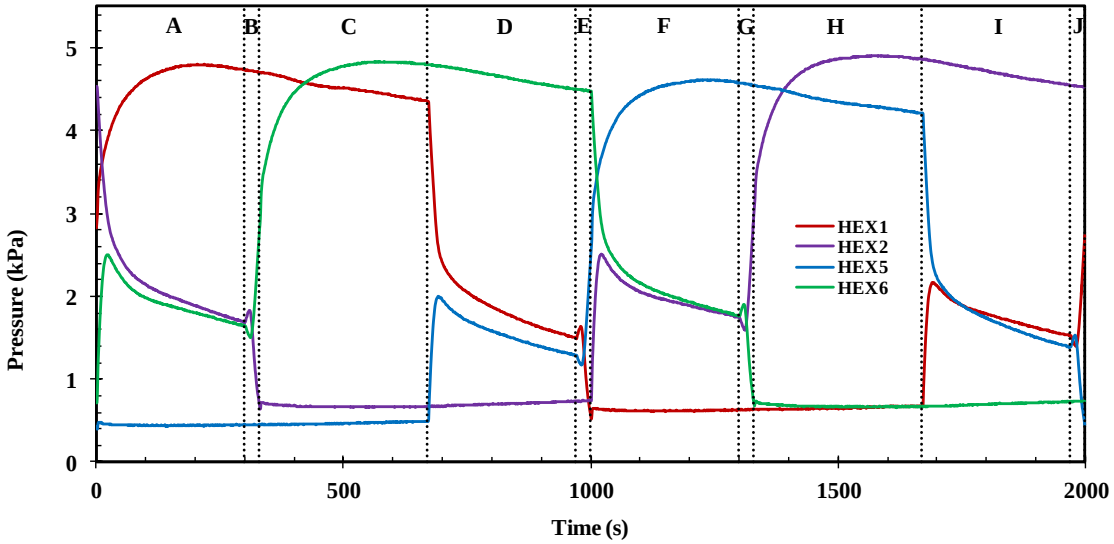

(b)

Figure 4.2: (a) Temperature histories and (b) Pressure histories of heat exchangers of the chiller

As a result, HEX2 starts to desorb and HEX6 to adsorb water vapor very fast. In mode B, HEX2 is in the pre-cooling process and HEX6 is in the pre-heating process. The temperature of HEX2 decreases and the pressure declines. The temperature and pressure of HEX6 increase. The next process is the desorption process for HEX2 and the adsorption

process for HEX6 (modes C, D and E). In this process, HEX2 operates on the evaporator pressure and HEX6 operates on the condenser pressure. The refrigerant in the evaporator will be evaporated and adsorbed by HEX2. At the same time, the adsorbed refrigerant of HEX6 will be released to the condenser in the adsorption process and then condensed in the condenser. Up to mode E is a first half-cycle, and the next process (mode F to J) is similar to mode A to E, but the adsorber and desorber positions will be changed in each of the HEX pairs, which is shown in Figure 4.2.

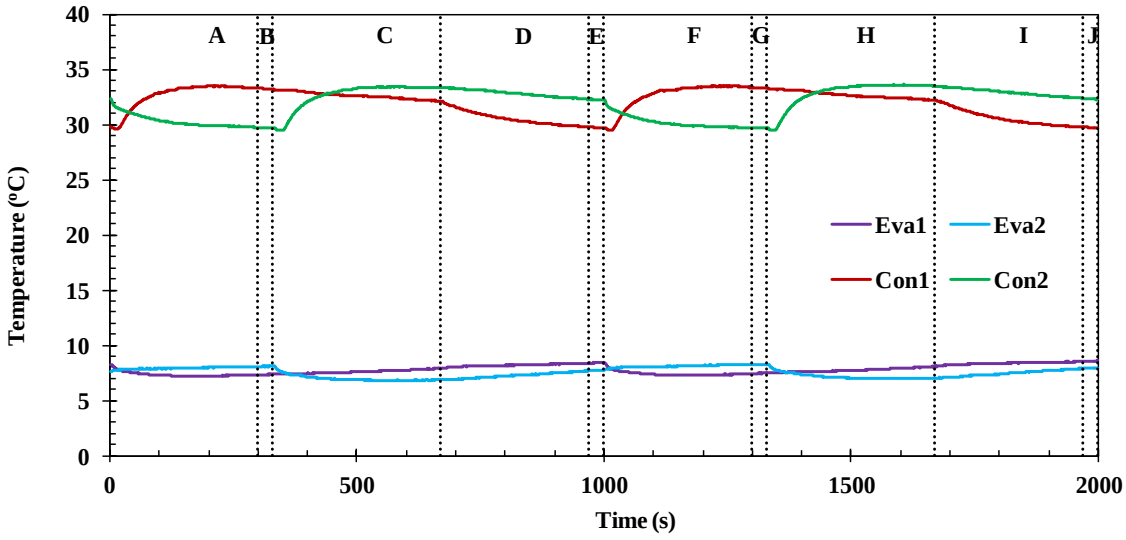

(a)

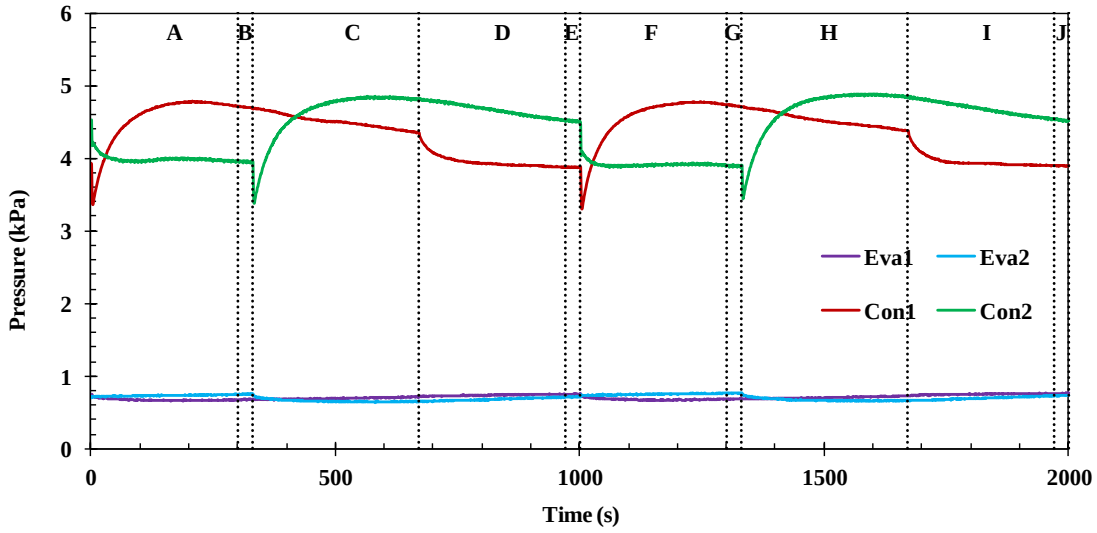

(b)

Figure 4.3: (a) Temperature histories and (b) Pressure histories of condenser and evaporator of the chiller.

Figure 4.3 shows that the pressure and temperature of condenser 1 increase drastically when the condensation process begins or when condenser 1 is connected to the HEX. The

heat rate from the refrigerant vapor received by the condenser is not equal to the heat rate adsorbed by the cooling condenser. The increase occurs until a certain point when the released refrigerant is condensed in the condenser in large quantities. After exceeding the maximum point, the pressure and temperature of condenser 1 will start to decrease while the pressure and temperature of condenser 2 will start to increase. The trend of evaporator temperature and pressure is the opposite trend of the condenser. When the evaporator is used during the evaporation process, the temperature as well as the pressure decrease until a minimum point and then increase.

4.4.2 Effect of Heat Source Temperature on Performance

The effect of the temperature of the heat source on performance is presented in Figure 4.4(a), where the chilled water outlet temperature was 9°C and the total cycle time was 1300 s. The COP and cooling capacity both increased with heat source temperature.

The reason that the COP and cooling capacity both increased with heat source temperature is explained in Figure 4.4(b), which shows that the concentration difference increases from point A to B if the heat source temperature increases. As the difference between the maximum and minimum concentration levels expands with the increase in heat source temperature, the cooling capacity as well as the COP improves with the increase in the heat source temperature. A greater amount of refrigerant will therefore be adsorbed and desorbed.

4.4.3 Effect of Cycle Time on Performance

The effect of the cycle time on performance (the COP and cooling capacity) is described by Fig. 4.5(a). Seven cycle times are chosen from 1000 s to 4000 s to represent the short cycle and the long cycle (Table 4.3). The experimental conditions were set up with the heat source temperature and chilled water outlet temperature at 60°C and 9°C, respectively.

The highest levels of performance were attained between cycle times of 2000 – 2500 s. When cycle times were less than 2000 s, sufficient time was not available for the process of adsorption/desorption. The result is therefore a low level of performance. In cycle times longer than 2500 s, the performance decreases drastically because the adsorption tends to be relatively less intense.

Longer cycle times cause more refrigerant to be adsorbed and desorbed. More cooling energy should therefore be produced in one cycle. However, an excessively long cycle will create a reduction in the average cooling power. Longer cycle times produce more cooling

power with a relatively lower consumption of driving heat.

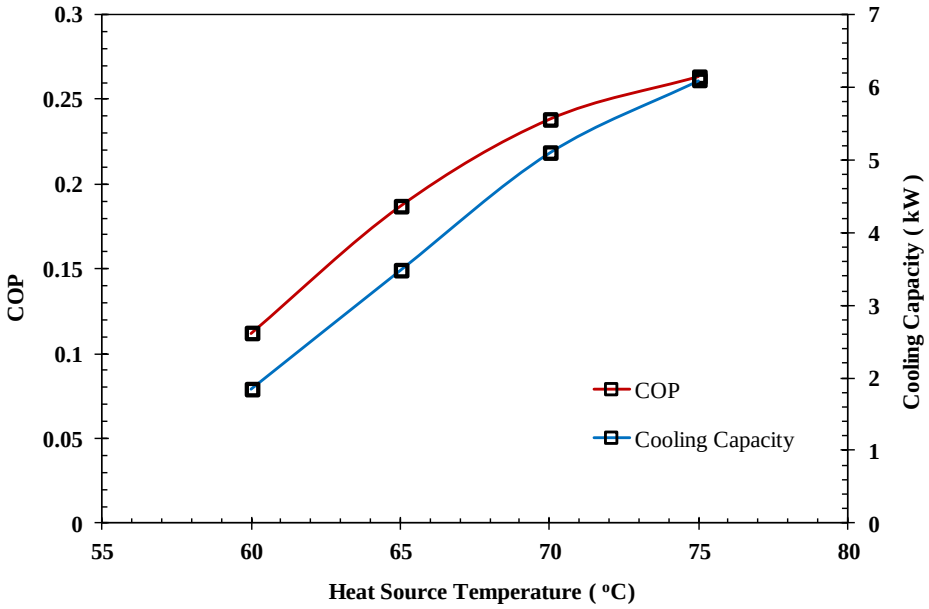

(a)

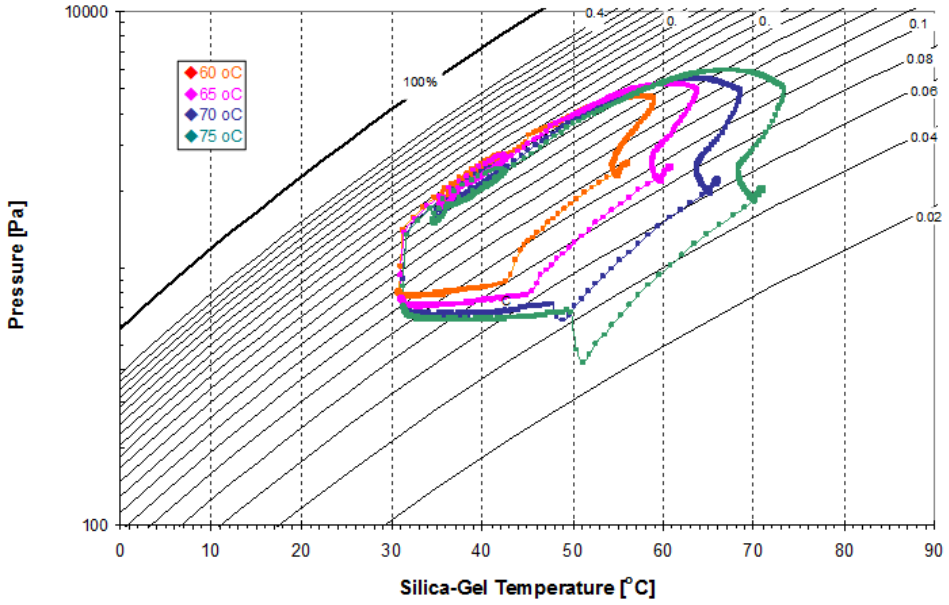

(b)

Figure 4.4: Effect heat source temperature on (a) performance and (b) P-T-X diagram.

The COP was therefore observed to increase uniformly within cycle times less than 2500 s. Further explanation of the effect of cycle time on performance can be illustrated by the P-T-X diagram in Figure 4.5(b). Two cycle times (1000 s and 2500 s) were chosen as representative of the short cycle and the long cycle. Longer cycle times give sufficient time to

reach the maximum-minimum concentration. The figure shows that the P-T-X diagram at longer cycle times generates more expansion than the short cycle time.

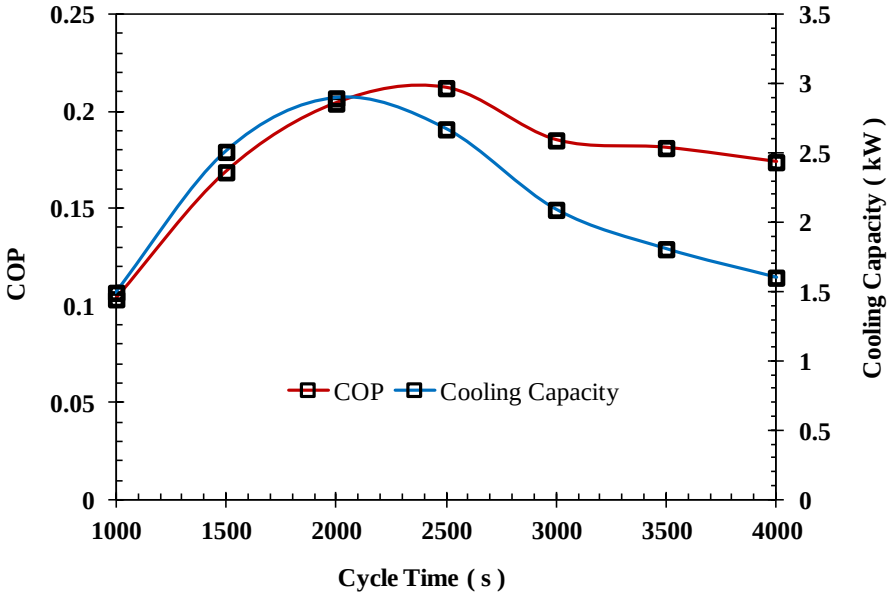

(a)

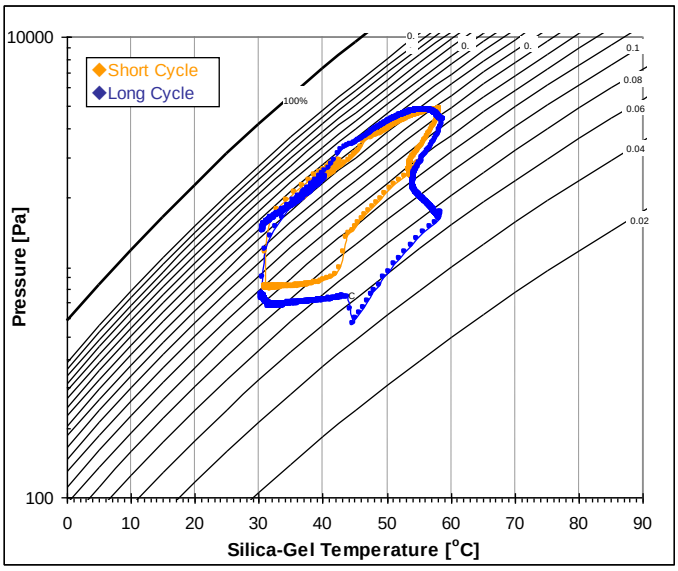

(b)

Figure 4.5: Effect cycle time on (a) performance and (b) P-T-X diagram

4.4.4 Effect Mass Recovery Time on Performance

The effect of mass recovery time is analyzed base on two focusing ideas. First, the effect of mass recovery time while the total cycle time is consider most, and the second one is emphasizing in fixing the adsorption/desorption time. Effect mass recovery time on performance is presented in Figure 4.6. Four mass recovery times are chosen (50s, 100s, 150s, and 200s). Cycle time, heat source temperature, and chilled water out temperature are set in

fixed condition (1300s, 60°C, and 9°C). The performance (COP and Cooling Capacity) increases until certain point and then decreases, succeeding mass recovery time increased. The optimum performance is obtained in mass recovery time 150 s. In this point of view, mass recovery process is very effective to improve the performance without increasing heat source temperature.

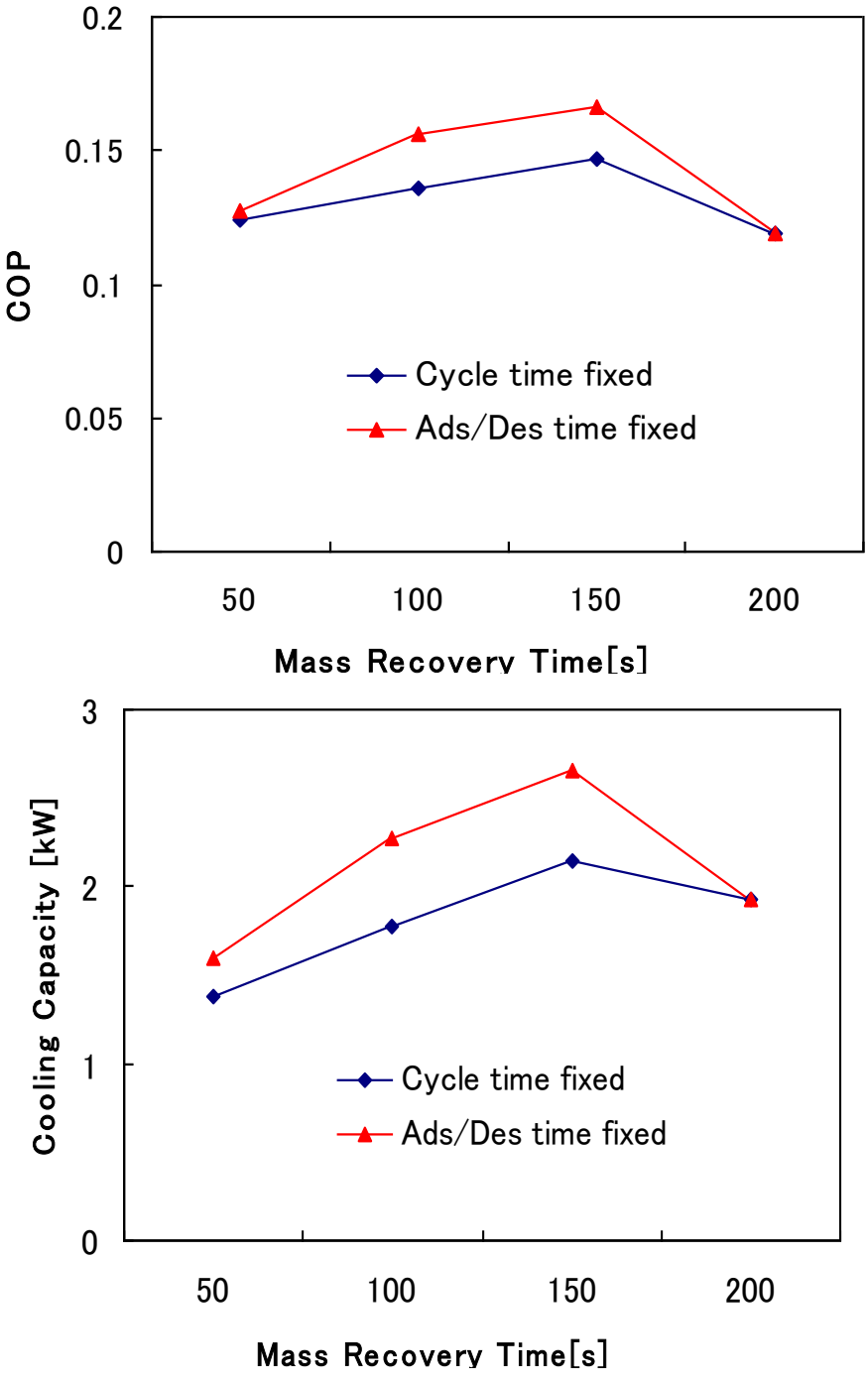

Figure 4.6: Effect mass recovery time on performance

Further illustration in mass recovery effect can be seen on P-T-X Diagram. Mass recovery time shorter than 150s, maximum concentration obtained is lower. It's mean that, optimum value of mass recovery time gives sufficient time to reach maximum concentration level. Mass recovery time longer than 150s causes performance decreases. The particular combination of cycle time and mass recovery time is one of the consideration values on the performance of the chiller.

Within the same total cycle time, the effect of mass recovery time produced lower performance compare than that of it implemented within the same adsorption-desorption time. As can be shown from Figure 4.7, mass recovery process in the cycle generates more desorption heat transfer from desorber through adsorb vapor. While keeping adsorption-desorption time on the cycle, mass recovery process is able to exploit the performance of the chiller.

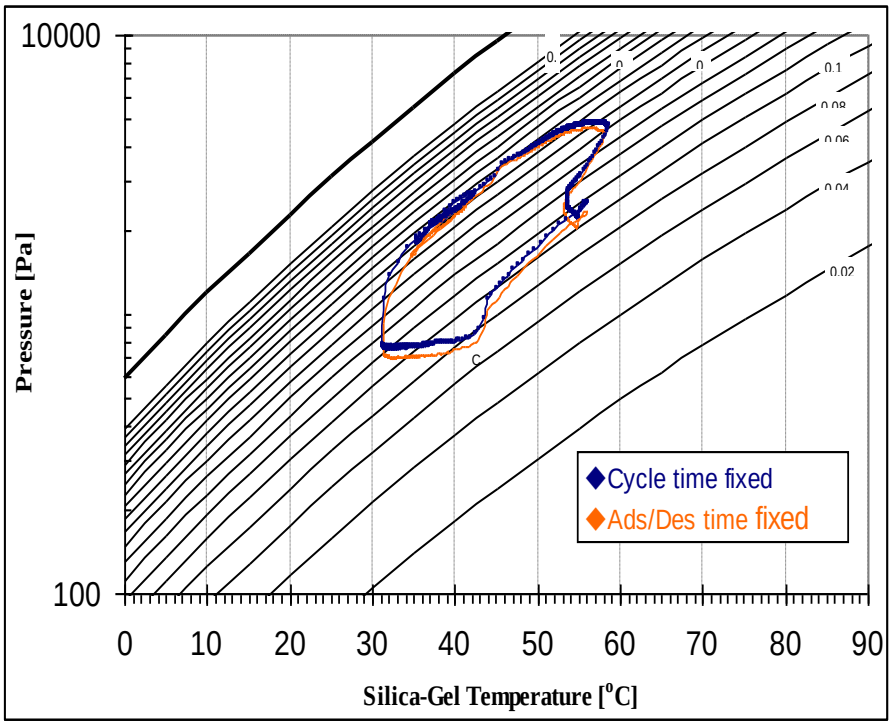

Figure 4.7: Effect mass recovery time on Duhring diagram

4.4.5 Discussion Optimum Performance

The global optimum performance is evaluated base on the unification among the mass recovery time and total cycle time which is applied during the experiment. Choosing the

global optimum value is based on which trends on the graph are showing the same tendency. The COP and cooling capacity of the unification among mass recovery time and total cycle time can be shown on Figure 4.8.

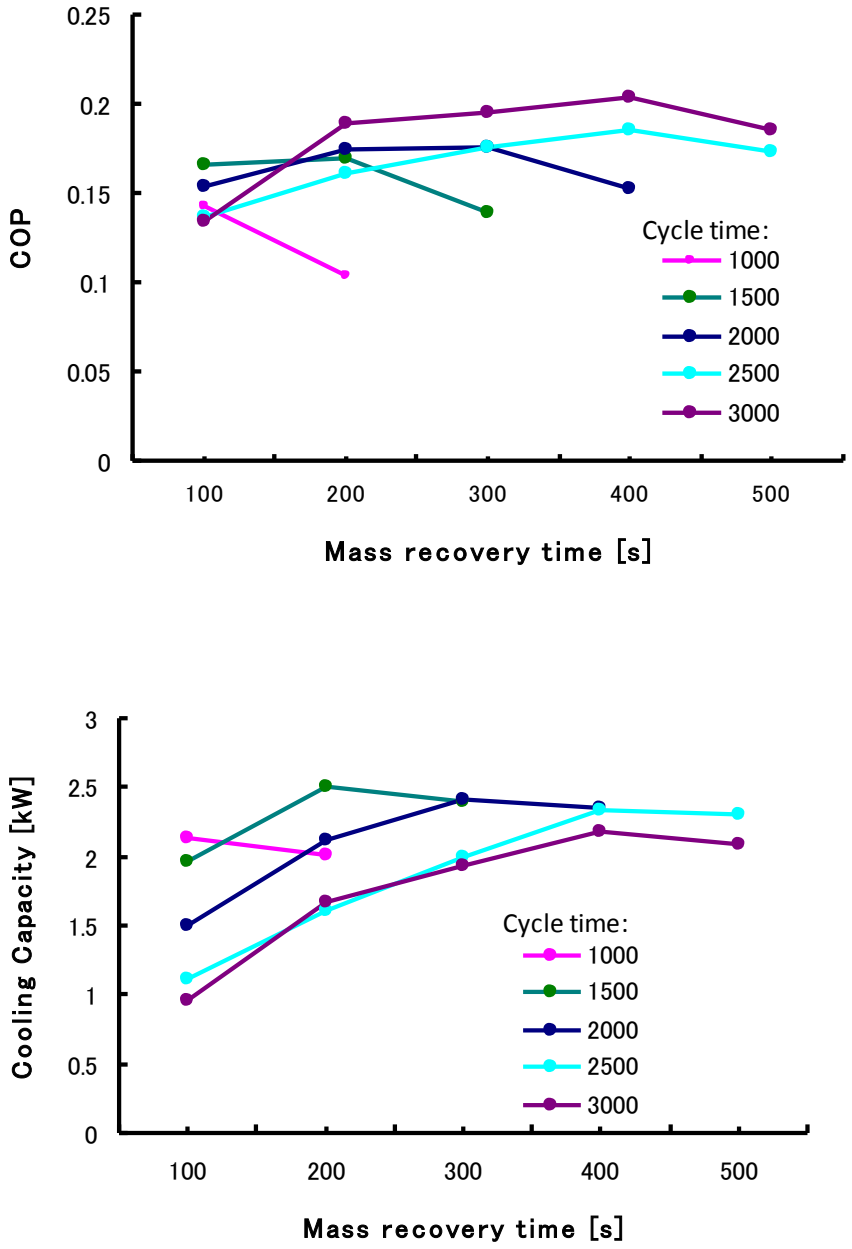

Figure 4.8: COP and cooling capacity of the unification among mass recovery time and total cycle time

Mass recovery time (100s, 200s, 300s, 400s, 500s,) and total cycle time (1000s, 1500s, 2000s, 2500s, and 3000s) will be combined among others. Heat source temperature and chilled water outlet temperature (60^{o}C and 9^{o}C) are arranged in fixed condition.

Because of the combination among mass recovery time and total cycle time should be in the right combination, it will make that one mass recovery time setting can not be applied in the total cycle time. For example, if we applied mass recovery time 400s in total cycle time 2000s, it will not be match because higher mass recovery time will made total cycle time increased.

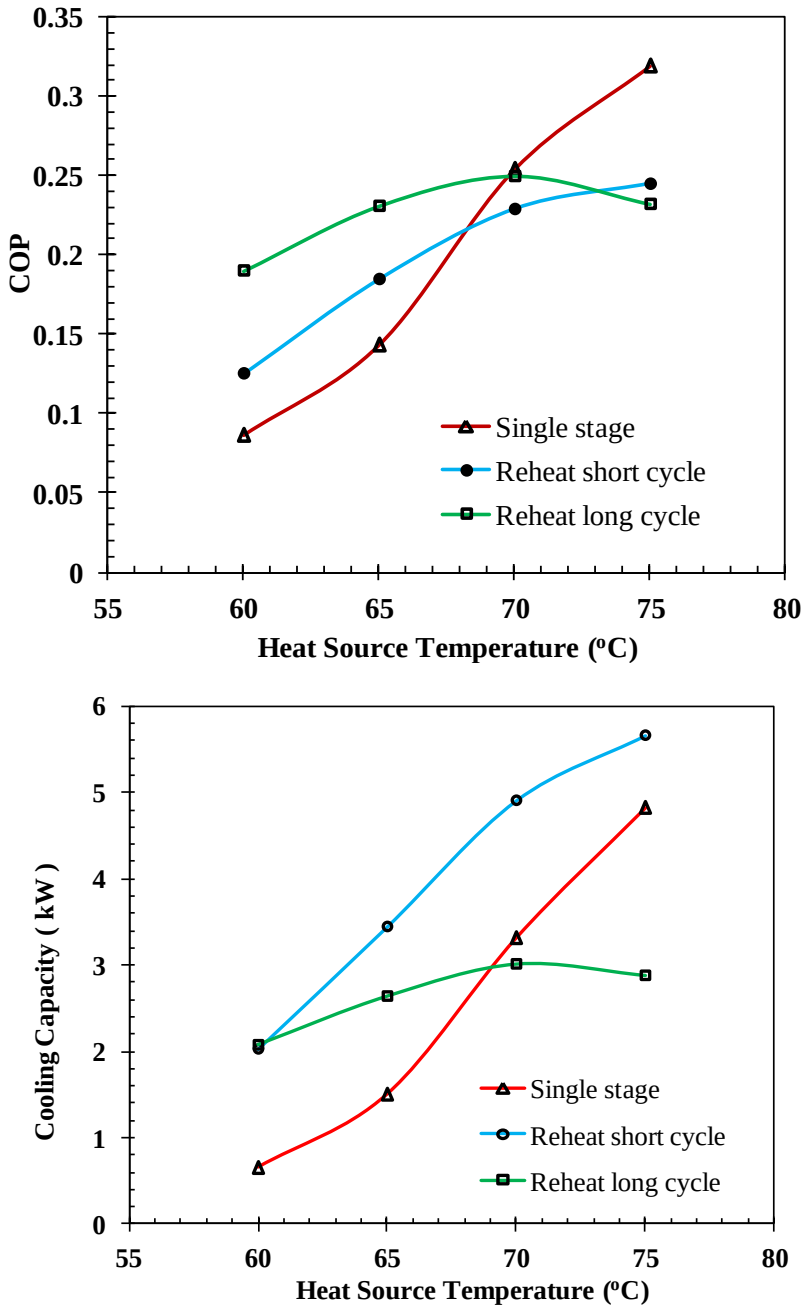

Figure 4.9: Performance comparison among re-heat short, re-heat long and single-stage

4.4.6 Performance Comparison between the Reheating Two-Stage Chiller and the Single Stage Chiller

A performance comparison between the reheating two-stage (short and long cycle) chiller and the single stage chiller is presented in Figure 4.9. The parameter conditions based on Table 4.3 were applied during the experiment. The four heat exchangers were used for a single stage cycle comparing the performance between the chillers.

Based on Figure 4.9, the reheating two-stage chiller with a long cycle provides better COP values than a short cycle time and a single stage. The COP expanded with the cycle time because the adsorption chiller with a long cycle time produced a relatively higher cooling effect. According to the figure, cycle time is responsive to the heat source temperature. For a low heat source temperature, the COP value for the reheating adsorption cycle with a long cycle time is better than the reheating short cycle and single stage. For a high heat source temperature, the COP of the single stage is superior.

The cooling capacity obtained from the reheating adsorption cycle with the long cycle and the short cycle is better than the single stage with a low heat source temperature. However, the short cycle time offered better cooling capacity with a relatively high heat source temperature compared to the other cycle.

4.5. CONCLUSION

The following concluding remarks can be drawn from the present study.

① Heat source temperature and cycle time are the influential factors for the reheating two-stage cycle chiller.

② The performance of the chiller increased with increasing heat source temperature.

③ A total cycle time of 2000 s to 2500 s gives better performance for the chiller.

④ For a relatively low heat source temperature, both short cycles and long cycles of the reheating two-stage cycle chiller offer better performance than the single stage chiller.

CHAPTER 5

CYCLE OPTIMIZATION ON RE-HEAT ADSORPTION CYCLE APPLYING FIXED CHILLED WATER OUTLET TEMPERATURE

In this chapter, a simulation model of re-heat adsorption cycles has developed to analyze the optimization of the cycle time, including adsorption/desorption time, mass recovery time and pre-heating/pre-cooling time, with chilled water outlet temperature fixed. The proposed cycle was compared with the four-bed without re-heat cycle in terms of COP and cooling capacity. The result shows that the performance of a re-heat cycle is superior to that of four-bed without re-heat, especially for low heat source temperature. For low heat source temperature (55-65 ^{o}C) both COP and cooling capacity of the re-heat cycle with optimization raised significantly compared to the high-heat source temperature (70-80 ^{o}C).

5.1. INTRODUCTION

The performance characteristic and the cycle operating conditions of adsorption chiller have investigated numerically. It's shown that the cycle time is one of the most influential parameters on the performance of the adsorption chiller. The performance model considering the operating condition effects has observed and concluded that the optimum cycle time of the chiller corresponding to maximum cooling capacity was increased significantly. Meanwhile, the performance comparison adsorption cooling system with optimization was concluded that time allocation of the cycle is relatively sensitive against the variation of heat source temperature. The pre-heating/pre-cooling time also affected the performance of the adsorption chiller.

The performance of an advanced adsorption chiller, namely re-heat cycle has been investigated by researches. However, optimization of the cycle never done and chilled water outlet temperatures are arrange in fluctuated. Maintaining a constant chilled water outlet temperature is also the equal importance to improve the conversion efficiency so that maximum cooling capacity can be derived.

The objectives of this study are (1) to developed a simulation numerically of four-adsorber/desorber re-heat adsorption cycle, (2) to optimized the cycle time and (3) to

compared the proposed optimized cycle with the optimized of four-adsorber/desorber conventional cycle. The optimization of the four-bed re-heat cycle are focusing in adsorption/desorption time, mass recovery time and pre-heating/pre-cooling time, especially in chilled water out temperature 9^{o}C.

5.2. SIMULATION METHOD

A complete simulation program was developed based on MATLAB software to solve all equations of adsorber/desorber energy balance, evaporator energy balance and condenser energy balance equation. In the beginning of the solution process, initial values are assumed and finally, those are adjusted by the iteration process. Once the satisfactory convergence criterion is achieved, then the process goes for the next time step. All input parameters such as adsorbent-refrigerant properties, flow rates of heat transfer fluids and heat exchangers specifications initially was given for which the system cyclic operation can be realized. Particle Swarm Optimization (PSO) was applied to optimize the cycle time based on maximum value of COP and cooling capacity which were chosen as the objective function and cycle time components (i.e., adsorption/desorption time, pre-cooling/pre-heating time and mass recovery time) were chosen as the variable. In PSO, a particle holds the values of variables and updates the values toward the optimal solution. After a number of updating calculations, all the particles hold the same value and the objective function value maximized. In this case, the number of particles and the number of iterations were considered as 20 and 500, respectively. It was observed that all particles reached their best position before 500 iterations.

Table 5.1 and Table 5.2 constituted the baseline parameter and standard operating conditions adapted in simulation, respectively.

5.3. RESULTS AND DISCUSSION

5.3.1. Temperature Histories

Figure 5.1 illustrates the temperature histories of the four-bed of the chiller with heat source temperature 60 ^{o}C and total cycle time 1300s.

It was seen that at the beginning, the temperature of bed2 decreased and that of bed4 increased suddenly after that temperature of bed2 is increased and bed4 decreased due to heating by hot water and cooling by cold water, respectively.

It is worth mentioning here that in the beginning (420s) bed2 and bed4 are in the mass recovery process where bed2 is in heating mode and bed4 in cooling mode (mode A),

respectively.

Table 5.1. Parameter's values in simulation

Symbol	Value	Unit
C_s	924	J/kgK
C_v	1.89E+3	J/kgK
C_w	4.18E+3	J/kgK
D_o	2.54E-4	m^2/s
E_a	2.33E+6	J/kg
L_w	2.50E+6	J/kg
Q_s	2.86E+6	J/kg
R	4.62E+2	J/kgK
R_p	3.00E-4	m
UA_{ads}	2.00E+3	W/m^2K
UA_{des}	2.23E+3	W/m^2K
UA_{eva}	2.36E+3	W/m^2K
UA_{con}	4.06E+3	W/m^2K
W_s	16	kg
$W_{con,w}$	5	kg
$W_{eva,w}$	25	kg

Table 5.2. Standard operating conditions

	Temperature (^oC)	Flow Rate (kg/s)
Hot water	60	1
Cooling water	30	1(ads) + 0.8(des)
Chilled water	14	0.8
Cycle time (Ads/Des+Mrc/Mrh+Ph/Pc)	(420 + 200 + 30)s	

Noted:
Ads/Des = adsorption/desorption
Mrc/Mrh = mass recovery
Ph/Pc = pre-heating/precooling

As results, bed2 starts to desorb and bed4 to adsorb water vapor very fast. In mode B, bed2 is in pre-cooling and bed4 in the pre-heating process. So that temperature of bed2 decreased and pressure decline. On the other hand, temperature of bed4 increased. The next process is desorption process for bed2 and adsorption process for bed4 (mode C, D and E). In this process, bed2 operates in evaporator pressure and bed4 operates in condenser pressure. Refrigerant in evaporator will be evaporated and adsorbed by bed2. At the same time, adsorbed refrigerant of bed4 will be released to the condenser in the adsorption process and then condensed in condenser. Up to mode E is a first half-cycle and the next process (mode F to J) is similar to mode A to E, only adsorber and desorber position will be changed each bed pair, which is obviously observed in this figure.

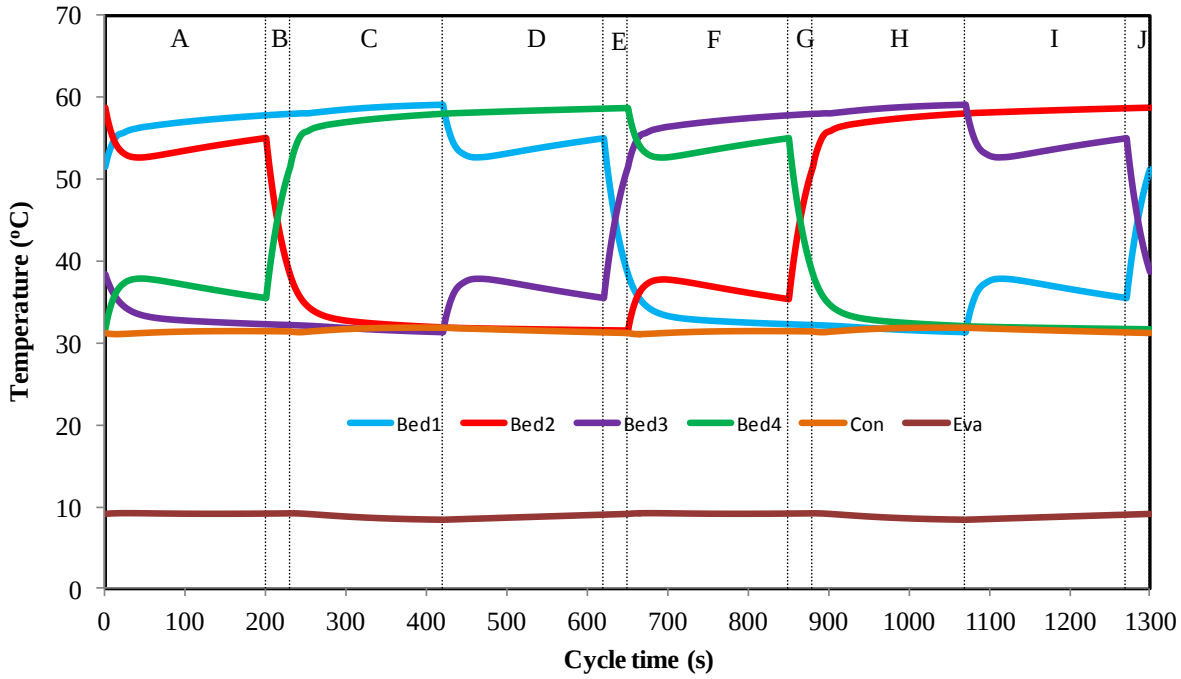

Figure 5.1: Temperature histories of the four-bed re-heat adsorption cycle

Figure 5.2 shown temperature histories comparison between experiment and simulation. Heat source temperature 60 ^{o}C and cycle time 1300s while temperature of chilled water outlet 9 ^{o}C are arrange in fixed condition. As can be seen that in every mode, between experiment and simulation illustrated the same tendency. The experimental results shown lower value compared than the simulation results because of the heat loses in the experiment which is neglected in the simulation. The figure also informed that the similarity of the trend prove that the simulation runs compatible.

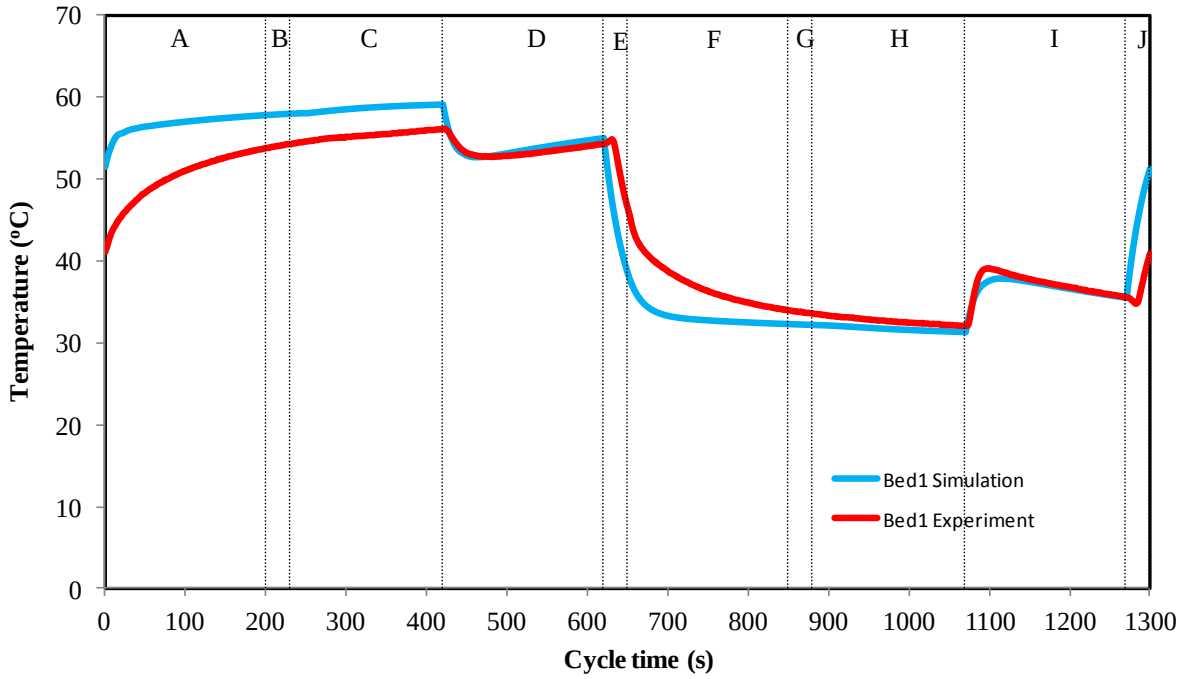

Figure 5.2: Temperature histories comparison between experiment and simulation

5.3.2. Water Content in Bed

Figure 5.3 illustrated the variation of water content in adsorber/desorber of bed. Heat source temperature at 60°C and fixed chilled water outlet temperature at 9°C are applied. Water contents in bed1, bed2, bed3 and bed4 were decreased during the desorption process because vapor is condensed into the condenser (i.e., mode A-B-C for bed1, mode H-I-J for bed2, mode F-G-H for bed3 and mode C-D-E for bed4) and increased during the adsorption process because bed was adsorbed the vapor from the evaporator (i.e., mode F-G-H for bed1, mode C-D-E for bed2, mode A-B-C for bed3 and mode H-I-J for bed4).

During pre-heating and pre-cooling process, water contents in all of beds were remained constant because all valves on the system were fully closed (i.e., mode E and mode J for bed1 and bed3 and mode B and mode G for bed2 and bed4).

In the mass recovery with heating process, water content in the bed1 was decreased (mode D) because the vapor transferred into the bed3, therefore, water content in the bed3 increased (mode D), respectively. In the mass recovery with cooling process, water content in the bed1 increased (mode I) because receive vapor from the bed3, therefore, water content in the bed3 decreased (mode I).

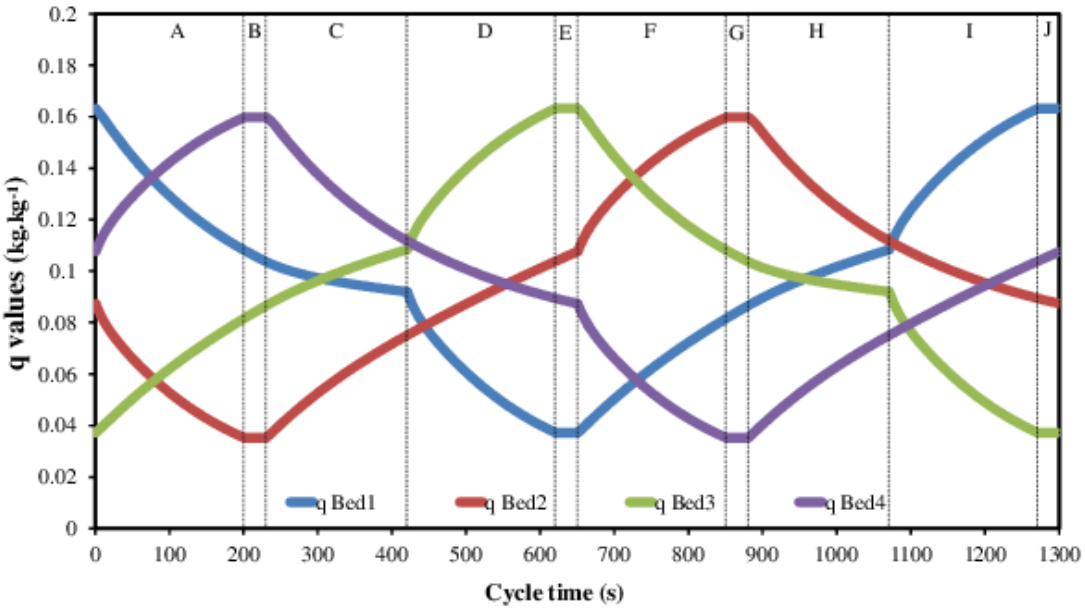

Figure 5.3: Water content in bed.

5.3.3. Performance of Cycle Time

The effect of cycle time for the performance and correlation among chilled water out temperature and mass flow rate of the four-bed re-heat cycle are presented in Figure 5.4.

Figure 5.4 (a) depicts the influences of cycle time on COP and cooling capacity. It was observed that COP increased along with cycle time. Cycle time 1000s to 5000 s with 500s escalation applied to show the performance characteristic. Chilled water out temperature applied in fixed condition at 9^{o}C while controlled mass flow rate based on Figure 5.4 (b). This figure informed that mass flow rate increased due to gain the chilled water out temperature 9^{o}C in cycle time from 1000s to 3000s and decreased when the cycle time more than 3000s. Cycle time from 2000s to 3000s required highest mass flow rate to gain chilled water outlet 9^{o}C.

The highest cooling capacity values attained at cycle time between 2000s and 3000s. Cycle time out of this range made cooling capacity lower. The reason is that the adsorption/desorption process cannot be occurred well within long cycle time and for short cycle time the process researches its equilibrium state, which causes the cooling capacity decline smoothly.

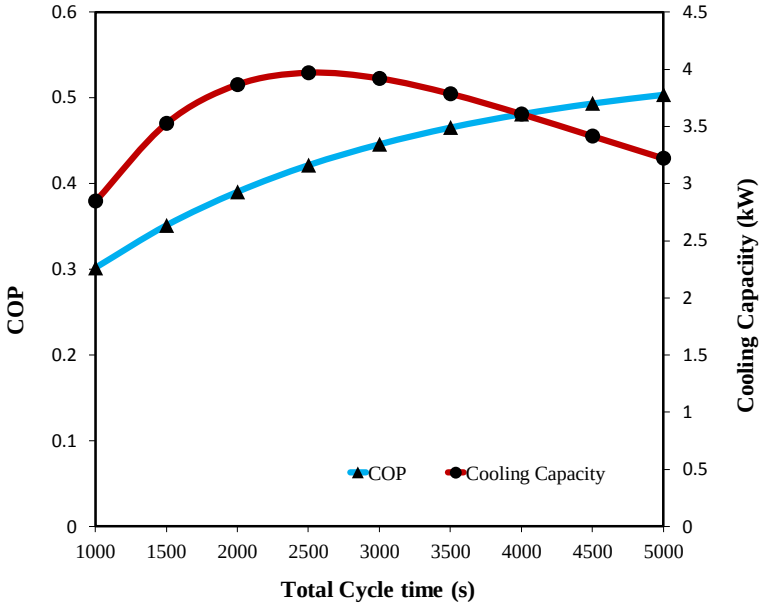

(a)

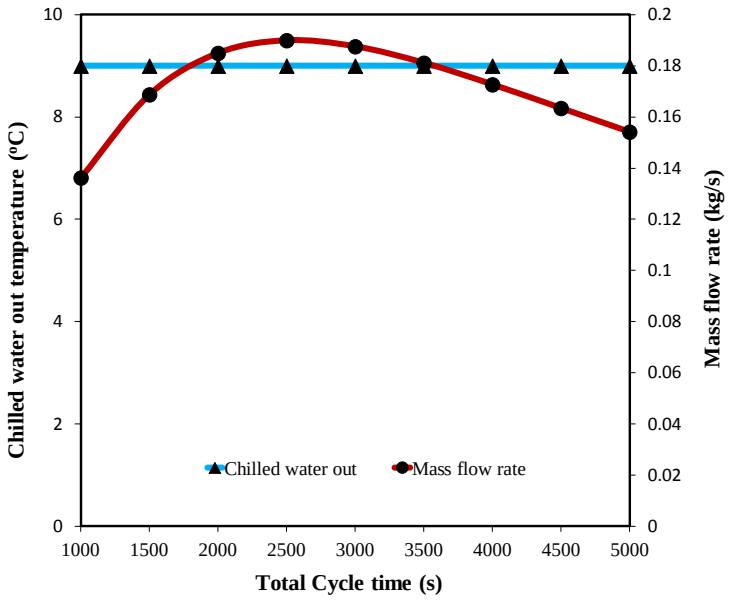

(b)

Figure 5.4: Performance of cycle time

5.3.4. Cycle Time Optimization

Cycle time optimization of the four-bed re-heat cycle presented in Figure 5.5(a) and the achievement of chilled water out temperature by controlling mass flow rate shown in Figure 5 (b) as well. The cycle optimizations consist of adsorption/desorption time, mass recovery time and pre-heating/pre-cooling time. Heat source temperature from 55 to 80 ^{o}C was chosen to show its characteristic. For low heat source temperature (55^{o}C) required longer cycle time

to gain the optimum performance. In contrast, the opposite tendency happened in high-heat source temperature (80^{o}C).

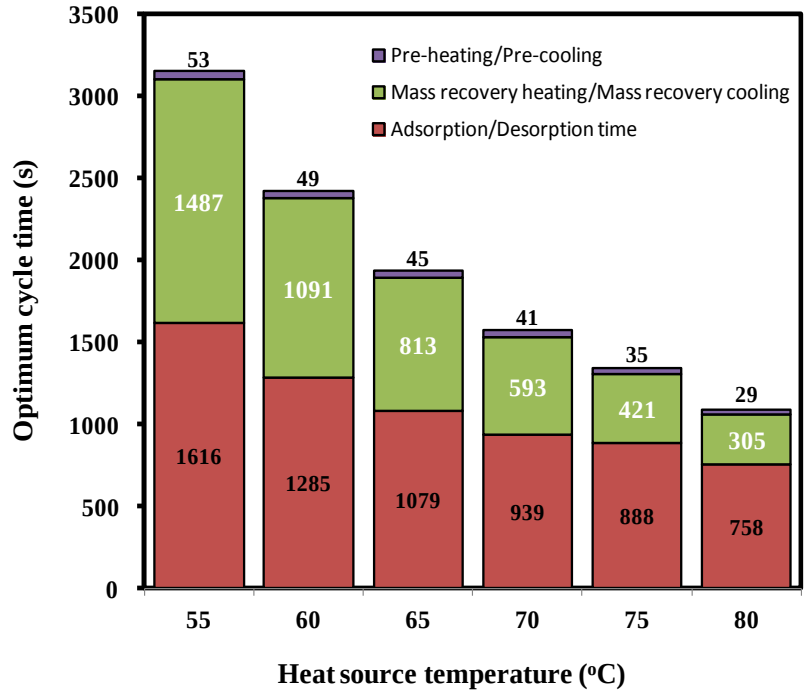

(a)

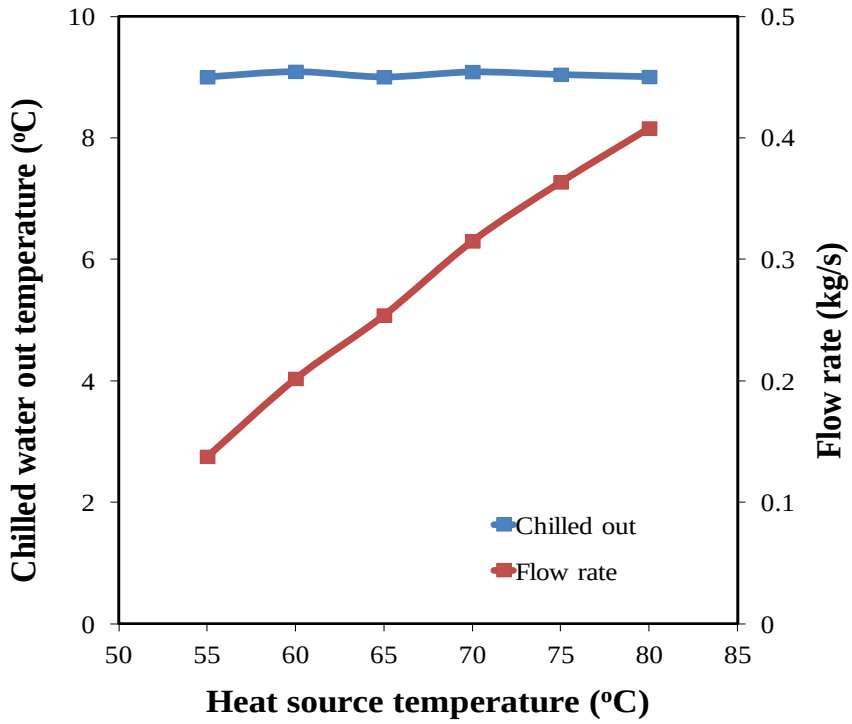

(b)

Figure 5.5: (a) Cycle time optimization and (b) The achievement of chilled water out temperature by controlling mass flow rate.

From the Figure 5.5(b) chilled water flow rate was increased with heat source temperature to maintain the chilled water outlet temperature at the constant temperatures. To gain chilled water outlet temperature 9^{o}C, mass flow rate should be controlled carefully. Based on Figure 5 (b), mass flow rate increased along with heat source temperature. Higher heat source temperature required more water consumption in evaporator caused the flow rate valve should be opened widely to keep chilled water outlet temperature 9^{o}C.

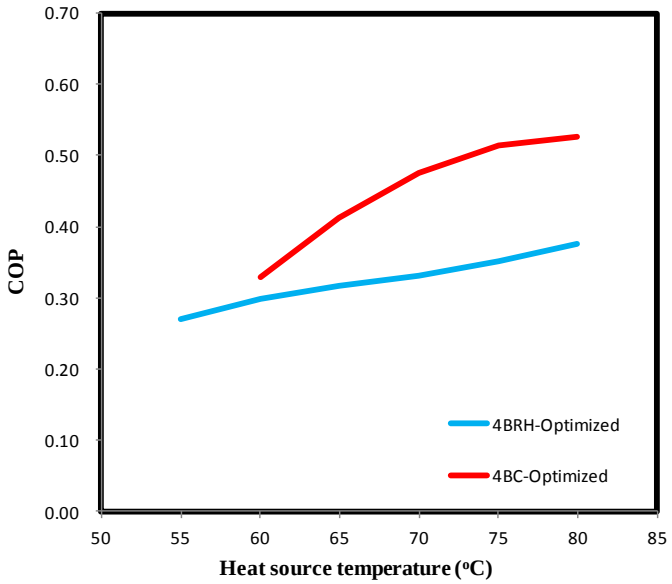

(a)

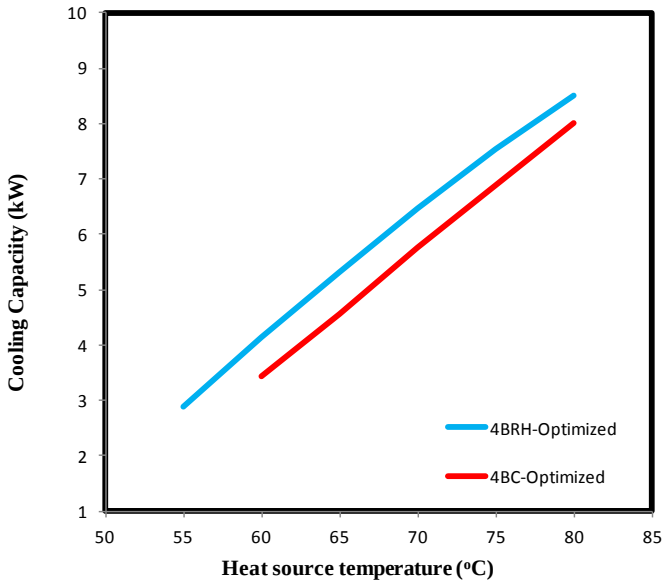

(b)

Figure 5.6: Performance comparisons.

From this point of view, cycle time selection based on Table 5.3, especially for low heat source temperature before optimization was not suitable for the best performance achievement and the optimized cycle time based on Figure 5 (a) should be applied. For the high heat source temperature, although the performance rose slightly, the optimization of cycle time still offering better performance.

Figure 5.6 presented the optimization performance comparison between re-heat cycle and conventional cycle. The conventional cycle consist of four-adsorber/desorber bed (heat exchanger), one evaporator and one condenser which is the upper-bed and the lower-bed never interacts with the evaporator and the condenser. The operation strategy of the conventional cycle through only four steps i.e desorption, pre-cooling, adsorption and pre-heating.

From Figure 5.6, we can observe that re-heat cycle in both COP and cooling capacity offering better performance compared to the conventional cycle, especially in low heat source temperature. For high-heat source temperature, even conventional cycle showing better COP compared than re-heat cycle but cooling capacity still lower. On the other hand, conventional cycle cannot be done in heat source temperature 55 ^{o}C if operated in the chilled water outlet 9 ^{o}C. From this point of view, re-heat cycle promising better performance for low heat source temperature. The optimization of cycle time should be applied in order to enhance the performance of the re-heat cycle.

5.4. CONCLUSION

The optimization of four beds re-heat cycle has observed during this study while applying chilled water out temperature fixed. Controlling in mass flow rate is a necessity due to gain fixed chilled water out temperature. Short cycle time (below 3000s) required mass flow rate higher than longer cycle time (up to 3000s). The COP increased along with cycle time and the highest cooling capacity values attained at cycle time between 2000s and 3000s.

Cycle optimization of the re-heat cycle offered better performance in both COP and cooling capacity. For the heat source temperature 55^{o}C shown the highest increment of 80% raised in both COP and cooling capacity, while 20% increment for heat source temperature 60^{o}C and 7% increment for heat source temperature 65^{o}C respectively. For relatively high-heat source temperature (70-80^{o}C), although there was the increment in both COP and cooling capacity, the value of escalation raised smoothly in about 1%.

CHAPTER 6

ADVANCED THREE-BED RE-HEAT COMBINED ADSORPTION CYCLE

In this chapter, the performances and the optimized cycle time of the advanced three-bed re-heat combined adsorption chiller is introduced. There are two type of advanced cycle in this study namely Advanced Three-Bed Conventional Re-Heat Combined Cycle and Advanced Three-Bed Three-Stage Re-Heat Combined Cycle. The chiller consists of three adsorbed/desorber heat exchanger, one evaporator and one condenser. Combined cycle refers to the adsorber/desorber of HEXs that one pair of bed operates in re-heat cycle while the other one operates in conventional cycle respectively. The governing equations of the present's chiller were using MATLAB and Particle Swarm Optimization (PSO). The objectives of the present study are to examine the simulation performance of three-hex re-heat combined chiller and the cycle time of the present chiller is optimized. The comparison with those of four-hex conventional chiller and four-hex re-heat chiller also presented.

6.1. INTRODUCTION

Heat driven adsorption system is one of the most promising systems due to use of low or near the environment temperature, as a driving heat source in its operation. By using water and silica gel as the adsorbent-refrigerant pair in the system indicates that the adsorption system is suitable for reduce the gas's emission and consume low energy can be achieved [28]. Some extensive investigations of the performances of the adsorption refrigeration chiller have been conducted considering various adsorbent/adsorbate pairs. Following are the examples: zeolite/water [29, 30], activated carbon/ammonia [31] and silica gel/water [32-34]. And the utilization of the low-temperature heat source have been proposed such as heat and mass recovery cycles [35], multi-stage chillers [36], the experimental investigation [40] and multi-bed chillers [10]. It was presented that those advanced chillers would achieve better performances compared with that of the conventional adsorption chiller.

To achieve better COP and/or cooling capacity values, most of the advanced chillers in adsorption refrigeration/heat pumps have been proposed. Alam has introduced the four

beds/hex adsorption chillers; namely, re-heat two-stage adsorption chiller and shows that the chiller can exploit the heat source temperature 50-90 ^{o}C [13]. Maintaining a constant chilled water outlet temperature is also of equal importance to improve the conversion efficiency of the chiller so that maximum cooling capacity can be delivered [15]. Wirajati et al. [26] identified the effect of the heat source temperature and the effect of cycle time on performance if the chilled water outlet temperature is fixed at 9°C experimentally.

The possibility of reducing the adsorber/desorber hex's utilization is still promising since the consideration of the smaller adsorption machine to be constructed [38-40] and can be performed for the relative low heat source temperature below 60 ^{o}C.

In this study, the author concern of reducing the number of hex utilization compare to the previous study that were based on the four-hex conventional and four-hex re-heat cycle has been investigated experimentally and numerically. By reducing the hex utilization and introducing the new mode operational strategy which is applied in the present chiller, the smaller compact machine can be designed. And the objectives of the recent study were to examine the performance of three-hex re-heat combined chiller and to optimized the cycle time of the present chiller. The comparison with those of four-hex conventional chiller and four-hex re-heat chiller also presented.

As a result, the first type and the second type of advanced cycle with the new strategy can utilize the minimum heat source temperature 55 ^{o}C and 45 ^{o}C respectively, while the chilled water out temperature keep in 9 ^{o}C.

6.2. SIMULATION AND OPTIMIZATION METHOD

A complete simulation program was developed based on Matlab software to solve all equations 3.3 – 3.14. In the beginning of the solution process, initial values are assumed and finally, those are adjusted by the iteration process. Once the satisfactory convergence criterion is achieved, then the process goes for the next time step. All input parameters such as adsorbent-refrigerant properties, flow rates of heat transfer fluids and heat exchangers specifications initially was given for which the system cyclic operation can be realized. Particle Swarm Optimization (PSO) was applied to optimize the cycle time based on maximum value of COP and cooling capacity which were chosen as the objective function and cycle time components (i.e., adsorption/desorption time, pre-cooling/pre-heating time and mass recovery time) were chosen as the variable. In PSO, a particle holds the values of variables and updates the values toward the optimal solution. After a number of updating calculations, all the particles hold the same value and the objective function value maximized.

In this case, the number of particles and the number of iterations were considered as 20 and 500, respectively. It was observed that all particles reached their best position before 500 iterations.

The values of physical properties parameters used in calculation and the standard operating condition adopted in simulation are shown in Table 6.22 and Table 6.3 respectively.

6.3. ADVANCED THREE-BED CONVENTIONAL RE-HEAT COMBINED ADSORPTION CHILLER PROCESS.

The three-bed re-heat combined adsorption chiller schematic and the Pressure-Temperature-Concentration (PTX) diagram are present in Figure 2.11 and Figure 2.12 while the mode strategy of the proposed chiller shown in Table 6.1 respectively.

Table 6.1**:** Mode Operational Strategy

HEX	A	B	C	D	E	F	G	H	I	J
1	Des			Mrh	Pc	Ads			Mrc	Ph
2	Ads			Mrc	Ph	Des			Mrh	Pc
3	Des			Pc		Ads			Ph	

6.3.1 RESULTS AND DISCUSSION

6.3.1.1 Water content in Hex

Figure 6.1 illustrated the variation of water content in adsorber/desorber of Hex. Heat source temperature at 55^{o}C and fixed chilled water outlet temperature at 9 ^{o}C are applied. Water contents in Hex was decreased during desorption process because vapor is condensed into the condenser (i.e., mode A-B-C for Hex1 and Hex3, mode F-G-H for Hex2) and increased during the adsorption process because Hex was adsorbed the vapor from the evaporator (i.e., mode A-B-C for Hex2, mode F-G-H for Hex1 and Hex3).

During pre-heating and pre-cooling process, water contents in all of Hex were remained constant because all valves on the system were fully closed (i.e., mode E and mode J for 1 and Hex3 and mode B and mode G for Hex2 and Hex4). In the mass recovery with heating process, water content in the Hex1 was decreased (mode D) because the vapor transferred into the Hex2, therefore, water content in the Hex2 increased (mode D), respectively. In the mass recovery with cooling process, water content in the Hex1 increased (mode I) because of

receiving vapor from the Hex2, therefore, water content in the Hex2 decreased (mode I). As can be seen from Figure 6.1(a), water content of Hex3 seems to be change marginally because of the heat source temperature 55^{o}C implementation was too low to condense the vapor in this Hex compare with the heat source temperature 70^{o}C in Figure 6.1(b).

Table 6.2. Parameter's values in simulation

Symbol	Value	Unit
C_s	924	J/kg K
C_v	1.89E+3	J/kg K
C_w	4.18E+3	J/kg K
D_o	2.54E-4	m^2/s
E_a	2.33E+6	J/kg
L_w	2.50E+6	J/kg
Q_s	2.86E+6	J/kg
R	4.62E+2	J/kg K
R_p	3.00E-4	m
UA_{ads}	2.00E+3	W/m^2K
UA_{des}	2.23E+3	W/m^2K
UA_{eva}	2.36E+3	W/m^2K
UA_{con}	4.06E+3	W/m^2K
W_s	16	kg
$W_{con,w}$	5	kg
$W_{eva,w}$	25	kg

Table 6.3. Standard operating conditions

	Temperature (^{o}C)	Flow Rate (kg/s)
Hot water	60	1
Cooling water	30	1(ads) + 0.8(des)
Chilled water	14	0.8
Cycle time (Ads/Des+Mrc/Mrh+Ph/Pc)	(420 + 200 + 30)s	

Noted:
Ads/Des = adsorption/desorption
Mrc/Mrh = mass recovery
Ph/Pc = pre-heating/pre-cooling

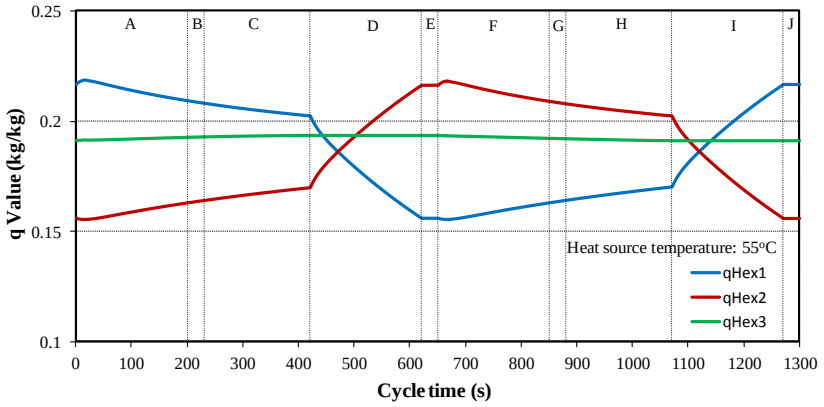

(a)

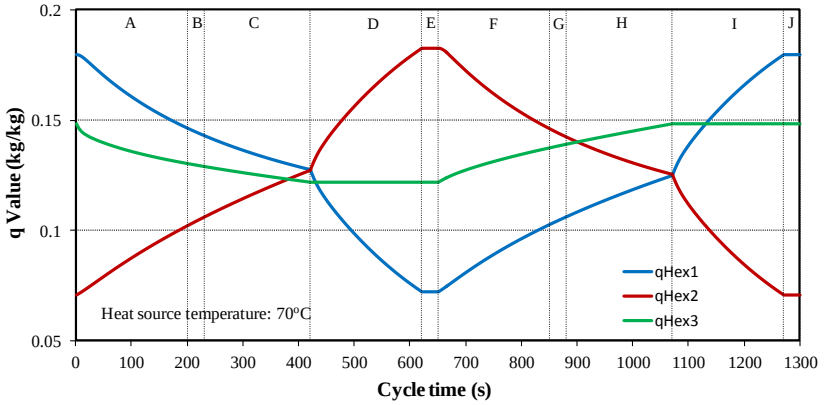

(b)

Figure 6.1: The variation of water content in adsorber/desorber of Hex comparation for heat source temperature (a) 55°C and (b) 70°C.

6.3.1.2 The Effect of Adsorption/Desorption Time on COP and Cooling Capacity

Figure 6.2 illustrates the simulation results of COP and cooling capacity with the adsorption/desorption time. Heat source temperature 60 °C, mass recovery time 100s and pre-heating/pre-cooling time 30s are chosen to investigated the effect of adsorption/desorption time between 100-800 s on the performance. The best cooling capacity values are attained for adsorption/desorption time between 300s and 350s. As can be seen from the figure, when adsorption/desorption times are shorter than 200s, there is not enough time for adsorption or desorption to occur effectively, thus the cooling capacity decreases suddenly. Conversely, if the adsorption/desorption times are longer than 300s, the cooling capacity decreases regularly because of the less intense of adsorption to its equilibrium or near equilibrium condition. The COP increases consistently with longer adsorption/desorption time because of the lower consumption of driving heat with longer duration adsorption/desorption time.

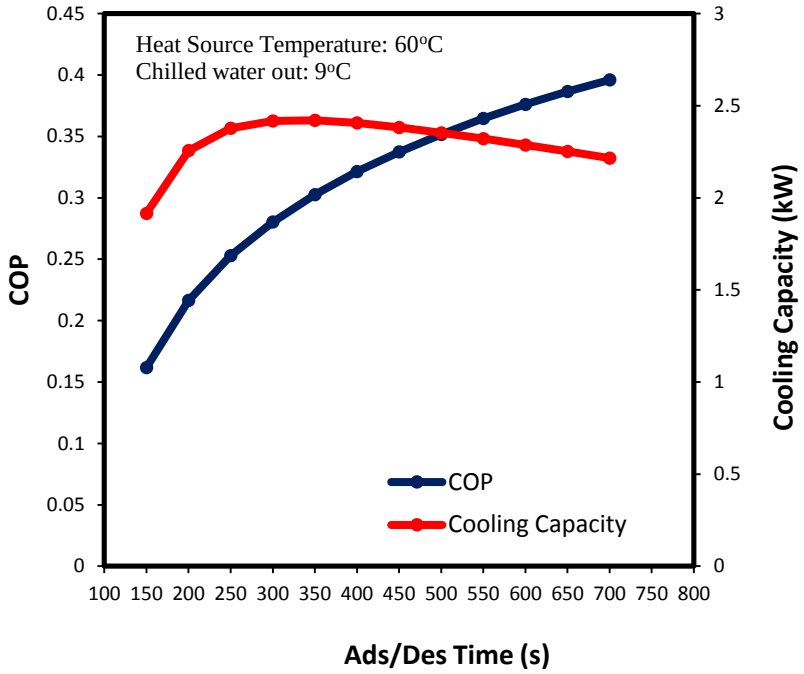

Figure 6.2: The Effect of Adsorption/Desorption Time on COP and cooling capacity.

6.3.1.3 The Effect of Pre-heating/Pre-cooling Time on COP and Cooling Capacity

Pre-heating/pre-cooling process in the adsorption chiller operation always required. The process is immediately connected to the saturated cold bed to the condenser and the regenerated hot bed to the evaporator. Figure 6.3 shows how the pre-heating/pre-cooling time affects the COP and cooling capacity of the present chiller. As can be seen, the cooling capacity raising significantly with the pre-heating/pre-cooling time until reaches a peak value at 60s and varies marginal thereafter, while the COP is always increasing respectively. By this point of view, the pre-heating/pre-cooling time at 60s indicates the optimum value for the cooling capacity but is the longer for the COP with the heat source temperature 60 ^{o}C.

6.3.1.4 The Effect of Mass Recovery Time on COP and Cooling Capacity

The mass recovery process can effectively improve the performance of the adsorption chiller driven by a low heat source temperature. The process seems to be a second adsorption/desorption process for the adsorber/desorber hex.

Figure 6.4 informed the effect of mass recovery time on COP and cooling capacity. Heat source temperature 60 ^{o}C, adsorption/desorption time 420s and pre-heating/pre-cooling 30s applying to investigates not only the effect of mass recovery time 50-350s but also to compare it with without mass recovery time (0s mass recovery time). It is seen that the chiller

without mass recovery worked quite inefficiently. The COP and cooling capacity without mass recovery are, respectively, 50% and 44% lower than those with 350s mass recovery times. By this point of view, the mass recovery is pivotal to this chiller, especially if operates for the low heat source temperature.

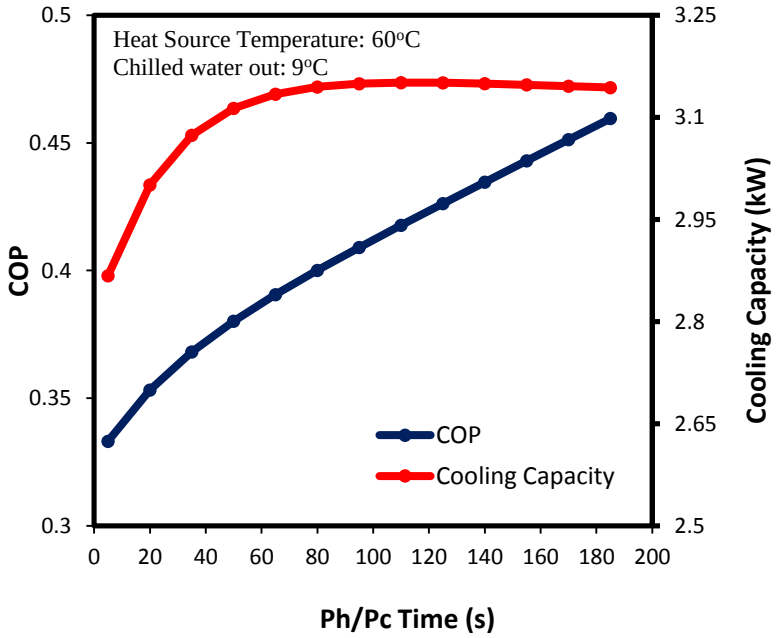

Figure 6.3: The Effect of Pre-heating/Pre-cooling Time on COP and cooling capacity.

6.3.1.5 The Effect of Adsorption/Desorption and Pre-Heating/Pre-Cooling Time on COP and Cooling Capacity

Figure 6.5 shown the effect of adsorption/desorption versus pre-cooling/pre-heating time on COP and cooling capacity. Chilled water out 9°C and standard operating condition base on Table 3 are implemented. It is worthy to mention here that, the range of adsorption/desorption and pre-cooling/pre-heating time influenced the range of cycle time with the total cycle time is 1950s.

Figure 6.5 informed that the COP increases with the increasing of adsorption/desorption time whilst the effect of pre-cooling/pre-heating time is marginal. As can be seen from Figure 6.5, the peaks value of cooling capacity reaches at adsorption/desorption and pre-cooling/pre-heating time 250 and 80s, respectively.

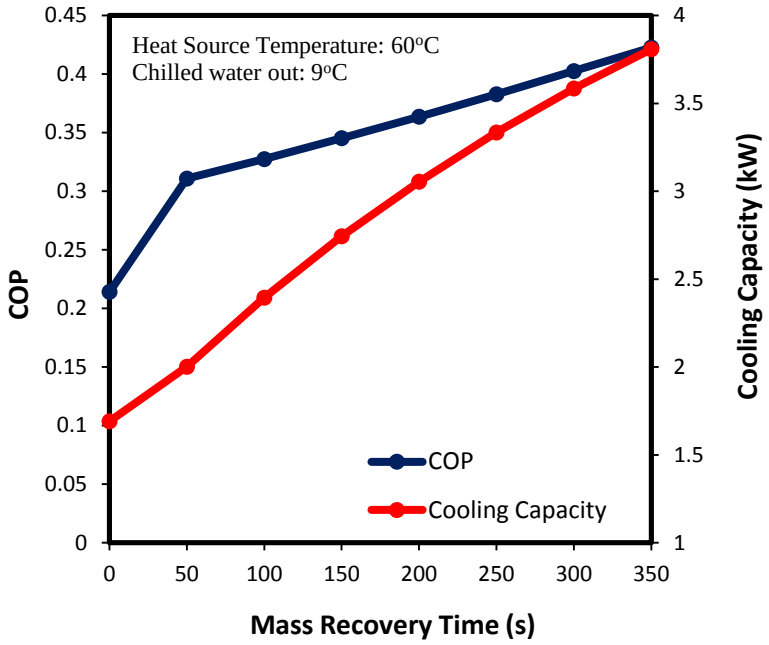

Figure 6.4: The Effect of Mass Recovery Time on COP and cooling capacity.

6.3.1.6 Cycle Time Optimization

Cycle time optimization of the three-hex re-heat combined cycle presented in Figure 6.6. The cycle optimizations consist of adsorption/desorption time, mass recovery time and pre-heating/pre-cooling time. Heat source temperature from 55 to 70°C was chosen to show its characteristic. For low heat source temperature (55 °C) required longer cycle time to gain the optimum performance. In contrast, the opposite tendency happened for the high-heat source temperature (70 °C).

Figure 6.6 has shown the total cycle time of three-hex re-heat combined cycles after and before optimization. The figure informed that the total cycle time was found to be decreased with the heat source temperature. For the low heat source temperature, cycle time optimization increased almost double compared to the cycle without optimization. The performance in both COP and cooling capacity of three-hex re-heat combined cycle shown the significant increment for the low heat source temperature.

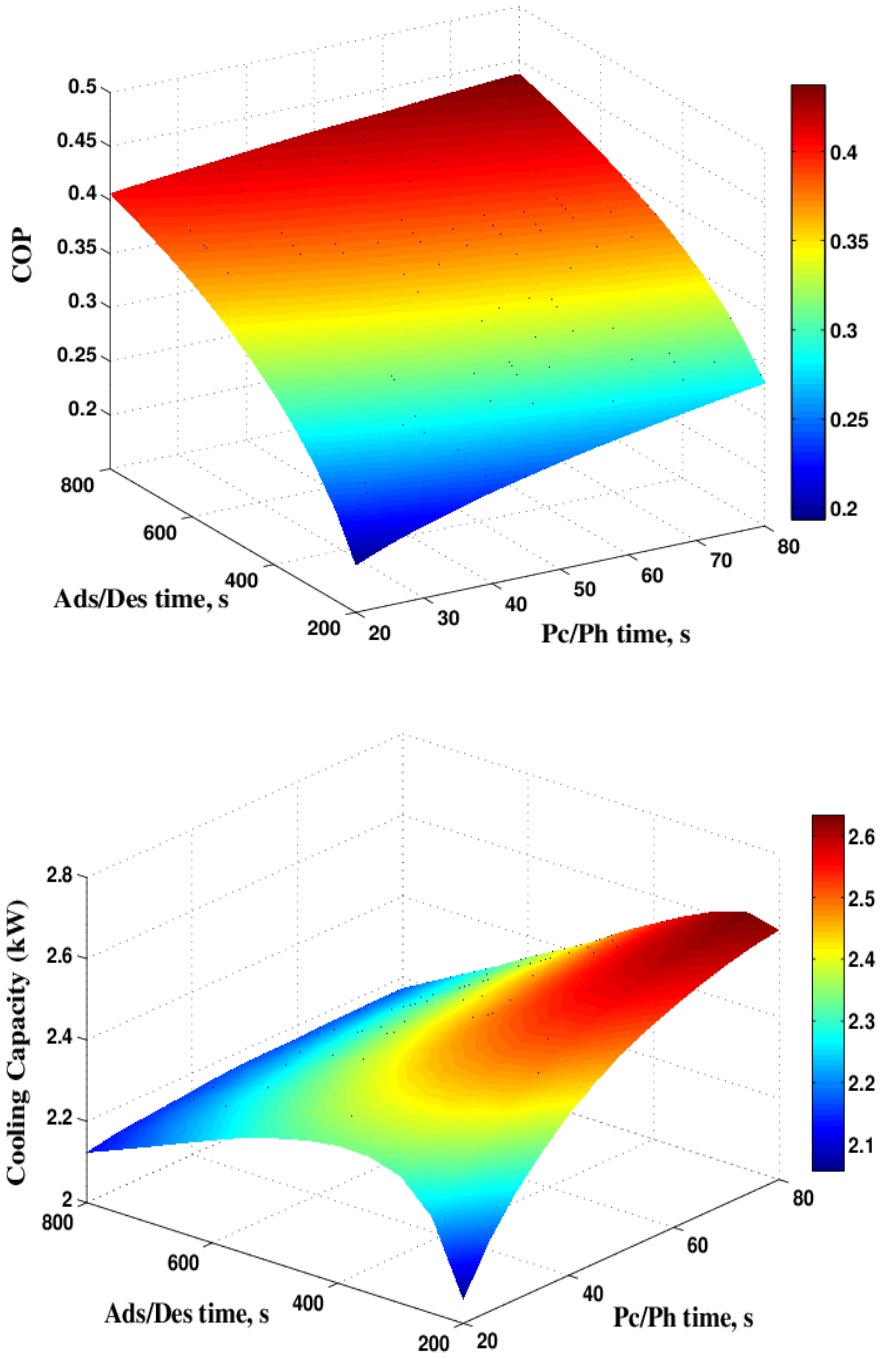

Figure 6.5: The effect of adsorption/desorption and pre-heating/pre-cooling time on COP and cooling capacity

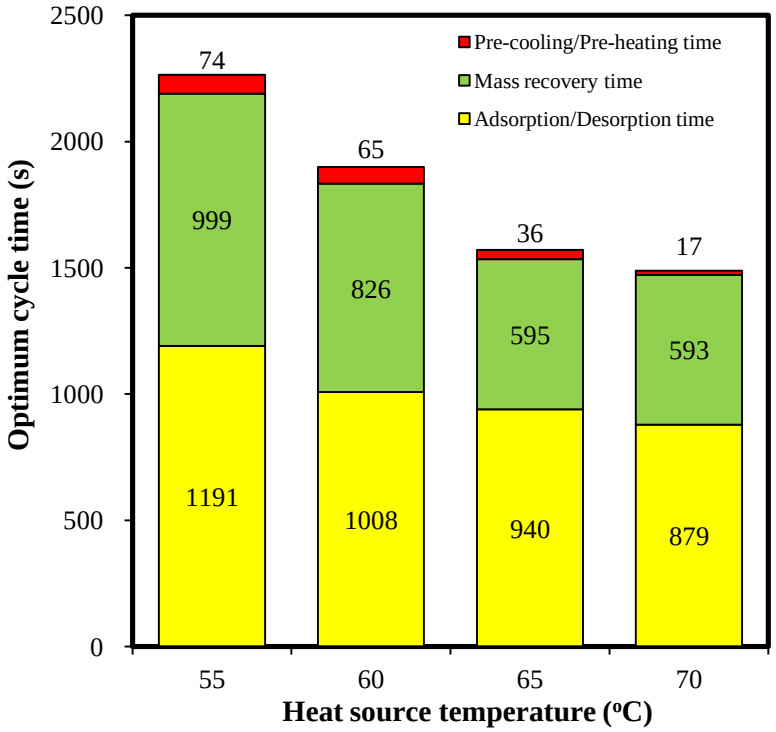

Figure 6.6: Cycle time optimization

Figure 6.6: Optimal cycle time comparison for heat source temperature 50 ^{o}C

6.3.1.7 Performance Comparison

Figure 6.7 and Figure 6.8 presents the comparison of the COP and the cooling capacity values of four-bed re-heat chiller, four-bed conventional chiller and three-bed re-heat combined chiller (as a present chiller).

COP is highly dependent on the temperature of heat source: the higher the temperature, the greater the COP value, as Figure 9 informed. The COP of three-bed re-heat combined chiller is superior compared to other chiller and it is shown the significant advantage of the three-bed re-heat combined cycle since the consideration of reducing the hex utilization and introducing the new mode operational strategy of the chiller.

Another observation of the heat source temperature effect on cooling capacity presents in Figure 6.8. From the figure we can observe that cooling capacity increased with the heat source temperature. For the low heat source temperature 55^{o}C, the four-bed re-heat chiller offering 20% slightly better cooling capacity compared to the three-bed re-heat combined. The reason is that there are four adsorber/desorber of HEX applied in the chiller and there are two pairs of HEX conduct the adsorption process at the same time, thus the cooling capacity higher. But the values of cooling capacity showed 14% increment when the three-bed re-heat

combined chiller was compared to the four-bed conventional chiller for the heat source temperature 60 ^{o}C. On the other hand, the four-hex conventional cycle is not work for the low heat source temperature 55 ^{o}C if the chilled water outlet temperature 9 ^{o}C arranged in fixed condition. By this point of view, reducing the beds while applying the mode strategy of three-bed re-heat combined chiller is promising since the consideration of the reducing of HEX's utilization.

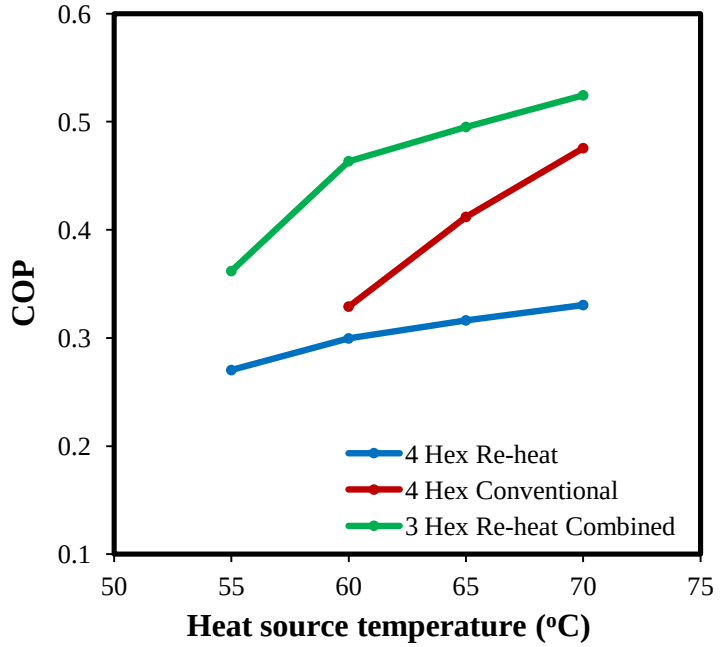

Figure 6.7: The COP comparison on the effect of heat source temperature

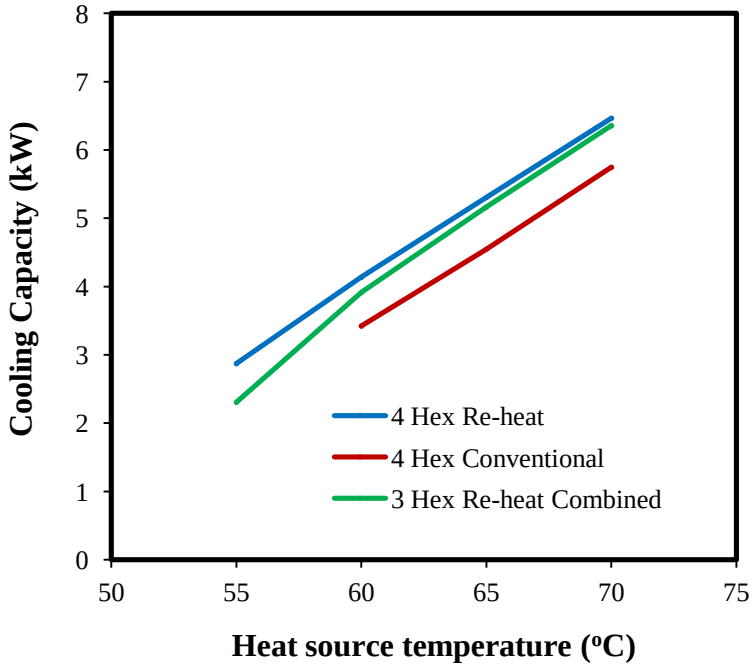

Figure 6.8: The cooling capacity comparison on the effect of heat source temperature

6.4. ADVANCED THREE-BED THREE-STAGE RE-HEAT COMBINED CYCLE

The three-bed three-stage adsorption chiller schematic and the Duhring diagram are present in Figure 2.13 and Figure 2.14, respectively. The chiller consists of three-adsorber/desorber of bed, one condenser and one evaporator. To complete a full cycle the bed operates continuously all together into eight modes, as can be shown in Table 6.4.

In this cycle, pressure lift from the evaporator level up to the condenser level is split into three progressive smaller pressure lifts as can be seen in Fig. 1(b). Bed1 and bed2 pressurize the vapor from the evaporation level to intermediate level. Then, bed3 pressurizes the vapor from the intermediate level to the condensation level.

Table 6.4. Mode Operational Strategy

Bed	A	B	C	D	E	F	G	H
1	Des	Mrh		Pc	Ads	Mrc		Ph
2	Ads	Mrc		Ph	Des	Mrh		Pc
3	Ads	Ph	Des	Pc	Ads	Ph	Des	Pc

Des: Desorption Mrh: Mass recovery heatin Ph: Pre-heating
Ads: Adsorption Mrc: Mass reovery cooling Pc: Pre-cooling

6.4.1. Results and Discussion

A complete simulation program was developed based on MATLAB software and used to solve all of the equations. Once all of the input parameters (i.e., adsorbent-refrigerant properties, flow rates of heat transfer fluids, and specifications of heat exchangers) are initially given, the cyclic operation can be simulated.

Particle Swarm Optimization (PSO)4) is used to optimize the cycle time in terms of SCP which was chosen as the objective function to be maximized, and the cycle time components (i.e., adsorption/desorption time, pre-cooling/pre-heating time, and mass recovery time) were chosen as the variables. In PSO, the particles contain the values of the variables, and the algorithm updates the values toward the optimal solution. After a number of updating calculations, all of the particles contain the same value, and the objective function achieves a maximized value. In this case, the number of particles and the number of iterations were 20 and 500, respectively. It was observed that all particles reached their best position prior to 500 iterations. Because the main objective is is to use a low heat source temperature

(i.e., less than 60 °C), the investigation was conducted for hot water temperatures of 45 °C and 50 °C.

6.4.1.1. Temperature Histories for Adsorber/Desorber Bed.

Figure 6.9 illustrates the temperature histories of the three-bed chiller with the heat source temperature.

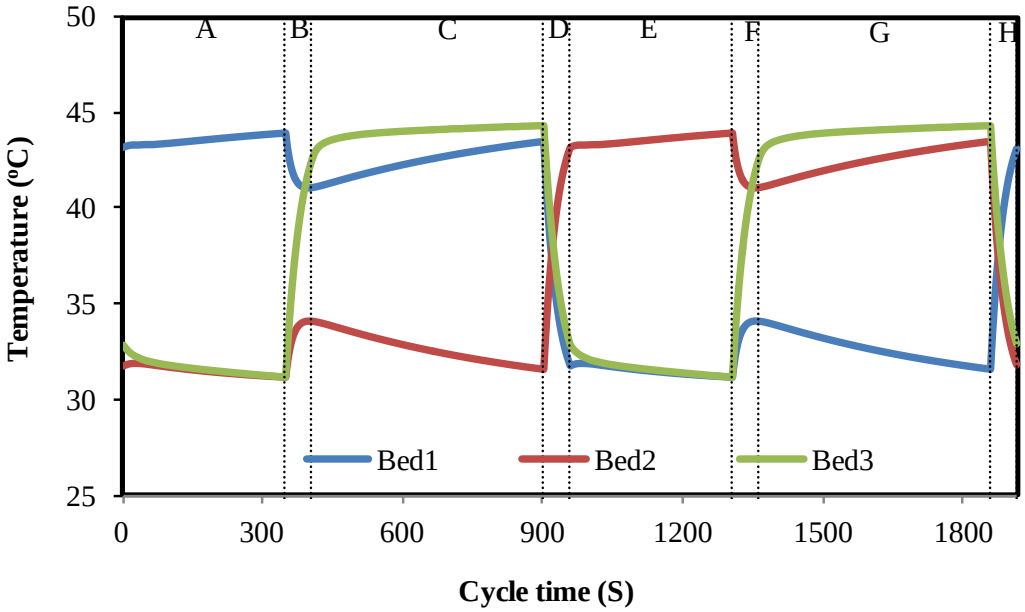

Figure 6.9: Temperature time curve characteristic for adsorber/desorber bed.

In the beginning of the process (mode A), the desorption process for bed1 and the adsorption processes for bed2 and bed3 were carried out with increasing and decreasing temperatures, respectively. In this process, bed2 and bed3 operated at the evaporator pressure, and bed1 operated at the condenser pressure.

In mode B, bed3 was operated in the pre-heating process, and thus, the temperature of bed3 increased because bed3 was heated by hot water and continued into mode C such that bed3 was switched into the desorption process.

In modes B and C, bed1 and bed2 were in the mass recovery state with heating and cooling and temperature changes accordingly.

During mode D, the temperature of bed1 and bed3 decreased, and the temperature of bed2 increased due to cooling by the cooling water and heating by the hot water. Mode D

occurred at the end of the half cycle. The temperature behavior of the remaining cycle was the same as in the previous cycle.

6.4.1.2. Water Content in Bed.

Figure 6.10 illustrated the variation of water content in adsorber/desorber of bed for full cycle.

The water content in the bed1 decreased during the desorption process because the vapor was transferred into bed3 in mode A, whereas that of bed2 increased because the bed adsorbed vapor from the evaporator. During the pre-heating and pre-cooling processes, the water content in all of the beds remained constant because all valves in the system were fully closed (i.e., mode B for bed 3 and mode D for bed1 and bed2). In the mass recovery with heating process (mode B-C), the water content in bed1 decreased because the vapor was transferred into bed2. In the mass recovery with cooling process, the water content in bed2 increased because of receiving the vapor from bed1.

During mode A, bed1 was connected to bed3, and during mode E, bed 2 was connected to bed3, where the vapor from the evaporator was consequently transferred from the lower pressure side to bed3. In these cases, bed3 worked continuously to send vapor from the intermediate pressure to condensation pressure, and a full cycle was properly completed.

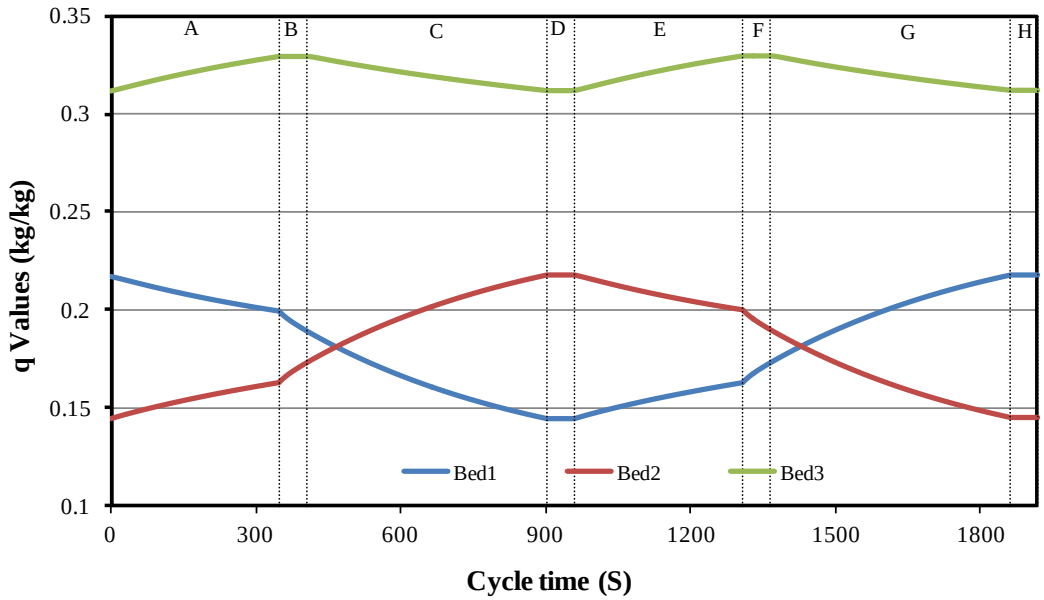

Figure 6.10: Water content characteristic of adsorber/desorber bed.

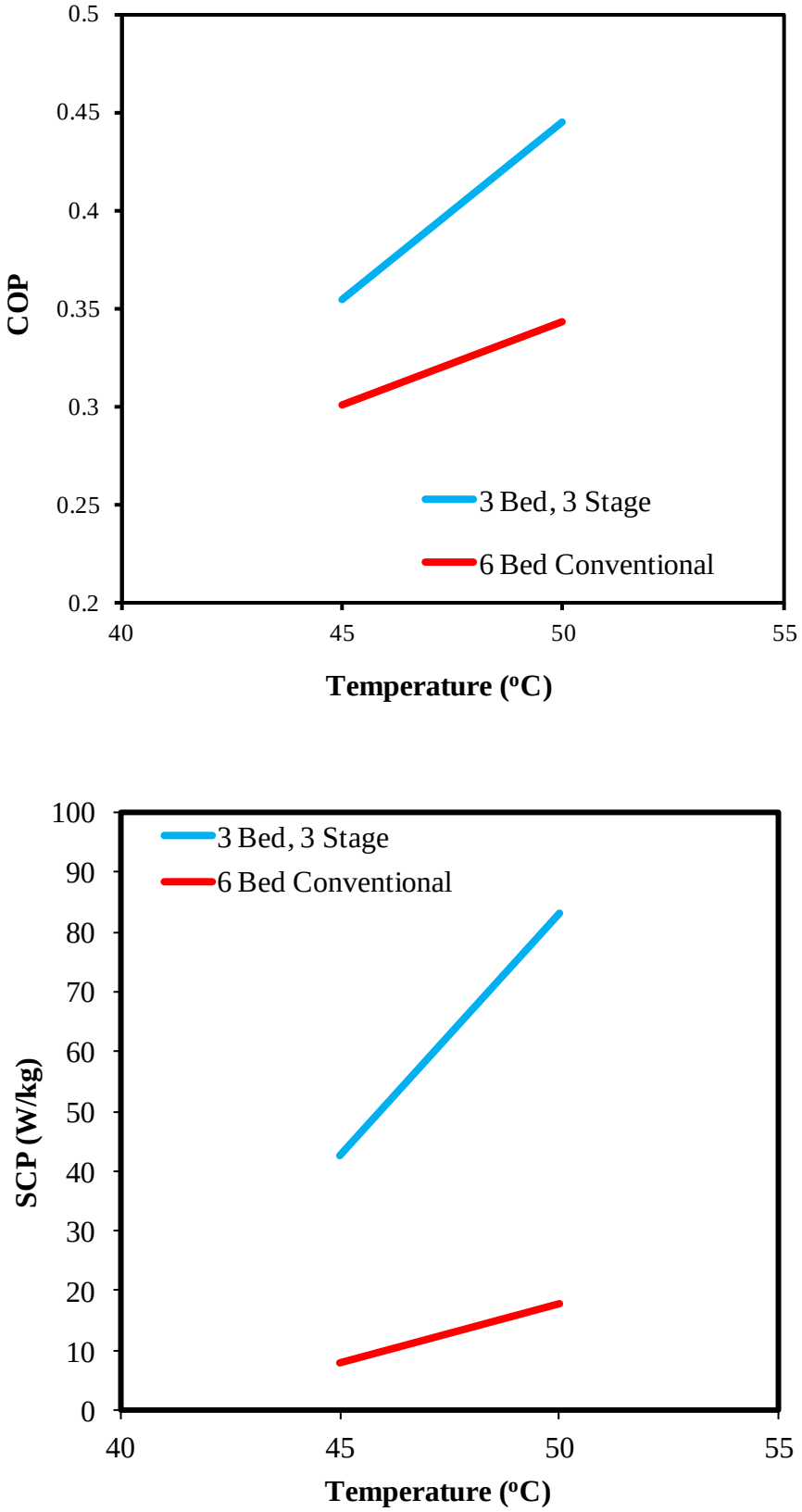

Figure 6.11: Optimization cycle time on the performance comparison.

6.4.1.3. Cycle Time Optimization

Cycle time optimization was conducted to compare the performance of the proposed cycle and the conventional six-bed three-stage cycle which Saha et al. [45] proved that it could work with low heat source temperature. Preferable cycle time depends on the cycle configuration, heat exchanger profile and heat source temperature. In order to compare the cycles properly, the cycle time should be selected to maximize the performance. Here, each cycle time of the two cycles were optimized in terms of specific cooling power.

Cycle time optimization of the three-bed three-stage and six-bed three-stage conventional cycle are presented in Table 6.5. As can be shown in Table 6.5, for the heat source temperature (45 ^{o}C) required longer total cycle time to gain the optimum performance compared to the heat source temperature 50 ^{o}C. The increment of this value because of the raising value of adsorption / desorption time, mass recovery time and pre-heating/pre-cooling time. Table 6.5 also informed the same tendency without any value in mass recovery time for six-bed conventional cycle.

Table 6.5 Optimized cycle time comparison

Adsorption Cycle	Heat Source Temperature (^{o}C)	Optimized Cycle Time (s)			Total Cycle Time (s)
		Ads/Des	Ph/Pc	Mrc/Mrh	
3Bed3Stage cycle	45	696	113	1106	1915
	50	407	95	890	1392
6Bed3Stage Conventional Cycle	45	1008	113	0	1121
	50	902	108	0	1010

The performance comparison of the proposed cycle at two different heat source temperatures is shown in Fig. 6.11. It is apparent that the present chiller can work at low heat source temperature at 45 ^{o}C while chilled water outlet was kept in constant at 9 ^{o}C. Based on Fig. 6.11, generally, the performance increased along with heat source temperature. The performance in both COP and cooling capacity of the proposed cycle is superior to the six-bed conventional three-stage cycle. While the same amount of silica gel in every bed, the

performance of the proposed cycle almost double higher than the 6 bed conventional. Because the proposed cycle uses half amount of silica gel compared with the conventional six-bed cycle, the proposed cycle is advantageous in terms of SCP. The proposed cycle has about 5 times higher SCP than the conventional cycle.

The results of optimized cycle time allocation of the three-bed three-stage cycle and the six-bed three-stage cycle are presented in Table 6.5. The results indicate that longer cycle time is required for both of the cycles when the heat source temperature is 45 ^{o}C than the case with 50 ^{o}C. The increment between two temperature cases resulted from the expansion of the adsorption/desorption process and the mass recovery process. From the viewpoint of total cycle time, the proposed cycle needs 1.4-1.7 times as long cycle time as the conventional cycle.

From this point of view, the three-bed three-stage cycle with the new operational strategy is promising because it can exploit low temperature heat sources. Furthermore, the proposed method also provides the potential to produce more compact three-stage adsorption machines by reducing the number of adsorber/desorber heat exchangers.

6.5. CONCLUSIONS

A simulation study of a three-bed three-stage adsorption cycle was carried out with cycle time optimization to evaluate the system performance. The ability to exploit a low heat source temperature and reduce bed utilization is the highlight of the examinations in this study. The simulation results showed that the proposed cycle with the new operational strategy could operate with a low heat source temperature of 45 °C which offers approximately five times higher performance in terms of SCP than the conventional six-bed three-stage adsorption cycle. Consequently, this work emphasizes that the proposed cycle is effective for utilization of a low-grade heat source even with three beds.

CHAPTER 7

OVERALL CONCLUSION

7.1 GENERAL CONCLUSIONS

In this dissertation, the author concern of studying the conventional adsorption cycle and re-heat adsorption cycle experimentally and numerically. The modification by reducing the utilization of hex and concerning the low heat source temperature has been investigated as well. The innovative designs of three-bed re-heat combined adsorption cycle are introduced. A computational simulation program has been developed based on MATLAB software. The PSO method was applied to optimize the cycle time to know the best performance of the analyzed adsorption systems. It was observed that optimal cycle time is specific for each heat source temperature, which was decreased with heat source temperature.

During experiment, cycle time is responsive to the heat source temperature. The four-bed re-heat cycle with a long cycle provides better COP values than a short cycle time and a four-bed conventional cycle. For a low heat source temperature, the COP value for the four-bed re-heat cycle with a long cycle time is better than the short cycle and four-bed conventional cycle. For a high heat source temperature, the COP of the four-bed conventional cycle is superior. The cooling capacity obtained from the reheating adsorption cycle with the long cycle and the short cycle is better than the single stage with a low heat source temperature. However, the short cycle time offered better cooling capacity with a relatively high heat source temperature compared to the other cycle.

The optimization of four beds re-heat cycle has observed during this study while applying chilled water out temperature fixed. Controlling in mass flow rate is a necessity due to gain fixed chilled water out temperature. Short cycle time (below 3000s) required mass flow rate higher than longer cycle time (up to 3000s). The COP increased along with cycle time and the highest cooling capacity values attained at cycle time between 2000s and 3000s. Cycle optimization of the re-heat cycle offered better performance in both COP and cooling capacity. For the heat source temperature 55^{o}C shown the highest increment of 80% raised in both COP and cooling capacity, while 20% increment for heat source temperature 60^{o}C and

7% increment for heat source temperature 65^{o}C respectively. For relatively high-heat source temperature (70-80^{o}C), although there was the increment in both COP and cooling capacity, the value of escalation raised smoothly in about 1%.

The effect of adsorption/desorption versus pre-cooling/pre-heating time on COP and cooling capacity has been investigated in three-bed re-heat combined cycle. It is worthy to mention here that, the range of adsorption/desorption and pre-cooling/pre-heating time influenced the range of cycle time with the total cycle time is 1950s. It was observed that the COP increases with the increasing of adsorption/desorption time whilst the effect of pre-cooling/pre-heating time is marginal. As can be seen from Figure 6.5, the peaks value of cooling capacity reaches at adsorption/desorption and pre-cooling/pre-heating time 250 and 80s, respectively.

As can be mentioned in chapter 1 of this thesis, it can be conclude the advanced three-bed three-stage re-heat combined cycle as a present chiller with the new operational strategy can utilize the minimum heat source temperature heat source temperature 45 ^{o}C which offering COP and cooling capacity 0.3 and 2 kW, respectively. This results finally answered the question.

7.2 REMARKS

In order to further development, the following investigation can be done for the proposed adsorption system

1. Investigating the new operational strategy for the advanced three-bed re-heat conventional combined cycle to gain the optimum performance.
2. Optimizing the new operational strategy for the three-bed re-heat conventional combined cycle.
3. Investigating the new mode operational strategy for the advanced three-bed three-stage re-heat combined cycle.
4. Optimizing the advanced three-bed three-stage re-heat combined cycle with new mode operational strategy.

REFERENCES

[1] A.O. Dieng , R.Z. Wang., (2001) Literature review on solar adsorption technologies for ice-making and air conditioning purposes and recent developments in solar technology, Renewable and Sustainable Energy Reviews., 5, 313–342.

[2] S.K. Farid, M.M. Billah, M.Z.I. Khan, M.M. Rahman, Uddin Md. Sharif., (2011) A numerical analysis of cooling water temperature of two-stage adsorption chiller along with different mass ratios, International Communications in Heat and Mass Transfer., 38, 1086–1092.

[3] Z.S. Lu, R.Z. Wang, Z.Z. Xia, Q.B. Wu, Y.M. Sun, Z.Y. Chen,. (2011) An analysis of the performance of a novel solar silica gel-water adsorption air conditioning, Applied Thermal Engineering., 31, 3636-3642.

[4] Ahmed R.M. Rezk, Raya K. Al-Dadah., (2012) Physical and operating conditions effects on silica gel/water adsorption chiller performance, Applied Energy., 89, 142–149.

[5] Z.Z. Xia ∗, R.Z. Wang, D.C. Wang, Y.L. Liu, J.Y. Wu, C.J. Chen., (2009) Development and comparison of two-bed silica gel–water adsorption chillers driven by low-grade heat source, International Journal of Thermal Sciences., 48, 1017–1025.

[6] A.S. Uyun, A. Akisawa, T. Miyazaki, Y. Ueda, T. Kashiwagi., (2009) Numerical analysis of an advanced three-bed mass recovery adsorption refrigeration cycle, Applied Thermal Engineering., 29, 2876–2884.

[7] T. Miyazaki, A. Akisawa., (2009) The influence of heat exchanger parameters on the optimum cycle time of adsorption chillers, Applied Thermal Engineering., 29, 2708–2717.

[8] B.B. Saha, S. Koyama, J.B. Lee, K. Kuwahara, K.C.A. Alam, Y. Hamamoto, A.

Akisawa, T. Kashiwagi., (2003) Performance evaluation of a low-temperature waste heat driven multi-bed adsorption chiller, International Journal of Multiphase Flow., 29, 1249–1263.

[9] E.C. Boelman, B.B. Saha, T. Kashiwagi., (1995) Experimental investigation of a silica gel-water adsorption refrigeration cycle-the influence of operating conditions on cooling output and COP, ASHRAE Trans: Research., 101(2), 358-366.

[10] H.T. Chua , K.C. Ng , A. Malek , T. Kashiwagi , A. Akisawa , B.B. Saha., (2001) Multi-bed regenerative adsorption chiller-improving the utilization of waste heat and reducing the chilled water outlet temperature fluctuation, International Journal of Refrigeration., 24, 124-136.

[11] Kim Choon Ng, Xiaolin Wang, Yee Sern Lim, B.B Saha, A. Chakarborty, S. Koyama, A. Akisawa, T. Kashiwagi., (2006) Experimental study on performance improvement of a four-bed adsorption chiller by using heat and mass recovery, International Journal of Heat and Mass Transfer., 49, 3343–3348

[12] D.C. Wang, Z.X. Shi, Q.R. Yang, X.L. Tian, J.C. Zhang, J.Y. Wu., (2007) Experimental research on novel adsorption chiller driven by low grade heat source, Energy Conversion and Management., 48, 2375–2381.

[13] K.C.A. Alam, M.Z.I. Khan, A.S. Uyun, Y. Hamamoto, A. Akisawa, T. Kashiwagi., (2007) Experimental study of a low temperature heat driven re-heat two-stage adsorption chiller, Applied Thermal Engineering., 27, 1686–1692.

[14] M.Z.I. Khan, K.C.A. Alam, B.B. Saha, A. Akisawa, T. Kashiwagi., (2007) Study on a re-heat two-stage adsorption chiller - The influence of thermal capacitance ratio, overall thermal conductance ratio and adsorbent mass on system performance, Applied Thermal Engineering., 27, 1677–1685.

[15] C.H. Tong, N.K. Choon, A. Malek, T. Kashiwagi, A. Akisawa, B.B Saha, A regenerative adsorption process and multi reactor regenerative adsorption chiller,

Espacenet Description:EP 1140314 (A1).

[16] Saha, B. B., Akisawa, A., Koyama, S., Thermally powered sorption technology, Japan ISTPST, 2003.

[17] Kim, Choon, N.G., Recent developments in heat-driven silica gel-water adsorption chiller, Heat Transfer Engineering, vol. 24, issue 3, pp. 1-3, 2003.

[18] Kashiwagi T, Akisawa A, Yoshida S, Alam KCA, Hamamoto Y. Heat driven sorption refrigerating and air conditioning cycle in Japan. Proceedings of the international sorption heat pump conference; pp. 50–62, 2002

[19] Saha, B.B., Boelman, E., Kashiwagi, T., Computer simulation of a silica gel-water adsorption refrigeration cycle – the influence of operating conditions on cooling output and COP, ASHRAE Trans, vol.101, pp. 348-357, 1995.

[20] Saha, B.B., Akisawa, A., Kashiwagi, T., Silica gel-water advanced adsorption refrigeration cycle, Energy, vol. 22, pp. 437-444, 1997.

[21] Karagiorgas, M., Meunier, F., The dynamics of a solid-adsorption heat pump connected with outside heat sources of finite capacity, Heat Recovery Systems and CHP, vol.7, pp. 285–299, 1987.

[22] Critoph, R.E., Zhong, Y., Review of trends in solid sorption refrigeration and heat pumping technology, Proc. IMechE, Part E: J. Process Mech. Eng., vol. 219, pp. 285-300, 2005.

[23] Saha, B.B., El-Sharkawi, I.I., Koyama, S., Lee, J.B., Kuwahara, K., Waste heat driven multi-bed adsorption chiller: heat exchanger overall thermal conductance on chiller performance, Heat Transfer Engineering, vol. 27, issue 5, pp. 80-87, 2007.

[24] Rahman, A.F.M.M., Miyazaki, T., Ueda, Y., Saha, B.B., Akisawa, A., Performance comparison of three-bed adsorption cooling system with optimal cycle time, Heat Transfer Engineering, vol.34, issue 11-12, pp.938-947, 2013.

[25] Alam, K.C.A., Kang, Y.T., Saha, B.B., Akisawa, A., Kashiwagi, T., A novel approach

to determine optimum switching frequency of a conventional adsorption chiller, Energy, vol. 28, pp. 1021-1037, 2003.

[26] Wirajati, IGAB., Akisawa, A., Ueda, Y., Miyazaki, T., Experimental investigation of a reheating two-stage adsorption chiller applying fixed chilled water outlet conditions, Heat Transfer Research, HTR-6774, DOI:10.1615/HeatTransRes.2014006774, 2014.

[27] Sakoda, A., Suzuki M., Fundamental study on solar powered adsorption cooling system, Journal Chemical Engineering of Japan, vol.17, pp.52, 1984.

[28] Kashiwagi, T.; Akisawa, A.; Yoshida, Y.; Alam, K.C.A.; Hamamoto, Y. Heat driven sorption refrigerating and air conditioning chiller in Japan. Proc. of the International Sorption Heat Pumps Conference, Kansai Science City, Japan, May 2002, 50–62.

[29] Tchernev, D.I.; Emerson, D.T.; High efficiency regenerative zeolite heat pump. ASHRAE Trans. 1988, Volume 2, pp. 2024-2032.

[30] Karagiorgas, M.; Meunier, F. The dynamic of a solid adsorption heat pump connect with outside heat source of finite capacity. J. Heat Recovery System. 1987, 7, 285-299.

[31] Critoph, R.E.; Vogel, R.E.R.; Possible adsorption pairs for use in solar cooling. Int. J. of Ambient Energy. 1986, 7, 183-190.

[32] Boelman, E.C.; Saha, B.B.; Kashiwagi, T. Experimantal investigation of silica gel – water adsorption refrigeration cycle – the influence of operating condition on cooling output and COP, ASHRAE Trans., 1995, 101, pp. 358-366

[33] Chua, H.T.; Ng, K.C.; Malek, A.; Kashiwagi, T.; Akisawa, A.; Saha, B.B. Modeling the performance of two-bed, silica gel-water adsorption chiller. Int. J. Refrig. 1999, 22, 94–204.

[34] Marlinda; Uyun, A.S.; Miyazaki, T.; Ueda, Y.; Akisawa, A. Performance analysis of a double effect adsorption refrigeration cycle with a silica gel/water working pair. Energies. 2010, 3, 1704-1720.

[35] Akahira, A.; Alam, K.C.A.; Hamamoto, Y.; Akisawa, A.; Kashiwagi, T. Mass recovery adsorption refrigeration cycle - improving cooling capacity. Int. J. Refrig. 2004, 27, 225–234.

[36] Mizanur Rahman, A.F.M.; Ueda, Y.; Akisawa, A.; Miyazaki, T.; Saha, B.B. Design and performance of an innovative four-bed, three-stage adsorption cycle. Energies, 2013, 6, 1365-1384.

[37] Alam, K.C.A.; Hamamoto, Y.; Akisawa, A.; Kashiwagi, T. Advanced adsorption chiller driven by low temperature heat source. Proc. of 21st International Congress of Refrigeration, Washington DC, USA, August 2003, Paper no. 0136 in CD ROM 17-22.

[38] Wirajati, I.G.A.B.; Ueda, Y.; Akisawa, A.; Miyazaki, T. The performance of three-bed re-heat combined adsorption chiller. Proc. of the International Sorption Heat Pumps Conference, Washington DC, USA , August 2003, Paper no. 1036.

[39] Khan, M.Z.I.; Saha, B.B.; Alam, K.C.A.; Akisawa, A.; Kashiwagi, T. Study on solar/waste heat driven multi-bed adsorption chiller with mass recovery, Renew. Energy, 2007, 32, 365–381.

[40] Uyun, A.S.; Miyazaki, T.; Ueda, Y.; Akisawa, A. Experimental investigation of a three-bed adsorption refrigeration chiller employing an advanced mass recovery cycle. Energies. 2009, 2, 531-544.

[41] Fan Y., Luo, L. and Souyri, B., 2007. Review of solar sorption refrigeration technologies: Development and applications, Renewable and Sustainable Energy Reviews, 11, pp. 1758-1775.

[42] Meunier F., 1978. Utilisation des cycle a sorption pour la production de froid par l'e´nergie solaire, Cahiers de I'AFEDES, 5, pp. 57-67.

[43] Srivastava N.C., Eames I.W., 1998. A review of adsorbents and adsorbates in solid - vapour adsorption heat pump systems, App. Therm. Eng., 18, pp. 707-7 14.

[44] Kennedy J. and Eberhart R., 1995. Particle Swarm Optimization. Proc. IEEE Int. Conf. Neural Networks, IV, pp. 1942-1948.

[45] Saha, B. B., Akisawa, A., and Kashiwagi, T., Silica gel water advanced adsorption refrigeration cycle, Energy, 1997, 22 (4), pp. 437–447.

APPENDIX A

DISSERTATION RELATED AUTHOR'S PUBLICATION

JOURNALS

1 **I Gusti Agung Bagus Wirajati**, Atsushi Akisawa, Yuki Ueda, Takahiko Miyazaki, Experimental Investigation of A Reheating Two-Stage Adsorption Chiller Applying Fixed Chilled Water Outlet Conditions, *Journal of Heat Transfer Research*, DOI:10.1615/HeatTransRes.2014006774. [Corresponding to Chapter 4 of the thesis]

2 **I Gusti Agung Bagus Wirajati**, Atsushi Akisawa, Yuki Ueda, Takahiko Miyazaki, Cycle Optimization on Re-Heat Adsorption Cycle Applying Fixed Chilled Water Outlet Temperature, *Journal of Heat Transfer Engineering*, Accepted (2014). [Corresponding to Chapter 5 of the thesis]

3 **I Gusti Agung Bagus Wirajati**, Muhammad Umair, Koji Enoki, Yuki Ueda and Atsushi Akisawa, Three-Stage Adsorption Cycle with Three-Beds of Silica Gel, *Trans. of the JSRAE*, 2014, [Corresponding to Chapter 6 of the thesis]

PROCEEDINGS AND CONFERENCES

1 **I Gusti Agung Bagus Wirajati** , Aep Saepul Uyun, K.C.A. Alam Takahiko Miyazaki, Atsushi Akisawa, Takao Kashiwagi, " Experimental Study on Adsorption Chiller with Reheat Two Stage Cycle", *Proceedings of the Asian Thermophysical Properties Conference Conference (ATPC2007)*, 21-24 August, 2007, Fukuoka, Japan

2 **I Gusti Agung Bagus Wirajati**, I Wayan Temaja, I Nengah Ardita, A. Akisawa, T. Kashiwagi, " Experimental Investigation of Fixed Chilled Water Outlet Condition on Reheat Two Stage Cycle- Adsorption Chiller", *Proceedings of the 1st International Conference on Sustainable Technology Development: Sustainable Technology Based on Environmental and Cultural Awareness (ICSDT2010)*, Udayana University, Bali, October 6-8, 2010.

3 **I Gusti Agung Bagus Wirajati** , Atsushi Akisawa, Yuki Ueda, Takahiko Miyazaki, "Cycle Optimization on Re-Heat Adsorption Cycle Applying Fixed Chilled Water Outlet Temperature", *Proceeding of 'International Symposium on Innovative Materials for Processes in Energy Systems 2013' (IMPRES2013,)* September 4-6, 2013, Fukuoka, Japan.

4 **I Gusti Agung Bagus Wirajati**, Atsushi Akisawa, Yuki Ueda, Takahiko Miyazaki, " The Performance of Three-bed Re-heat Combined Adsorption Chiller", *Proceeding of 'International Sorption Heat pumps Conference (ISHPC 2104)*, March 31-April 3, 2014, Washington, USA.

5 **I Gusti Agung Bagus Wirajati**, Muhammad Umair, Koji Enoki, Yuki Ueda and Atsushi Akisawa, "Three-Stage Adsorption Cycle with Three-Adsorption Beds", *Proceeding of '2014 JSRAE Annual Conference*, Saga, Japan, 2014 September 10-13.